INORGANIC CARBON UTILIZATION AND THE ROLE OF PHOSPHOENOLPYRUVATE CARBOXYKINASE IN THE PHOTOSYNTHESIS OF THE MARINE MACROALGA *UDOTEA*

By

BETH ANN BURCH

A DISSERTATION PRESENTED TO THE GRADUATE SCHOOL
OF THE UNIVERSITY OF FLORIDA IN PARTIAL FULFILLMENT
OF THE REQUIREMENTS FOR THE DEGREE OF
DOCTOR OF PHILOSOPHY

UNIVERSITY OF FLORIDA

1993

To My Dear Husband, Greg

and

In Loving Memory of My Parents,

John and Doris Lilly

ACKNOWLEDGMENTS

I wish to thank Dr. George Bowes, my major professor, for his support and encouragement throughout my graduate career. The helpful suggestions provided by the supervisory committee, Dr. Steve Davis, Dr. Richard Smith, Dr. Charlie Guy, and Dr. Charles Allen are gratefully acknowledged. A special note of appreciation to Dr. Steve Davis, who so graciously volunteered to take his personal boat to Crystal Bay at all times of year in order to collect some of the plant samples. I appreciate the suggestions and help with research methodologies given by Dr. Julia Reiskind during the course of my tenure in Dr. Bowes' laboratory. A thank you goes to Dr. Charles Guy for allowing me to use some of his laboratory equipment in experiments. I am grateful to the research staff of the laboratory of the Florida Keys Land and Sea Trust in Marathon, Florida for their help in collecting some of the plant samples and for use of the laboratory facilities. This research was funded by the United States Department of Agriculture, Science and Education Administration, Competitive Research Grants Office, Photosynthesis Program Grants 88-37130-3703 and 90-37130-5576.

I am indebted to my husband, Greg, for his enduring love and support through my completion of this research and dissertation.

TABLE OF CONTENTS

LIST OF TABLES

LIST OF FIGURES

KEY TO ABBREVIATIONS

A	absorbance
ATPase	adenosine triphosphate synthetase
AZ	acetazolamide
Bicine-NaOH	n,n-bis(2-hydroxyethyl)glycine-sodium hydroxide
BSA	bovine serum albumin
CA	carbonic anhydrase
CAM	Crassulacean acid metabolism
cAMP	cyclic adenosine monophosphate
CHES-NaOH	2-(n-cyclohexylamino)ethanesulfonic acid-sodium hydroxide
Chl	chlorophyll
C_i	inorganic carbon
DBAZ	dextran-bound acetazolamide
DCMU	3-(3,4-dichlorophenyl)-1,1-dimethylurea
DHAP	dihydroxyacetone phosphate
DIC	dissolved inorganic carbon
DIDS	4,4'-diisothiocyanatostilbene-2,2'-disulfonic acid
DTT	dithiothreitol
DW_A	dry weight after acid treatment
EZ	ethoxyzolamide
F-1,6-BP	fructose-1,6-bisphosphate
F6P	fructose-6-phosphate
Hepes-NaOH	n-(2-hydroxyethyl)piperazine-n'-(2-ethanesulfonic acid-sodium hydroxide
$K_{0.5}$	apparent Michaelis-Menten constant
LN_2	liquid nitrogen
MDH	malate dehydrogenase

MES	2-(n-morpholino)ethanesulfonic acid
MES-NaOH	2-(n-morpholino)ethanesulfonic acid-sodium hydroxide
MPA	3-mercaptopicolinic acid
OAA	oxaloacetate
PCO	photorespiratory carbon oxidation
PCR	photosynthetic carbon reduction
PEP	phosphoenolpyruvate
PEPC	phosphoenolpyruvate carboxylase
PEPCK	phosphoenolpyruvate carboxykinase
3-PGA	3-phosphoglycerate
PIPES-NaOH	piperazine-n,n'-bis(2-thanesulfonic acid)-sodium hydroxide
PMSF	phenylmethylsulfonyl fluoride
pro	protein
PVP-40	polyvinylpyrrolidone with molecular weight of 40,000 kilodaltons
Rubisco	ribulose-1,5-bisphosphate carboxylase/oxygenase
RuBP	riubulose-1,5-bisphosphate
Tris-HCl	tris(hydroxymethyl)aminomethane-hydrochloric acid
V_{max}	maximum velocity
μCi	micro Curie

Abstract of Dissertation Presented to the Graduate School
of the University of Florida in Partial Fulfillment of the
Requirements for the Degree of Doctor of Philosophy

INORGANIC CARBON UTILIZATION AND
THE ROLE OF PHOSPHOENOLPYRUVATE CARBOXYKINASE
IN THE PHOTOSYNTHESIS OF THE MARINE MACROALGA *UDOTEA*

By

Beth Ann Burch

December 1993

Chairman: George Bowes
Major Department: Botany

Udotea is a marine, green, siphonaceous macroalga with C_4-like photosynthetic characteristics. At pH 8.2, 15 mM dissolved inorganic carbon (DIC) was required to saturate photosynthesis, which is 7-fold greater than the concentration in natural seawater. Carbon dioxide was the preferred DIC species for photosynthesis. Acidification of the thallus surface occurred in the light and the dark, which could produce CO_2 for diffusion into the siphons. External carbonic anhydrase activity was lacking. In pH drift experiments, the highest final pH value attained was only 8.95, which is in the range typical of CO_2-only users. However, some HCO_3^- use was indicated by enhanced photosynthesis when the HCO_3^- concentration was increased at a given CO_2 concentration. Photosynthesis was inhibited 13 to 33% by 4,4'-diisothiocyanostilbene-2,2'disulphonate and 34% by the plasma-membrane ATPase inhibitor vanadate, which also halted thallus acidification. Thus, ATP may have a role in the DIC uptake process. Calcium chloride was necessary for photosynthetic DIC uptake, but not O_2 evolution. This is consistent with calcification by *Udotea*, as 50% of the dry weight of the alga was composed of carbonate salts.

The kinetics of isolated phosphoenolpyruvate carboxykinase (PEPCK) were analyzed to determine how this enzyme operates for carboxylation in *Udotea* photosynthesis. Unlike carboxylation by ribulose-1,5-bisphosphate carboxylase/oxygenase, the PEPCK carboxylation reaction was O_2 insensitive though CO_2 was the substrate. The carboxylation pH optimum of 6.8 was lower than for decarboxylation, and at this pH, which is close to the probable pH of the cytosol, where PEPCK appears to be located, the carboxylation V_{max} was nearly 2-fold greater than that of decarboxylation. For carboxylation, the K_m values for CO_2, phosphoenolpyruvate (PEP), and ADP were 2.1 mM, 1.7 mM, and 30 μM, respectively; for decarboxylation, the K_m values for oxaloacetate (OAA) and ATP were 35 and 2 μM. Dihydroxyacetone phosphate, 3-phosphoglycerate, and ATP inhibited carboxylation, while fructose-1,6-bisphosphate stimulated it by lowering the K_m(PEP) from 1.6 mM to 0.5 mM. Fructose-6-phosphate and CO_2 inhibited decarboxylation. These observations raise the possibility of metabolite regulation of the carboxylation/decarboxylation ratio. Both reactions were competitively inhibited with respect to PEP and OAA by 3-mercaptopicolinic acid. The carboxylation rate was enhanced 6-fold in the presence of malate dehydrogenase isolated from *Udotea*.

CHAPTER 1
GENERAL INTRODUCTION AND LITERATURE REVIEW

The Marine Macroalga *Udotea*

Habitat and Morphology

Udotea conglutingata (Ellis and Solander) Lamouroux and *U. flabellum* (Ellis and Solander) Lamouroux used in this investigation are marine, green, calcified, macroalgae that belong to the Family Udoteaceae of the Order Caulerpales, Class Chlorophyceae and Division Chlorophyta (20, 153). These algae can be found in tropical to sub-tropical marine waters (21), growing in soft mud or calcareous sand, often among seagrasses (45). The thallus of *Udotea* is composed of intertwining siphons with cell walls of β-1,3-xylan (21, 23), which exists in a hollow helix conformation (97). No cellulose was detected.

Thalli are heteroplastidic with photosynthetic chloroplasts and starch-storing amyloplasts (153). Chloroplasts of *Udotea* have lamellae with various numbers of thylakoids and a thylakoid-organizing body of concentric double membranes at one end (153). The accessory photosynthetic pigments siphonein and siphoxanthin are also found in members of this family (153). In adult thalli, amyloplasts are found further down in the thalli than the chloroplasts (24).

Sexual reproduction in members of the Udoteaceae seldom happens (21), but when it does occur, diploid dioecious thalli produce haploid gametes in a holocarpic manner, where an entire siphon is converted from the vegetative state to one where the nuclear division products are haploid gametes (101, 153). Gametes are released into the water when the siphon bursts open at the tip, and thallus death then follows (21). Anisogamous germ cells of two opposite mating types fuse, producing a

diploid zygote, which then develops into a protosphere, which has starch-containing chloroplasts (21). Upon maturation, the new thallus that develops from the protosphere becomes heteroplastidic. Vegetative reproduction, which is the most frequent type of reproduction in *Udotea*, occurs when new thalli arise from a branched rhizoidal system (21).

These habit and reproductive features of *Udotea* indicate that it possesses a number of derived and highly derived characteristics. Although its evolutionary development was in a different direction from that which eventally led to the vascular land plants, *Udotea* is by no means a "primitive" alga; rather, it belongs to a group considered "most derived (153)."

Calcification

Udotea conglutinata and *U. flabellum* are calcified representatives of this genus. The calcification mechanism in algae is tied closely with photosynthesis, as no $CaCO_3$ is deposited until the plant is photosynthetically active (22, 23, 24).

The mechanism of calcification in these two species differs slightly in that *U. conglutinata* deposits aragonite crystals of $CaCO_3$ intracellularly within organic layers of a sheath that begins at the cell wall and forms an outer wall of the siphons (19). Some deposits also occur in the intersiphonous areas of the thallus. In addition, crystals of calcium oxalate are deposited in the vacuole in a randomly oriented fashion (56).

In contrast, *U. flabellum* lacks calcium oxalate crystal deposits in its vacuoles (56). At the outer surface, the siphons are highly branched, forming a developed cortical surface (19). In this cortex region, $CaCO_3$ is deposited between layers of the siphon wall, while away from the exterior surface, $CaCO_3$ aragonite crystals are deposited in the inter-siphon spaces (19). Both primary and secondary crystal deposits occur in the cortex region, and this pattern is somewhat similar to what occurs in sheath calicification, exhibited in *U. conglutinata* (19).

Thus, *U. flabellum* exhibits both intra- and intercellular calcification (19).

Regardless of where $CaCO_3$ precipitation occurs, this mechanism requires an enclosed space where a high pH can be generated, in this case, by the removal of CO_2 for use in photosynthetic carbon assimilation (23). It has been suggested that the Ca^{2+} for precipitation in calcareous macroalgae comes from an intracellular pool (98). The trans-membrane Ca^{2+} transport may be achieved by an ATPase that exchanges 2 H^+ per Ca^{2+}, thus helping to generate the external high pH needed for $CaCO_3$ precipitation (98).

Photosynthesis

Terrestrial plants have been divided into four categories based on the biochemistry of their photosynthetic mechanism. These categories are C_3, C_4, C_3-C_4 intermediates, and Crassulacean acid metabolism (CAM). The categories do not follow taxonomic lines, as one genus contains representatives from three of the four photosynthetic categories. The C_3-C_4 intermediate category will not be discussed.

C_3 Photosynthetic Category

By far the vast majority of plants in the North American flora fits into the C_3 category. The leaf mesophyll of plants in this group is differentiated into a palisade layer on the adaxial side and a spongy layer on the abaxial side. Chloroplasts are dispersed throughout the mesophyll layer and are usually lacking in the bundle sheath. The chloroplasts are all the same, i.e., the thylakoids are stacked into grana, have both photosystems I and II, and have the full complement of photosynthetic carbon reduction (PCR) cycle enzymes. Of the seed plants, both gymnosperms and angiosperms (including monocots and dicots) are represented, so vascular bundle arrangement varies somewhat. Stomates are found on both leaf surfaces, although usually more prevalent on the abaxial surface. Guard cells are functional and open

during the daytime to facilitate the exchange of CO_2, O_2, and water vapor between the leaf and the surrounding atmosphere (51).

The C_3 plants use the PCR cycle to fix atmospheric carbon into carbohydrate. Ribulose 1,5-bisphosphate carboxylase/oxygenase (Rubisco) is the predominant carboxylating enzyme, and it incorporates atmospheric CO_2 directly into 3-phosphoglycerate (3-PGA). Because of the active site conformation of Rubisco, which allows either CO_2 or O_2 to react with ribulose 1,5-bisphosphate (RuBP), the enzyme also catalyzes the first step in photorespiration or the photorespiratory carbon oxidation (PCO) cycle. Rubisco must be activated by CO_2 and Mg^{2+} to be catalytically competent (32, 89, 92). Carbon dioxide, rather than HCO_3^- or CO_3^{2-}, is the carbon species utilized for both activation and catalysis, and the activator and catalytic CO_2 molecules are distinct according to kinetic and spectroscopic measurements (75, 89). A CO_2 molecule and Mg^{2+} cation must bind to each of the eight catalytic sites for Rubisco to be completely activated (81). Light affects Rubisco in two important ways: light induces changes in the chloroplast such as increasing the stromal pH from around 7 to approximately 8.2 (92) and increasing Mg^{2+} concentration in the stroma by about 3 mM (92). These changes increase enzyme activity (32) and activate Rubisco via Rubisco activase. The binding of CO_2 and Mg^{2+} to the catalytic sites of the enzyme is facilitated (129, 154).

In the PCO cycle, RuBP is oxidized to 3-PGA and 2-P glycolate, the latter of which is dephosphorylated in the chloroplast, and the resulting glycolate enters the peroxisome, where it is metabolized to glycine. Glycine then migrates to the mitochondrion where CO_2 is released in the conversion to serine (91). The PCO cycle decreases net carbon fixation by 20 to 40% (16) because O_2 directly competes for CO_2 at the Rubisco active site. This photorespiration decreases the amount of RuBP available for carboxylation, and one third of the fixed CO_2 is released. The CO_2 compensation point, the concentration of CO_2 at which

the net carbon exchange in the light is zero, is achieved when the CO_2 released by the PCO cycle just balances that reduced by the PCR cycle. For terrestrial plants, the CO_2 released in photorespiration is a large component of the CO_2 compensation point, but the CO_2 released by dark respiration is not. When the plants are placed into 1% O_2, where photorespiration is all but eliminated, measurable respiratory CO_2 release is virtually zero (54). The operation of the PCO cycle causes the CO_2 compensation points in C_3 plants to be quite high, in the range of 30 to 70 μL CO_2 L^{-1} (16). Photorespiratory CO_2 release is energetically expensive because CO_2 must first be reduced to RuBP with NADPH and ATP produced in the light reactions before oxidation to glycolate can occur (90), and the process itself requires NADH and ATP to function. The release of NH_3 and its subsequent refixation is also a costly process.

Evidence that both carboxylation and oxygenation occur at the same site includes 1) inhibition of the two processes by carboxyarabinitol 1,5-bisphosphate (similar in structure to the C_6 intermediate formed immediately after carboxylation of RuBP), 2) activation of both functions to the same degree by CO_2 and Mg^{2+}(91), and 3) demonstration that $K_m(CO_2)$ equals $K_i(O_2)$ and $K_m(O_2)$ equals $K_i(CO_2)$ (26). However, although the ratio of CO_2 to oxygen is relatively constant at all temperatures, oxygenation is favored over carboxylation at the higher temperatures because CO_2 is less soluble in water than O_2 under these conditions (65, 86, 107), and Rubisco has a lower affinity for CO_2 at higher temperatures (104, 132). Therefore, the optimum temperature for C_3 photosynthesis ranges from 15 to 25°C (16).

C_4 Photosynthetic Category

In some terrestrial plants, an additional metabolic pathway has arisen which serves to concentrate CO_2 in the vicinity of the Rubisco active site, thereby decreasing photorespiration (48). The origin of the C_4 photosynthetic mechanism appears to be polyphyletic, and for

terrestrial plants it is found only in the more advanced angiosperms (115). It occurs most frequently in herbaceous plants including annual and perennial herbaceous monocots and dicots.

Plants in this photosynthetic category exhibit Kranz anatomy in which the bundle sheath surrounding the vascular tissue is distinctive and composed of large, closely packed cells that are larger than the mesophyll cells. Chloroplasts in the bundle sheath are arranged specifically in accord with the type of C_4 metabolism the plant uses (48). Plants of the NADP-malic enzyme type contain dimorphic chloroplasts (48). Those of the mesophyll cells have grana, pyruvate P_i dikinase, and relatively high levels of NADP-malic dehydrogenase, but lack Rubisco and have the enzymes of only the reductive phase of the PCR cycle. However, the Kranz cell chloroplasts lack grana but have Rubisco and all of the PCR cycle enzymes (48).

All C_4 plants have two carboxylation reactions. In the first reaction, HCO_3^- is the form of dissolved inorganic carbon (DIC) used. Carbonic anhydrase (CA) facilitates the equilibrium between this species and atmospheric CO_2. Phosphoenolpyruvate is carboxylated with HCO_3^- by phosphoenolpyruvate carboxylase (PEPC), resulting in the production of the C_4 acid oxaloacetate (OAA). Oxaloacetate is either reduced to malate or transaminated to aspartate, which is then transported to the bundlesheath cells. Either malate is decarboxylated directly or aspartate is deaminated and reduced to malate, which is then decarboxylated by one of three enzymes (48).

In the NADP-malic enzyme subgroup of C_4 plants, which includes *Zea mays* and *Saccharum officinarum*, OAA from carboxylation in the mesophyll cell cytosol is reduced to malate and then translocated to the bundle sheath cell chloroplasts, where the malate is oxidized and decarboxylated to pyruvate and CO_2. The pyruvate is transported back to the mesophyll cell chloroplasts, where it is phosphorylated to PEP by pyruvate P_i dikinase. The CO_2 is then refixed by Rubisco in the

chloroplasts of the bundle sheath cells. Chloroplasts in the bundle sheath cells of these species are agranal and deficient in photosystem II activity (48). They are located near the centrifugal wall of the bundle sheath cells. The predominant transport metabolites in this subgroup are malate and pyruvate (48).

In the NAD-malic enzyme subgroup, exemplified by *Panicum miliaceum* and *Amaranthus retroflexus*, OAA from PEPC carboxylation is transaminated to aspartate in the cytoplasm of the mesophyll cells and then transported to the mitochondria of bundle sheath cells. Aspartate is deaminated to OAA in the mitochondria and then reduced to malate, which is oxidized and decarboxylated to pyruvate and CO_2. Pyruvate is transaminated to alanine in the bundle sheath cell cytosol. Alanine moves back into the mesophyll cell cytosol and is deaminated to pyruvate, which them moves into the chloroplasts, where phosphorylation occurs via pyruvate P_i dikinase to regenerate PEP. The liberated CO_2 is refixed by Rubisco in the chloroplasts of bundle sheath cells. Chloroplasts of the bundle sheath cells in these species do have grana and are located in the centripetal position in the cells. These plants also have many more large mitochondria in the centripetal position of the bundle sheath cells compared to other groups. Here the major transport metabolites are aspartate and alanine (48).

Plants in the PEPCK subgroup, such as *Panicum maximum* and *Chloris gayana*, transaminate the OAA produced by PEPC to aspartate in the cytoplasm of mesophyll cells, and aspartate is then moved to the cytosol of bundle sheath cells. Here deamination produces OAA which is decarboxylated to pyruvate followed by ATP-dependent formation of PEP in the cytoplasm. The PEP is dephosphorylated to pyruvate, which is then transaminated to alanine. Alanine then moves into the cytosol of the mesophyll cells. Alanine is deaminated to pyruvate which enters the chloroplasts and is phosphorylated to PEP via pyruvate P_i dikinase. As above, the CO_2 is refixed by Rubisco in the bundle sheath cell

chloroplasts. These plants have granal chloroplasts toward the centrifugal position in the bundle sheath cells. The major transport metabolites in this subgroup are also aspartate and alanine (48).

In the C_4 photosynthetic mechanism, less than 5% of the CO_2 assimilated from the atmosphere enters 3-PGA directly. Instead, the CO_2 that enters the PCR cycle comes almost exclusively from the decarboxylation of the organic acids; essentially Rubisco is isolated from the atmosphere (48). This arrangement is beneficial for the plant in that the CO_2 concentration is elevated or concentrated. Photosynthesis by C_4 plants is independent of O_2 concentrations ranging from 2 to 21% (115). Because the CO_2/O_2 ratio is increased in C_4 plants, the limitations imposed by CO_2 and O_2 solubility characteristics with increasing temperature are overcome (86), which has a role in elevating the temperature optimum in these species into the 30 to 47°C range (16). The function of the elaborate C_4 acid system is to concentrate CO_2 and in doing so, essentially eliminates the photorespiratory release of CO_2. However, some 2-P glycolate does form, and there is carbon flux through the glycolate pathway (108). A measurable indicator of less CO_2 release from the leaf is the very low CO_2 compensation point measured for C_4 plants, usually in the range from 0 to 10 $\mu L\ CO_2\ L^{-1}$ (16). Dark respiration does not constitute any measurable component of the CO_2 compensation point, as evidenced by these low values. The C_4 acid mechanism, then, is an effective means by which to reduce photorespiratory CO_2 release.

Although less CO_2 is photorespired in the C_4 pathway, thereby reducing energy loss in the form of NADPH and ATP used to produce RuBP and energize the PCO cycle, C_4 plants do require an additional two or three ATP molecules to fix CO_2 because of the last step of the sequence where pyruvate is converted to PEP by pyruvate P_i dikinase (48). Under conditions of higher temperature and irradiance, C_4 plants have a major advantage over C_3 plants in that C_4 plants are not affected by the

decrease in CO_2 solubility with increased temperature because of the CO_2 concentrating mechanism (48). However, under lower irradiance levels and temperature, C_3 plants can match or even exceed the net carbon gain exhibited by C_4 plants (48).

CAM Photosynthetic Category

Crassulacean acid metabolism can actually be considered a form of C_4 photosynthesis. Atmospheric CO_2 is converted to HCO_3^- by CA and fixed by PEPC into OAA, which is then reduced to malate. Decarboxylation then occurs by either NAD-malic enzyme or PEPCK, and the liberated CO_2 is fixed into carbohydrate by Rubisco. Obligate CAM species utilize the CAM pathway for carbon fixation all the time, while facultative CAM species can shift dramatically the physiology and biochemistry of carbon fixation from C_3 to CAM mode. Water availability determines the photosynthetic metabolism; low availability induces CAM (144). These plants exhibit variable CO_2 compensation points. During the early part of the day, during Phase III of the CAM cycle, in which the malate stored at night is decarboxylated, the CO_2 compensation point is low because the decarboxylation concentrates CO_2 in the vicinity of Rubisco. The CO_2 level may rise to be greater than 1% or 10,000 $\mu L\ L^{-1}$. Although the O_2 concentration increases as photosynthesis proceeds, the favorable CO_2/O_2 ratio limits photorespiration (144). In addition, the difference in $K_m(CO_2)$ and $K_m(O_2)$ for Rubisco favors CO_2 fixation. However, toward the end of the day, during Phase IV when all of the stored malate has been depleted, the stomates open, and the plant carries on C_3 photosynthesis. The CO_2 compensation point in this phase has been measured at 50 $\mu L\ CO_2\ L^{-1}$, and a burst of CO_2 results when plants in this phase are artificially placed in the dark; both characteristics point to an active photorespiration process. Although CAM species can photorespire, the CO_2 released can serve as an internal carbon source for photosynthesis (111). But unlike C_4 plants, CAM species lack Kranz anatomy (59). PEPC and Rubisco are located in the same cells, but their

activities are temporally separate; fixation by PEPC at night results in the storage of malate in the vacuole until daylight when malate transport and decarboxylation and subsequent fixation of the released CO_2 by Rubisco begins (113). Plants with this photosynthetic pathway usually occur in arid habitats, where the mechanism aids in water conservation. However, *Isoetes howellii*, a submersed aquatic plant, also exhibits this type of carbon metabolism (83) as a means of overcoming the carbon limitations in its environment.

Marine Algal Photosynthesis

In numerous marine macroalgae studied thus far, photosynthesis is characterized by O_2-insensitive photosynthesis, low CO_2 compensation points, and low photorespiration rates, but some species do not share these attributes (77). Such characteristics make the algae photosynthetically more similar to the terrestrial C_4 plants than to the C_3 species. This feature is intriguing in that the algae are considered to be "primitive" among plants. The C_4 photosynthetic mechanism is considered "advanced," as it involves specialized anatomy and compartmentalized enzymes with ample shuffling of metabolites between cells. One wonders how these "primitive" plants can utilize such an "advanced" form of metabolism. In contrast, Raven and Osmund (119) have concluded that some subtidal macroalgae, including the green *Codium fragile*, and the browns *Dictyota dichotoma*, *Padina vickersii*, *Sargassum filipendula*, and *Fucus vesiculosus*, possess photosynthetic capacity that cannot be used during steady-state, light-saturated photosynthesis unless the inorganic carbon concentration is increased, a scenario reminiscent of the terrestrial C_3 species. Thus, the inorganic carbon concentration in marine waters is not sufficient to saturate photosynthesis for some algae, just as the atmospheric concentration of CO_2 does not saturate photosynthesis in the terrestrial C_3 species.

One of the challenges a plant faces in a marine environment is obtaining inorganic carbon for photosynthesis. Because dissolved gases

diffuse about 10,000 times more slowly in water than they do in air (25), a submersed plant must be able to overcome this physical limitation in its environment. A survey of marine macroalgae across the algal divisions indicates that the DIC concentration in seawater is too low to overcome the effects of O_2 on photosynthesis unless the alga employs some sort of carbon concentrating mechanism (71). Such mechanisms may involve direct HCO_3^- uptake or C_4 acid metabolism.

With regard to the particular species of DIC utilized by an alga, one must consider the influence of the pH and salinity of seawater on the proportion of each of the inorganic carbon species. The pH of seawater is in the 8.0-8.2 range and the salinity around 35 parts per thousand. Under these conditions, with the water in equilibrium with the atmosphere, the predominant species is HCO_3^-, present at a concentration of about 2 mM. Only 10 μM of the total carbon is CO_2 (133). It has been determined that CO_3^{2-} is not a photosynthetically active species, even when its relative proportion dramatically increases, as may occur in a rockpool containing photosynthesizing algae (93), so further discussion will focus on only HCO_3^- and CO_2. The macroalgae examined show a range of affininities for HCO_3^- (94). A common method of assessing this ability is based on measuring the photosynthetic rate and comparing it to the rate expected based on the CO_2 produced as a result of HCO_3^- dehydration (77). If the observed photosynthetic rate exceeds the spontaneous CO_2 supply rate, the species likely is using HCO_3^- in addition to CO_2 (77). However, before a specific HCO_3^- utilization mechanism can be hypothesized, a lack of external CA must be demonstrated. This enzyme located outside the plasma membrane facilitates the conversion of HCO_3^- to CO_2 or vice versa, depending on the pH. The CO_2 can diffuse across the membrane into the cell (77), while HCO_3^- cannot because of the charge on the molecule. Based on this criterion, most marine macroalgae studied have been found to need HCO_3^- in addition to the CO_2 spontaneously supplied

by dehydration to support the observed photosynthetic rate (6, 77), and the algae show a consistently high capacity for inorganic carbon transport (14).

The inorganic carbon disequilibrium technique can also be used to ascertain the species of inorganic carbon preferred by a plant. The plant is given either CO_2 or HCO_3^- under conditions where the time for equilibrium to be established between the two carbon species is prolonged by low temperature. Based on whether photosynthesis occurs more rapidly in the presence of either CO_2 or HCO_3^-, this rate difference indicates which particular carbon species is preferred by that plant (77).

Of course, the enzymes involved in inorganic carbon utilization are a key component of the photosynthetic mechanism. In all macroalgae examined, Rubisco has been determined to be the primary carboxylase (11, 71). In addition, the variability in photosynthetic rates observed for the marine macroalgae correlates well with the measured carboxylase activity (14), even to the extent that the photosynthesis to carboxylase activity ratio is close to one. Rubisco activity plays a role in regulating the photosynthetic capacity where internal CO_2 concentration is high and photorespiration is suppressed, but other factors also have a role in limiting the photosynthetic rate under such conditions (14).

Chlorophyta

Nearly all green macroalgae examined to determine their photosynthetic mechanism exhibit a C_3-type pattern, where the initial and primary carboxylating enzyme is Rubisco (11, 71, 77, 123). Studies with $^{14}CO_2$ have shown that the radioactivity first appears in 3-PGA, the first product of Rubisco carboxylation. Only later, during the chase time, does the ^{14}C appear in the C_4 organic acids malate and aspartate, thereby indicating that these compounds are produced later in the metabolic sequence rather than being early products that are rapidly turned over, losing the ^{14}C to other molecules (123).

The green macrophyte *Prasiola stipitata*, which grows in the very high splash zone, has a low CO_2 compensation point and the photosynthetic rate is saturated at the seawater concentration of inorganic carbon (118). External HCO_3^- is used for photosynthesis and no CAM-like features occur (118).

One green macrophyte studied extensively is *Ulva*. Some species of this ubiquitous alga move HCO_3^- across the plasma membrane into the cytoplasm, which saturates photosynthesis at the inorganic carbon (C_i) concentration found in natural seawater (10). Despite a low CO_2 compensation point and O_2-insensitive photosynthesis, *Ulva* is biochemically a C_3 plant. Activity of PEPC is detectable, but the level is just one-tenth that of Rubisco. The data from radioactive labeling studies corroborate this finding; the first compound labeled with ^{14}C is 3-PGA, and the radioactivity subsequently appears in sugars (11). Thus, it is suggested that a carbon concentrating mechanism based on HCO_3^- uptake is responsible for these features (11).

During photosynthesis, the entire surface of *U. fasciata* reaches pH 10; no zones of acidification such as occur in the green alga *Chara* were detected (12). For *U. lactuca*, no carbonic anhydrase activity could be measured external to the cytoplasm (12, 47). When the CA is inhibited by acetazolamide (AZ), CO_2 from the unstirred layer cannot support the observed photosynthetic rate; thus, it is concluded that HCO_3^- uptake occurs, although CO_2 use at times cannot be excluded (12).

Therefore, HCO_3^- is the preferred species transported in *U. lactuca* (13). The mechanism for this movement could be HCO_3^-/H^+ antiport or HCO_3^-/OH^- symport (12, 47). It is hypothesized that HCO_3^- is transported across the plasma membrane and then converted intracellularly to CO_2 which moves to the chloroplast and can then be used by Rubisco for catalysis. Whether the HCO_3^- translocation occurs via facilitated diffusion as occurs in red blood cell membranes or by active transport remains to be determined (47). In *U. fasciata*, the

internal carbon concentration can reach 2.3-6.0 mM with the bulk concentration of the surrounding medium at 0.02-1.5 mM, which indicates that active C_i accumulation occurs (13). With a cytoplasmic pH of 7.2 and high internal CA activity, the internal CO_2 concentration could be high enough to suppress photorespiration and saturate carboxylation, even though this Rubiso has $K_m(CO_2)$ of 70 μM (13).

A slightly different mechanism for C_i uptake may occur in *U. rigida*. This alga has both an external and internal CA (15). HCO_3^- is converted to CO_2 outside the cells, and CO_2 passes through the plasma membrane. Support for this mechanism comes from studies with dextran-bound AZ (DBAZ), which inhibits only external CA. In the presence of DBAZ, photosynthesis is inhibited at pH 8.6 when HCO_3^- is virtually the only inorganic carbon source, but no inhibition occurs at pH 6.5, where ample CO_2 is present (15). However, active HCO_3^- transport cannot be excluded based on these data (15). In addition, the external alkalinization of the thallus is inhibited in the presence of DBAZ. Ethoxyzolamide (EZ) also inhibits photosynthesis, at both pH 6.5 and pH 8.6; however, adding CO_2 to the medium at pH 8.6 overcomes the inhibition (15). The internal CA plays an important role in the C_i utilization mechanism in this alga.

Photosynthesis in *Codium decorticatum* appears C_3-like with O_2-sensitive photosynthesis and minimal PEPC and PEPCK activities (123). The high CO_2 compensation point is also sensitive to O_2. The DIC in natural seawater does not saturate photosynthesis, but saturation occurs at 5 mM DIC (123, 124). Both the cytoplasm and isolated chloroplasts have CA activity, and some of the chloroplast activity is associated with the membranes (123). There is also a report of extra-cellular CA activity in *Codium* (40). In addition, higher photosynthetic rates can be obtained with the addition of HCO_3^- to the photosynthetic medium, which indicates that the alga is able to use HCO_3^- (124), as is also reported for *C. fragile* (119).

The green microalga *Stichococcus bacillaris* has high CA activity and a high affininty for CO_2. In a medium of pH 5.0, the cells can concentrate internal CO_2 to a level 20 times greater than that in the bathing medium, and this concentrating does not occur at pH 8.3 (102). Therefore, *Stichococcus* is a CO_2-user, and it is suggested that this concentration is accomplished via an active CO_2 transport mechanism (102).

A green macroalga with photosynthetic metabolism that stands in stark contrast to other green algae investigated is *Udotea flabellum*. However, *U. flabellum* exhibits O_2-insensitive photosynthesis and a low CO_2 compensation point, both of which suggest a low level of photorespiration (123), similar to a number of the green algae. A comparison of photosynthetic rates measured at pH 5.0 and 8.0 indicates that the rate is higher at the higher pH, which suggests that the alga is able to use HCO_3^- for photosynthesis (123). At pH 5.0, EZ has a limited effect on photosynthesis, but at pH 8.0, the rate decreases 39%, which shows that CA activity has a role in *Udotea* photosynthesis (123).

Examining photosynthesis in this alga with $H^{14}CO_3^-$ and with and without 3-mercaptopicolinic acid (MPA), an inhibitor of PEPCK, indicates that decreased label is found in the photorespiratory products when PEPCK is operating and that the C_4 organic acids malate and aspartate are early products that rapidly lose their radioactivity (123). Such a mechanism is reminiscent of the metabolism of the terrestrial C_4 species. However, in those plants, the initial carboxylation reaction is catalyzed by PEPC, and the activity of this enzyme in *U. flabellum* was barely detectable (123). PEPCK has substantial activity, though, such that it rivals Rubisco activity (123). Inhibiting the PEPCK activity with MPA causes an increase in the photorespiratory intermediates along with a decrease in the radioactivity found in malate and aspartate (123).

Carbonic anhydrase activity in this alga may be related to HCO_3^- use, but it is not a component of the mechanism to overcome the O_2 inhibition of photosynthesis. Rather, it appears that PEPCK activity may be the key to reduce photorespiration. In contrast to other algae, it is doubtful that the β-carboxylation catalyzed by PEPCK functions for anapleurosis. Instead, the C_4-like metabolism depends on active PEPCK because inhibiting the activity with MPA decreases the photosynthetic rate by 70%, increases the Warburg effect, reduces the C_4 acid label by 66%, and increases label in the PCO cycle intermediates by 3-fold (122, 123). These effects of MPA on photosynthesis cannot be explained by an HCO_3^- utilization mechanism in *U. flabellum*, nor is it likely that the effects of MPA place PEPCK in the role of simply refixing photorespired CO_2; the effects are too large for this to be the case (122). Also, in the absence of DIC, exogenously-supplied malate is able to stimulate photosynthesis, but if MPA is present, no such stimulation occurs (122).

Because Kranz anatomy associated with terrestrial C_4 species is not present in *Udotea*, a C_4-type mechanism would have to involve an organellar separation of events (122). This type of separation has been reported for the freshwater angiosperm *Hydrilla verticillata*, which also lacks Kranz anatomy (25, 27). A parallel function between PEPCK of *Udotea* and PEPC of terrestrial C_4 species is suggested; the activities of other enzymes typically associated with C_4 metabolism are present in *Udotea* at high enough levels that it is reasonable to assume that C_4 photosynthetic biochemistry could occur (122, 123). Thus, for *Udotea*, the evidence appears quite convincing that a type of C_4 biochemistry occurs which is dependent on PEPCK activity. However, this mechanism has not been reported for any other marine macroalgae.

Phaeophyta

The photosynthetic characteristics of the brown algae investigated display a mixture of features. For example, *Turbinaria turbinata* and *Lobophora variegata* exhibit a Warburg effect on photosynthesis at 0.5

and 2.5 mM DIC, respectively (71). Although *Turbinaria* has a detectable malate pool, it does not appear to function in a CAM-like mechanism (71). Another brown, *Dilophus guineensis*, has high PEPC and PEPCK acitivities, but Rubisco is the major carboxylating enzyme (71). Of the brown algae surveyed by Kremer and Küppers (85), the PCR cycle is the only light-dependent carboxylation system, and greater than 90% of the early photosynthetic products are phosphorylated compounds, with 3-PGA being predominant, thereby lending support to the assertion that these plants operate C_3 photosynthesis (85). They suggest that when PEPCK activity is high, the enzyme functions for light-independent carbon fixation. In addition, no PEPC activity is reported for the species they examined (85).

However, in contrast to *Turbinaria* and *Lobophora*, the eulittoral brown algae appear C_4-like in their photosynthetic features: low CO_2 compensation points, and O_2-insensitive photosynthesis (79, 141), which suggests that an inorganic carbon concentrating mechanism is present in these algae. In addition, photosynthesis is saturated with inorganic carbon at the concentration of 2 mM found in natural seawater (141), so these algae are able to photosynthesize faster than would be expected based on the dehydration rate of HCO_3^- alone (79).

Some Fucaceae, of which *Ascophyllum nodosum* is a member, for example, have C_4-like physiology but C_3-like biochemistry. They demonstrate an active membrane transport of CO_2 and/or HCO_3^- , although the location of the transporter, whether at the plasma membrane or chloroplast membrane, remains to be determined (78, 141). *A. nodosum* has a H^+ buffering system that is independent of the ion exchange in the cell wall (5). This alga also has a photosynthetic buffering capacity connected to the H^+ buffer, which is an adaptation to the alga's growing in the intertidal region. These buffering systems enable the plant to produce O_2 in excess of the inorganic carbon taken up for photoreduction (5). *A. nodosum* has high PEPCK activity, which may be involved in

producing the pool of CO_2-exchanging organic acids that function as the photoreductant buffer (5) as a complement to or an integrated part of a CAM-like system (6). The benefit of these two buffering systems to the alga is that they allow some photosynthetic electron transport to be maintained, even when exogenous carbon is in short supply. These systems could afford protection against photoinhibition (5).

When CA is inhibited in *A. nodosum*, the CO_2 compensation point increases 25-fold and the apparent $K_{0.5}(CO_2)$ for photosynthesis increases 8-fold, resulting in a shift of photosynthetic gas exchange characteristics from C_4-like to C_3-like (77). The rate of photosynthesis equals the rate of CO_2 production and diffusion from the bulk phase when external CA is inhibited. Therefore, it appears likely that CO_2 is the species assimilated, and the C_4 physiological characteristics depend in part on the operation of an external CA (77).

Two other species hypothesized to have an active HCO_3^- uptake mechanism are *Fucus distichus* and *Pelvetiopsis limitata*, which have no external CA, but have photosynthetic rates that exceed the photosynthetic rate possible based on spontaneous HCO_3^- dehydration alone (42). Some algae of the Laminariales, including *Laminaria digitata*, *L. hyperborea*, *L. saccharina* and *Alaria esculenta*, and some others of the Fucales, such as *Halidrys siliquosa*, have some C_4-like gas exchange characteristics, but the CO_2 compensation points are higher than found in the Fucaceae, yet all have measurable external CA activity (141). These species appear to be less avid "HCO_3^- users," but what features they do exhibit are probably due to active inorganic carbon influx as part of a concentrating mechanism (141).

Both *Fucus* and *Laminaria* exhibit light-dependent external alkalinization of the surrounding medium, and this process is inhibited by adding DCMU, a light reaction inhibitor that blocks electron flow between quinone and the B protein, to the systems at pH 8.0 but not at pH 6.0 (64). Species of both genera have an external CA, as AZ inhibits

the alkalinization at pH 8.0 (64). The proposed mechanism for C_i uptake is that an external CA converts HCO_3^- from the surrounding medium to CO_2 which then moves into the cells for photosynthesis. It is not known whether CO_2 movement occurs by diffusion only or whether an active uptake process is involved (64). The site of CO_2 transport has yet to be determined; it may be at the plasma membrane and/or the chloroplast envelope. Carbon dioxide is pumped from the external medium into the cytosol by using energy from photosynthetic electron flow rather than from mitochondrial respiration (140).

Another study of *Laminaria digitata* and several other species of brown algae that are C_i-limited in natural seawater showed that when photosynthesis is saturated by red light, a blue light pulse stimulates the photosynthetic rate (55). The effect is hypothesized to involve an increase in the CO_2 supply to the plant; whether this is an effect on the external CA or H^+ efflux pump in the plasma membrane or on the carbon-fixing enzymes in the chloroplast remains to be determined (55).

Photosynthesis in *Dictyota dichotoma*, *Padina vickersiae*, *Sargassum filipendula*, and *Fucus vesicuolus* can use HCO_3^-, at least at pH 9.4 and 2 mM DIC (119). Of the four taxa, *F. vesicuolus* is able to take up HCO_3^- effectively and is carbon saturated at ambient concentration of DIC, similar to *A. nodosum* (77). Members of the Phaeophyceae are noted for exhibiting high PEPCK activity, but these organisms biochemically exhibit C_3-like photosynthesis with 3-PGA appearing as the first product (85). Subsequent studies using ^{14}C show a large amount of the radioactive carbon is located in malate, and then the malate is rapidly metabolized to mannitol (85). In *F. vesicuolus*, a substantial portion of ^{14}C appears in malate and aspartate, thus suggesting active β-carboxylation. However, rapid turnover of these organic acids does not occur, indicating that these compounds are really metabolic end-products (85). In addition, Rubisco from *A. nodosum* has a carboxylase/oxygenase activity ratio of about six, which is similar to

that found in higher plants with C_3 photosynthesis (77). For a long time, the PEPCK enzyme has been said to function in light-independent carbon fixation. However, in *A. nodosum*, dark fixation of carbon does not exceed 5% of the light fixation rate, and usually the dark fixation rate is much lower (77). Thus, the role of PEPCK in this group remains unclear, but it is suggested that DIC accumulation accounts for the observed gas exchange features that make some algae in this group appear C_4-like in their metabolism (77). It is currently believed that a biochemically based C_4-like photosynthetic metabolism is not widespread among the algae (77).

Rhodophyta

An investigation of photosynthesis in the red algae indicates that more than 90% of the early photosynthetic products are phosphorylated compounds, with 3-PGA constituting the largest proportion (85). These data support Rubisco as the major carboxylating enzyme, suggesting that the red alga incorporate inorganic carbon by the C_3 mechanism (85).

In *Laurencia papillosa*, photosynthesis is inhibited by O_2 at 0.5 mM DIC (71). However, the algal extract has high PEPC and PEPCK activities. Malate pools can be detected with levels greater at night than during the day, but the fluctuation is not large enough to imply the operation of a CAM mechanism (71). Thus, this alga probably operates a C_3-type photosynthetic mechanism.

Photosynthesis in *Chondrus crispus* whole thalli, thalli pieces, and protoplasts has been examined (136, 137, 138), and all the data are in agreement. The photosynthetic rate saturates at 3-4 mM DIC, and inorganic carbon does not accumulate internally, according to measurements using the silicone oil centrifugation technique (137, 138). This alga has an external CA that functions to dehydrate HCO_3^- to CO_2, and the CO_2 then passes across the plasma membrane (137, 138). Carbonic anhydrase activity is important for the function of this mechanism, as the initial carbon fixation rate decreases when CA is inhibited (137).

The CO_2 translocation appears to be passive, since inhibitor studies do not suggest the presence of the band 3 anion transporter, a Na^+/K^+ transporter, or any involvement of Na^+ in a transport mechanism (138). Therefore, internal accumulation of inorganic carbon cannot occur, as metabolic energy would have to be expended to do so. This alga can use HCO_3^- in seawater via an indirect mechanism where a conversion to CO_2 by CA occurs first, and then CO_2 moves into the algal cells. Intracellular CA also plays an important role in this carbon utilization mechanism (138).

Another red macroagla, *Gracilaria conferta*, exhibits O_2-insensitive photosynthetic rates and a low CO_2 compensation point under ambient DIC conditions (73). Rubisco is the major carboxylating enzyme, although PEPC and PEPCK activities are measurable. Inorganic carbon fixation occurs via the PCR cycle and supporting evidence for photosynthetic C_4 acid metabolism is lacking (73). Photosynthesis saturates at close to ambient DIC conditions and HCO_3^- is believed to be the main source of inorganic carbon. However, it is not known whether active uptake of HCO_3^- occurs or if dehydration to CO_2 occurs prior to uptake (73).

In *Gracilaria tenuistipitata*, an indirect HCO_3^- utilization mechanism based on dehydration of HCO_3^- to CO_2 by an external CA has been proposed (63), similar to the mechanism hypothesized for *Chondrus crispus*. Carbonic anhydrase activity has been measured extracellularly and intracellularly, including an association with the chloroplast membranes (63). During photosynthesis, alkalinization of the surrounding medium depends on the C_i concentration and is inhibited by an inhibitor of external CA (63). However, the photosynthetic rate for thalli and protoplasts is higher at pH 6.5 as compared to pH 8.6, which indicates that CO_2 is the preferred C_i species. At alkaline pH, the photosynthetic rate exceeds that which could be attained based on spontaneous HCO_3^- dehydration alone, and when the external CA is

inhibited, the photosynthetic rate drops to that which would be expected based on the spontaneous dehydration of HCO_3^- to CO_2 (63).

In the presence of HCO_3^-, *Porphyridium purpureum* has an intracellular pH of 7.3, but when the cells are carbon starved, the pH falls to 6.0. Ethoxyzolamide blocks HCO_3^--dependent alkalinization of the cytosol, so it is believed that CA and HCO_3^- are important for cytosolic pH regulation (102). As is true for any enzyme, the activity of CA is pH-dependent, so a synergistic interaction may occur between CO_2 uptake and HCO_3^- transport (102). Li^+ also inhibits HCO_3^--dependent photosynthesis in *Porphyridium*.

Bacillariophyta

An investigation of photosynthesis in the diatom *Phaeodactylum tricornutum* indicates that a HCO_3^- transporter is present that depends on Na^+ for its operation, as Li^+ inhibits the HCO_3^--dependent photosynthetic O_2 evolution (46, 102). It is hypothesized that the Na^+/HCO_3^- symport in air-grown and 5% CO_2-grown cells at the plasma membrane is driven by Na^+/H^+ antiport (46). Carbonic anhydrase plays an important role in converting the HCO_3^- transported into the cells into CO_2 for use by Rubisco (46, 102). Inhibition of CA by AZ at pH 8.0 increases the apparent $K_{0.5}(CO_2)$ 2.5-fold, but inhibition by EZ increases the $K_{0.5}(CO_2)$ 10-fold (46).

Summary

The marine algae display a range of photosynthetic characteristics. Some have very C_3-like gas exchange features in having photosynthesis that is inhibited by O_2, high CO_2 compensation points, and photorespiration. Others display C_4-like gas exchange characteristics, where the photosynthetic rate is not inhibited by O_2, the CO_2 compensation points are low, and photorespiration is low. Despite these features, in all algae examined thus far, the primary carboxylating enzyme is Rubisco, which points to the operation of a C_3-like photosynthetic mechanism. The C_4-like gas exchange features are

accounted for by inorganic carbon concentrating mechanisms that involve either HCO_3^- uptake or a CO_2 pump. The net result is to diminish oxygenation by Rubisco, which results in the appearance of C_4-like photosynthesis. However, *Udotea flabellum* is unique in that substantial evidence exists that supports the operation of C_4-like biochemistry based on the high activity of PEPCK found in this alga, and this biochemistry may account for the C_4-like gas exchange characteristics of this alga.

Phosphoenolpyruvate Carboxykinase

Phosphoenolpyruvate carboxykinase was discovered in chicken liver in 1953 by Utter and Kurakaski and later found to be present in all forms of liver and kidney tissue, as well as mammary, muscle, and adipose tissue (152). Utter also worked with pyruvate carboxylase, and between these two enzymes, the mechanistic basis for the entry of carbon into gluconeogenesis was established (69), as these enzymes function to bypass the step in glycolysis catalyzed by pyruvate kinase (69). In addition, this enzyme is present in a variety of other organisms: plants, algae, bacteria, fungi, yeasts, flatworms, roundworms, insects, and molluscs (152).

In most organisms, PEPCK catalyzes the synthesis of PEP from OAA as part of a pathway to synthesize carbohydrates according to the following reaction: OAA + ATP <===> PEP + CO_2 + ADP + P_i with Mn^{2+} as a cofactor (E.C. 4.1.1.49). Depending on the organism, other nucleotides that participate in the reaction include GTP (E.C. 4.1.1.32) or ITP. The reaction is readily reversible, but in general, the decarboxylation reaction is two to eight times faster than the carboxylation reaction (152). An exchange reaction between OAA and CO_2 is also catalyzed by PEPCK and proceeds about 30 times more rapidly than the carboxylation reaction (152). The Mn^{2+} ions have two roles in catalysis: the ion binds directly to the enzyme in a one to one ratio and facilitates the

binding of PEP (152); it also forms a complex with the nucleotide species, and the complex is the catalytically active form (31, 33, 116).

Algae

The green macroalga *Udotea flabellum* has PEPCK carboxylation activity that equals the Rubisco activity (123). In this alga, PEPCK functions in the operation of a C_4-like photosynthetic system that reduces photorespiration. Malate and aspartate appear as early photosynthetic products that turn over within one minute, and low amounts of radioactive label are present in photorespiratory compounds (123). This PEPCK enzyme is inhibited by incubation with MPA, and as a result, less malate and aspartate are produced as early photosynthetic products, and more photorespiratory intermediates are detected (122). Thus, the C_4-like photosynthetic system and decreased photorespiration are linked to PEPCK activity hypothesized to be located in the cytosol (122).

The brown alga *Laminaria hyperborea* has PEPCK that uses ATP/ADP in catalysis. The enzyme functions for carboxylation in an anapleurotic role for replenishing the Krebs cycle to enhance growth in young fronds before light intensities are high enough for net photosynthesis to occur (159). The enzyme in *Ascophyllum nodosum* has a molecular weight of 60 kD and a pH optimum for carboxylation of 7.9 (84). In this species, PEPCK catalyzes light-independent carbon fixation with CO_2 as the substrate (78).

The unicellular alga *Euglena gracilis* has high PEPCK activity when grown autotrophically with CO_2 in the light. Higher activity is present when an additional carbon source, such as glucose, is supplied to the cells and no PEPCK activity is detectable in cells grown in CO_2 in the dark (117). However, the highest activity occurs when the cells are grown in the dark with both CO_2 and glucose. When *Euglena* is grown heterotrophically with lactate as the carbon source, PEPCK in the cytosol functions in gluconeogenesis to provide glucose for the cells

(117). PEPCK in this *Euglena* strain is suited to anaerobic CO_2 fixation and is suggested to be the key enzyme for the methylmalonyl CoA pathway for odd-numbered fatty acids and alcohols, where propionyl CoA is incorporated into wax monoesters in fermenting *Euglena* (117). The enzyme is activated by a combination of Mn^{2+} and Mg^{2+}, unlike other PEPCK enzymes. This PEPCK uses GTP/GDP for catalysis, and free sulfhydryl groups of the enzyme are essential for activity (117).

The marine diatom *Skeletonema costatum* has PEPCK that uses ADP that functions in β-carboxylation which is superimposed on the C_3 photosynthetic pathway (104). Turnover of C_4 acids does not occur and the Rubisco activity is always greater than that of PEPCK. Two pools of PEPCK may exist in this diatom: one pool is always activated, allowing for carboxylation in the light, while the second pool is inactivated in the light but activated in the dark. For this dark carboxylation, a substrate synthesized in the light, perhaps a polyol, is used as a source for PEP, thereby involving polyols in the primary metabolism of diatoms (104).

The diatom *Phaeodactylum tricornutum* has high PEPCK activity which has an absolute requirement for ADP and Mn^{2+} (72). The enzyme has a molecular weight of about 70 kD as determined by gel filtration and a pH optimum for carboxylation of 6.2 (72). This enzyme catalyzes carboxylation *in vivo* and uses HCO_3^- as the inorganic carbon source. The carboxylation reaction may provide an additional source of ATP for the cells (72).

Higher Plants

In terrestrial plants, one subgroup of those with C_4 photosynthesis has high PEPCK activity located in the bundle sheath cells, where the enzyme functions in the cytosol as a decarboxylase (156). In this subgroup, the PEPCK activity is 40 to 50 times greater than that in the other C_4 subgroups or the C_3 species (67).

Three well-studied species with this metabolism include *Chloris guyana*, *Urochloa panicoides*, and *Panicum maximum* (33). The PEPCK is a hexamer of 64 kD subunits with a total molecular weight of 380 kD and is active as a decarboxylase in the pH range from 7.4 to 8.2 (33). At pH 8.0, decarboxylation proceeds ten times faster than carboxylation in *C. guyana* (67). Although ATP/ADP is used in catalysis, the enzyme has a wide nucleotide specificity (33). The inorganic carbon species used as a substrate for the *U. panicoides* enzyme is CO_2 (74). Decarboxylation activity of this PEPCK is inhibited by 3-PGA, fructose-6-P (F6P), fructose-1,6-bisphosphate (F-1,6-BP) and excess ATP but stimulated by Cl^- (33). Decarboxylation is also inhibited 40% by 0.5 mM CO_2 (74). Actually, CO_2 and HCO_3^- inhibit PEPCK decarboxylation activity to nearly the same extent; this inhibition may be involved in dark regulation of the enzyme (74).

PEPCK activity in *Chloris guyana* has no pyruvate kinase activity associated with it (67). In contrast to PEPCK from chicken liver, this enzyme does not require the presence of a thiol-reducing compound for maximal activity. However, as for all other PEPCK enzymes, Mn^{2+} is essential for activity, and this ion cannot be replaced by any other divalent metal cation (33, 67, 151). The Mn^{2+} binds to the enzyme at its own site, and it also binds with the ATP as $MnATP^{2-}$, as this species is the actual substrate for the enzyme (33). In the presence of Mn^{2+}, Mg^{2+} inhibits the reaction (33).

In *Spartina anglica*, the levels of pyruvate, alanine, and 3-PGA cannot account for all the PEP produced by PEPCK in the C_4 cycle (134). Either PEP moves directly from the bundle sheath cells to the mesophyll cells or more than one pathway of PEP metabolism is involved in this C_4 cycle (134).

The reaction mechanism for PEPCK carboxylation in *Panicum maximum* is fully ordered with ADP binding to the enzyme first, followed by PEP and then CO_2. The OAA is released prior to ATP (2). However, the

enzyme from *C. guyana* has a fully random kinetic mechanism where CO_2, ADP, and PEP can bind in any order (2). Because CO_2 can bind before the other substrates, the enzyme must have a CO_2 binding site.

In the C_4 species *Urochloa panicoides*, two decarboxylation systems are present in the bundle sheath cells. NAD malic enzyme decarboxylates malate in the mitochondria while PEPCK decarboxylates OAA in the cytosol (34, 66). Studies with radioisotopes indicate that PEP comes from aspartate via OAA while pyruvate comes from malate; 2-oxoglutarate is required in this system, presumably for OAA formation (34). The major source of ATP for PEPCK activity is phosphorylation in the mitochondria rather than photophosphorylation in the chloroplasts. For this system to work, malate has to be oxidized by NAD malic enzyme at one-third the rate that PEPCK operates to produce one NADH per three ATP utilized (34). In the bundle sheath cells, mitochondrial electron transport contributes little to NADH oxidation; rather, NADH is oxidized primarily by reducing OAA to malate (66). In these mitochondria, Krebs cycle activity is not enhanced.

There is PEPCK in plants other than grasses. In apple, for example, PEPCK activity peaks at the pre-climacteric stage and shortly after the fall of the petals; its role is to metabolize organic acids (17). In other species with C_3 photosynthesis, such as orange, lemon, avocado, and grape, PEPCK functions in the fruits to fix CO_2 in the dark (17).

The carboxylation and decarboxylation reactions of *Panicum* PEPCK are inhibited completely by 100 μM MPA while the exchange reaction is inhibited to a lesser extent (120). The inhibitor MPA at 100 μM concentration did not affect the activity of Rubisco or NAD-malate dehydrogenase (MDH), and NAD and NADP malic enzyme are only partially inhibited (120). The activity of PEPC is stimulated 70% by 1 mM MPA (120). Thus, in *Panicum*, MPA substantially inhibits only PEPCK. However, in *Spartina*, MPA is not a specific inhibitor of PEPCK because

HCO_3^--dependent O_2 evolution by bundle sheath strands was inhibited at pH 6.0, but not at pH 8.0 by MPA (134).

Fungi

Yeast

In yeast, *Saccharomyces cerevisiae*, PEPCK is a tetramer (152) with one binding site per subunit (50) that utilizes the ATP/ADP nucleotides for reaction. The optimum pH for enzyme stability and catalysis is 6.5 (147). The molecular weight per subunit is about 64 kD with a holoenzyme molecular weight of approximately 261 kD (147). The enzyme functions in gluconeogenesis, but if a glucose source is available to the yeast, catabolite repression occurs, where PEPCK is degraded more rapidly in the presence of the glucose because the enzyme is not needed to make more glucose (106, 160). This catabolite repression is in contrast to *Euglena*, where PEPCK is synthesized in the presence of glucose (117).

Gluconeogenesis must occur in a respiring yeast cell, as the cytochrome system and protein synthesis in mitochondria are necessary for the pathway to function (160). The catalytic sites on the enzyme contain active thiols, and each subunit has 10 cysteines that must be in the reduced form for the enzyme to be active (36). There is a Mn^{2+} binding site in addition to the site where ATP/ADP-Mn^{2+} binds. When ATP/ADP-Mn^{2+} is bound to the active site, it affords protection against inactivation of the essential arginine residues of the site (36, 95).

Anaerobe of rumens

An anaerobic fungus of rumens, *Neocallimastix frontalis*, has a PEPCK enzyme that is 608 amino acids long (125). The catalytic regions, with the sulfide binding site and and nucleotide binding domain, are highly conserved among fungal organisms and animals; however, the amino acid sequence of the yeast enzyme bears no similarity to the sequence of the rat, chicken, or fruit fly (125). Thus, although the enzymes may catalyze similar reactions, the proteins themselves have various

structures. It should be noted that the yeast enzyme utilizes ATP/ADP while the other enzymes mentioned above use GTP/GDP.

Bacteria

In *Veillonella parvula*, an anaerobic bacterium of the human oral cavity, PEPCK functions in gluconeogenesis as a roundabout way of synthesizing PEP during lactate metabolism (38). The photosynthetic bacterium, *Rhodospirillum rubrum*, has PEPCK that operates as a carboxylase with CO_2 as substrate (44). *Bacteroides fragilis*, a bacterium of the gut, has PEPCK that acts when low CO_2 concentrations are present. It refixes the CO_2 released from the decarboxylation of succinate to propionate to allow more ATP to be synthesized during glucose catabolism (37).

Protozoa

In *Trypanosoma cruzi*, the organism that causes sleeping sickness in humans, the PEPCK is located in membrane-bound glycosomes. The enzyme has a molecular weight of 84 kD and is composed of two subunits containing cysteine residues that are important for catalytic activity (150). The primary function of the enzyme is thought to facilitate the reoxidation of NADH from glycolysis by producing OAA that can be reduced to malate, and it also is involved in producing succinate, an end product of glucose metabolism (110). In addition, it functions to facilitate the complete oxidation of the amino acid skeletons that enter the Krebs cycle and operates in biosynthesis, functioning as a decarboxylase (150). Unlike PEPCK in yeast, this enzyme is not subject to repression by glucose (150).

In *Leishmania mexicana*, a blood fluke, PEPCK is also located in glycosomes, which are unique to the trypanosomatids (105). This enzyme catalyzes CO_2 fixation and operates at a key branchpoint in the metabolism of *Leishmania* with PEP. High activity of MDH when PEPCK activity is also high, in the amastigote stage, may work to bring about succinate production in conjunction with fumarate reductase (105).

Platyhelminthes

The filiarial worm *Setaria digitata*, a facultative anaerobe, uses PEPCK to fix CO_2 and ferment lactate (8). This enzyme utilizes ATP/ADP for catalysis. The PEPCK in the liver fluke *Fasciola hepatica* operates for reverse gluconeogenesis at the branchpoint of PEP to control the ratio of fermentation products by competing with pyruvate kinase for PEP (88). Catalysis by PEPCK results in the production of acetate and propionate, while pyruvate kinase activity leads to lactate production (88). Thus, the PEPCK functions as a carboxylase in an anaerobic environment using IDP (88). The enzyme is evenly distributed between the cytosol and the mitochondria, has an optimum pH range of 5.7 to 6.7, and has an absolute requirement for Mn^{2+} for catalysis. The activity of this PEPCK appears to be modulated only by the reaction substrate and product concentrations, and MPA is a potent inhibitor of catalysis (88). After OAA is produced by PEPCK, it is rapidly converted to malate by an active malate dehydrogenase, and the malate moves to the mitochondria (88).

Nematodes

In the helminth *Ascaris suum*, PEPCK functions as a glycolytic CO_2-fixing enzyme and is the point at which the metabolisms of this parasite and its host diverge (116). This enzyme is functional as a monomer with a molecular weight of about 80 kD and utilizes GTP/GDP for catalysis (116). As for other PEPCK proteins, Mn^{2+} binds directly to the enzyme to activate it. The active nucleotide complex can be formed with either Mn^{2+} or Mg^{2+} (116).

In the nematode *Trichinella spiralis*, PEPCK functions as a carboxylase in the fumarate reductase pathway for the production of n-valerate, acetate, and propionate (18). This enzyme uses ITP/IDP with an optimum pH of 6.6, and 98% of the enzyme is located in the cytosol with the other 2% in the mitochondria (18).

Vertebrates

Many of the investigations on PEPCK have been performed with chicken and rat tissue. In animals, PEPCK functions in liver and kidney tissue for gluconeogenesis, and since it catalyzes the first committed step of the pathway, it is also the rate-determining enzyme for the metabolic sequence that produces glucose from OAA (69). In gluconeogenesis, PEPCK and pyruvate carboxylase by-pass the glycolytic step catalyzed by pyruvate kinase. Within the livers and kidneys of humans, cows, sheep, cats, dogs, and guinea pigs, PEPCK is evenly distributed between the cytosol and mitochondria. In rats, mice, and hamsters, a larger proportion of PEPCK activity is found in the cytosol. In the livers of chickens, pigeons, and rabbits, more PEPCK activity is found in the mitochondria, but the distribution in the kidney is fairly even between the mitochondria and the cytosol (69).

Chickens

This PEPCK is a monomer with a molecular weight of 70 kD, composed of 622 amino acids (43). The nucleotide used in the reaction is GTP/GDP (130). In the mitochondrial enzyme from embryo liver, the enzyme is activated by micromolar concentrations of Mn^{2+} in the presence of millimolar concentrations of Mg^{2+} (131). The OAA-CO_2 exchange reaction is activated synergistically by Mn^{2+} and Mg^{2+} (131).

The regulation of PEPCK is different in birds and mammals in that avian livers are unable to synthesize glucose from pyruvate or amino acids (69). However, chickens have a high glucose concentration in the blood, and avian kidney tubules are able to use both pyruvate and lactate. In liver, lactate is the major precursor for glucose synthesis (69). Gluconeogenesis from pyruvate and amino acids requires transfer of reducing equivalents and carbon from the mitochondria to the cytosol. In tissue with a cytoplasmic PEPCK, malate from the mitochondria moves to the cytosol, where it is oxidized by MDH to OAA, thereby producing NADH (69).

In contrast, in tissues that have very low cytosolic PEPCK activity, such as chicken liver, the cytosolic NADH arises from the transformation of lactate to pyruvate in the cytosol. The low level of cytosolic PEPCK activity in chicken liver cells is attributed to post-translational regulation, as considerable levels of PEPCK mRNA are present (157). Thus, the cytosolic enzyme in the kidney in a starvation state uses gluconeogenesis to convert the amino acids resulting from protein degradation into glucose (69). During starvation, the mRNA level for the cytosolic enzyme increases, after which PEPCK is synthesized (157).

The mitochondrial PEPCK functions as a part of the Cori cycle to oxidize lactate to pyruvate (69). The cytosolic and mitochondrial enzymes are synthesized from two different mRNA molecules (43), they exhibit subtle differences in ligand interactions at the active site, the proteins have different molecular weights, and they do not cross-react to antibodies produced from the other form of the enzyme (69). Another difference between the two enzymes is that the cytoplasmic form catalyzes the OAA-CO_2 exchange reaction at a rate 30-100% greater than that catalyzed by the mitochondrial enzyme (130). The mitochondrial enzyme is synthesized in the cytoplasm as a precursor, having a signal peptide that is later excised after its arrival in the mitochondrion (69). In fact, the cytosolic and mitochondrial forms from one species share only 56% homology in their amino acid sequences, while there are many similarities between the cytoplasmic enzyme from species from different classes, such as the chicken and rat (43, 69). Synthesis of the mitochondrial PEPCK is constitutive (43), while synthesis of the cytosolic enzyme increases in response to epinephrine, glucocorticoids, thyroid hormones, and glucagon which acts via cAMP (43, 69). Insulin inhibits cytosolic PEPCK synthesis.

In chicken liver cells, PEPCK is also found in the nucleus (145). The enzyme in this location functions for anapleurosis, in the nuclear

synthesis of N-acetyl-neuraminic acid, and the synthesis of glycosylated high mobility group proteins, which are non-histone proteins associated with the nuclear protein matrix (145).

Rats

In rat liver cytosol, PEPCK functions in gluconeogenesis (149) and is a protein of 621 amino acids with a molecular weight of approximately 70 kD (9, 31). The enzyme utilizes GTP/GDP and is activated by micromolar concentrations of Mn^{2+} (31). The mRNA is about 2600 nucleotides long, and a portion of the gene favors Z-DNA formation (9). The hormone regulation of gluconeogenesis in rats and chickens is similar. Glucagon via cAMP and glucocorticoids stimulate PEPCK activity while insulin inhibits it (9). These hormones exert their effects by altering enzyme synthesis via mRNA amounts and translation (9). In rats that were starved and re-fed, serotonin increases the level of mRNA coding for the cytosolic form of PEPCK in the kidney, liver, and small intestine. The level is higher than found in the same tissues after 24 hours of starvation, and the serotonin stimulates cAMP levels within one minute of treatment (162), thus further affirming that production of PEPCK occurs in response to cAMP levels.

Other Mammals

In camels, PEPCK functions in gluconeogenesis to maintain the high level of blood glucose found in these animals (1). More enzyme occurs in the kidney relative to the liver, but both isozymes have a molecular weight of 80 kD and pH optimum for activity of 7.2.

Rabbit PEPCK in the liver occurs in both the mitochondria and cytosol. The molecular weight of the cytosolic form is 68 kD, while that of the mitochondrial form is 56 kD as determined by gel filtration (58). The cytoplasmic form functions in gluconeogenesis from amino acids, but the function of the mitochondrial enzyme is unclear. It may be involved in remobilizing lactate as a part of the Cori cycle (58).

Differences in molecular weight and function suggest differences in the amino acid sequence between the two forms (58).

In mouse pancreatic islets, the PEPCK uses ITP/IDP for catalysis and is activated by Mn^{2+} (68). Preincubation of the enzyme with $ATPMg^{-}$ inhibits the Mn^{2+}-stimulated activity over time. Two fishes have been examined for their PEPCK activities. In the carp hepatopancreas, one form of PEPCK is present that has a molecular weight of 83 kD as determined by SDS electrophoresis and a pH optimum of 7.7 for decarboxylation and 7.2 for carboxylation (87). The liver of the rainbow trout has isozymes with molecular weights and pH optima similar to the carp enzyme (87). The enzymes function in gluconeogenesis. Of metal ions, Mn^{2+} is the best activator (87).

Summary

The PEPCK enzymes that utilize ADP/ATP for catalysis are generally either tetramers, as in yeast, or hexamers, as in the higher plants. The subunits typically have molecular weights in the 65 kD range. In contrast, the enzymes that use GDP/GTP for catalysis are monomers that have molecular weights in the 70 to 80 kD range. In most organisms where PEPCK is found, the most common location of the enzyme is in the cytosol, and the optimum pH for catalysis ranges from 6.2 to 7.9 among the organisms. For its reactions, PEPCK is Mn^{2+}-specific. The ion binds to a site directly on the enzyme and may also form a nucleotide complex for the reactions. In organisms where PEPCK functions as a carboxylase, CO_2 is the inorganic carbon substrate for the enzyme. In the algae, PEPCK functions as a carboxylase for anapleurosis and synthesis of fatty acids. In the higher plants, the enzyme operates as a decarboxylase in one of the C_4 photosynthetic subgroups. In the vertebrates, PEPCK is a decarboxylase in the gluconeogenic pathway. Thus, this enzyme catalyzes a range of reactions for metabolism, and its activity in both directions is inhibited by MPA.

In *Udotea*, where PEPCK operates presumably in the cytosol, the enzyme is hypothesized to function as an oligomer that uses ADP/ATP for its reactions. The Mn^{2+} ion also appears to be important for the reactions to proceed. This PEPCK activity appears to be crucial for the operation of the C_4-like photosynthetic mechanism, as its inhibition with MPA shifts the photosynthetic metabolism to C_3-like. Thus, *Udotea* PEPCK appears to share some features with PEPCK enzymes from some algae, yeast, and the higher plants. One of the purposes of this investigation was to learn more about the characteristics of PEPCK in *Udotea* to understand better how it plays a role in the C_4-like photosynthetic mechanism of this alga.

CHAPTER 2
INORGANIC CARBON UTILIZATION
IN THE MARINE MACROALGA *UDOTEA*

Introduction

Udotea, a marine siphonaceous macroalga of the Chlorophyta, has been found to exhibit C_4-like photosynthetic characteristics, but the mechanism which produces these features requires more adequate investigation. C_4-like gas exchange properties, such as O_2-insensitive photosynthesis, low CO_2 compensation point, and low photorespiration rate can be attributed to one of two general mechanisms: HCO_3^- utilization or C_4 acid metabolism. It is evident that C_4 acids are an important part of the photosynthetic metabolism of *Udotea*, as high activities of enzymes typically associated with this type of metabolism are found in this alga (123). In addition, during light fixation of $^{14}CO_2$, there is an early appearance of C_4 acids which turn over rapidly, suggesting that these acids are not just metabolic end-products (123). The purpose of this investigation was to determine if *Udotea* also uses HCO_3^- as a part of its photosynthetic carbon assimilation mechanism. Bicarbonate utilization could occur via an indirect mechanism, in which an external CA converts HCO_3^- from the seawater into CO_2 that either diffuses across the plasma membrane as proposed for the red alga *Chondrus crispus* (138) or be actively transported across, as reported for the green microalga *Chlorella* (126). Alternatively, could be used directly in a system where the ion is transported across the plasma membrane on a carrier which may or may not require energy to operate (135).

Since *Udotea* is a calcareous alga, the role of calcification during inorganic carbon asssimilation must also be considered, as

calcification and photosynthesis are closely linked in other calcifying organisms (24).

The results presented in this paper suggest that CO_2 is the primary species of inorganic carbon used in photosynthesis, but some energy-dependent HCO_3^- use also occurs. A possible model for calcification is also considered.

Materials and Methods

Materials

Specimens of the marine macroalga *Udotea conglutinata* (Ellis and Solander) Lamouroux (division Chlorophyta) were collected with intact holdfasts in late fall, spring, and summer at the mouth of the Crystal River in the Gulf of Mexico, Florida, in water ranging from 1.0-1.5 m in depth. After collection, the plants were washed clean of epiphytes and transplanted into 20 L aquaria with mollusc shell fragments on the bottom, filled with filtered, aerated, natural seawater. The aquaria were placed into a growth chamber under a 25°C/12-h photoperiod with a quantum irradiance of 5-10 μmol m^{-2} s^{-1} (400-700 nm) and a 23°C scotoperiod. The seawater was changed every three to four weeks. Algae used for the investigations appeared healthy and had lush green color.

Gas Exchange Experiments

Net photosynthetic rates were determined as O_2 evolution with a Hansatech electrode system at 25°C and 21% and 2% gas phase O_2 (equivalent to 220 and 22 μM O_2, respectively) in synthetic seawater buffered with 10 mM Tris-HCl, pH 7.7, 10 mM Tris-HCl, pH 8.2, or 10 mM CHES-NaOH, pH 9.0, containing various amounts of dissolved inorganic carbon, added as $NaHCO_3$. The artificial seawater was prepared according to Drechsler and Beer (47) and contained 450 mM NaCl, 10 mM KCl, 10 mM $CaCl_2$, and 30 mM $MgSO_4$. The salinity of this solution was determined by the HW Harvey method (96). A 10 mL sample of water to which four drops of 0.41 M K_2CrO_4 had been added was titrated with 0.16 M $AgNO_3$ solution until a brick-red color persisted with stirring. The salinity, in parts

per thousand, was equivalent to the volume of $AgNO_3$ solution needed to titrate the 10 mL sample. The quantum irradiance during the photosynthetic measurements was 300 μmol m^{-2} s^{-1} (400-700 nm). The rate of CO_2 production in the photosynthetic medium arising from hydration and dehydration of the various inorganic carbon species present in seawater was calculated according to equation 6 from Johnson (76) using the constants determined for seawater with a salinity of 34 parts per thousand at a temperature of 25°C.

The calculation for the hydration rate of CO_2 in seawater is presented according to the method of Johnson (76).

$$\delta(CO_2)/\delta t = -(K_{CO2} + K_{OH} - K_W/a_H)(CO_2) = (k_d a_H + K_{HCO3-})(HCO_3^-)$$

M = mol L^{-1}

For seawater at 25°C and 34 parts per thousand salinity:

$K_{CO2} = 0.0362\ s^{-1}$

$K_{OH} - K_W = 13.4 \times 10^{-11}$ mol L^{-1} s^{-1}

$K_d = 3.52 \times 10^4$ L mol^{-1} s^{-1}

$K_{HCO3-} = 1.17 \times 10^{-4}\ s^{-1}$

$a_H = [H^+]$

At pH 8.2 and 2 mM DIC:

$[H^+] = 6.31 \times 10^{-9}$ M

$[CO_2] = 0.00601(DIC) = 1.20 \times 10^{-5}$ M

$[HCO_3^-] = 0.898(DIC) = 0.001796$ M

Therefore, substituting into the equation:

$$\delta(CO_2)/\delta t = -[0.0362 + (13.4 \times 10^{-11})/6.31 \times 10^{-9}](1.20 \times 10^{-5})$$
$$+ [(3.52 \times 10^4)(6.31 \times 10^{-9}) + 1.17 \times 10^{-4})](0.001796)$$
$$\delta(CO_2)/\delta t = -[0.0362 + 0.0212](1.20 \times 10^{-5}) = (3.39 \times 10^{-4})(0.001796)$$
$$= -(0.0574)(1.20 \times 10^{-5}) + 6.09 \times ^{-7}$$
$$= -(6.89 \times 10^{-7}) + (6.09 \times 10^{-7})$$
$$= -8 \times 10^{-8}\ s^{-1} \times M = -0.08 \times 10^{-6}\ s^{-1} \times M$$
$$= -4.8 \times 10^{-6}\ min^{-1} \times M$$

The effect of $CaCl_2$ on photosynthesis was measured in artificial seawater prepared with and without $CaCl_2$. Sections of thallus, about 15 mm by 15 mm, from the tip of the thalli, were incubated for 15 min in unbuffered, artificial seawater with or without 10 mM $CaCl_2$ at a quantum irradiance of 150 μmol m^{-2} s^{-1} (400-700 nm). The photosynthetic rate measurement in the presence of 2 or 5 mM DIC commenced with adding the alga to the oxygen electrode chamber, which already contained 2 mL artificial seawater buffered with 10 mM Tris-HCl, pH 8.2. Photosynthesis was measured for 15 min. An aliquot of the reaction mixture in the O_2 electrode chamber was removed to measure the initial total inorganic carbon. A 100 μL sample was injected into 3 mL 0.1 N H_3PO_4 bubbled with N_2 in a flask, and the CO_2 released was measured with an infra-red gas analyzer and recorded on an integrator against a known concentration of a $KHCO_3$ standard. Another aliquot of the reaction solution was removed after the photosynthesis measurement to record the total DIC remaining.

The influence of several potential effectors on photosynthesis was examined, including 40 mM KI, 0.24 mM DIDS, and 0.1 mM vanadate. The vanadate solutions were prepared according to three different methods. In the first method, solution A, 5 mM Na_3VO_4 was dissolved in 20 mM NaOH and allowed to stand overnight at room temperature (57). In the second method, solution B, Na_3VO_4 was dissolved in deionized water (20 mL) to produce a 5 mM solution and heated for 3 h at 40°C (109). After cooling, the volume was readjusted to 20 mL with deionized water, and the pH was adjusted to 9.5 with MES powder. The absorbance of a 0.1 mM solution was recorded at 268 nm against a water blank in order to determine the true concentration of the solution. The molar extinction coefficient used was 1.44×10^{-4} as determined by Cantley *et al.* (35). The pH was then adjusted to 7.2 with MES powder and the solution was stored in a glass stoppered flask at room temperature until used. In the third method, solution C, the solution was prepared on the day of

the experiment as 100 mM solution in 20 mL deionized water (142). The pH was adjusted to 9.5 with MES powder, and the solution was boiled until colorless. After cooling, the pH was adjusted to 7.5 with MES powder, followed by a second boiling. After cooling, the volume was adjusted to 20 mL with deionized water and the pH adjusted to 7.5 with MES powder. Potential effectors were added into the standard reaction mixture, consisting of artificial seawater buffered with 10 mM Tris-HCl at pH 8.2, to which $NaHCO_3$ was added to achieve various DIC concentrations.

The O_2 electrode system was also used to determine which species of inorganic carbon was used for photosynthesis. These photosynthetic measurements were performed at 9°C to slow the equilibration between CO_2 and HCO_3^-. The procedure that Cooper *et al.* (44) used to determine the DIC substrate of carboxylation enzymes was modified for use on thalli pieces. The *Udotea* thallus section was placed into a chamber containing 2 mL artificial seawater buffered with 10 mM Tris-HCl at pH 8.2, at a quantum irradiance of 300 μmol m^{-2} s^{-1} (400-700 nm). When a stable line was achieved on the chart recorder, either 5 mM $NaHCO_3$ or 5 mM $NaHCO_3$ acidified with 0.1 N HCl was added to the chamber with a Hamilton syringe. If an acidified solution was used, the acidification was done in the syringe, and the solution was added to the reaction chamber only after bubbles of CO_2 appeared in the syringe. In this manner, a significantly larger proportion of either CO_2 or HCO_3^- was added to the reaction chamber. The photosynthetic rate was followed for a maximum of one minute.

pH Drift Experiments

Udotea thalli without holdfasts were placed into 60 mL glass-stoppered bottles containing unbuffered, artificial seawater to which 2 mM $NaHCO_3$ was added (94). The pH of the starting solution was recorded and a sample was removed to measure the true concentration of total inorganic carbon present at the start of the experiment. The stoppered

bottles were placed into a shaking water bath maintained at 32°C under a quantum irradiance of 200 μmol m^{-2} s^{-1} (400-700 nm) for 6 h. After removal from the water bath, the bottles were allowed to return to room temperature, at which time the final pH of the solution was measured. An aliquot of water was removed to measure the remaining total DIC, and the alkalinity of the water was measured by titrating a 10 mL sample of the water with 0.12l N HCl to pH values of 4.2, 3.9, and 3.7 (94). The quantities of acid added and the exact pH values achieved were used to calculate the alkalinity of the samples. The *Udotea* thalli were removed and the fresh weights recorded. The thalli were then dried in a 70°C oven for at least 24 h and dry weights determined. The HCO_3^- dehydration rate was calculated using equation 6 and the constants from Johnson (76).

Carbonate Salts in the Algal Skeleton

Thalli that had been oven-dried were placed into Petri dishes and treated with 6 N HCl to liberate the carbonates in the plant skeleton. After bubbling ceased, the acid was pipetted off and the remaining thalli allowed to dry. After drying, the weights were measured and compared to the fresh weights and the dry weights prior to acid treatment.

Carbonic Anhydrase Assay

Carbonic anhydrase was assayed according to the method of Drechsler & Beer (47). At 10-12°C, the time for a pH change of two units was recorded for a solution of 5.8 mL artificial seawater, 0.2 mL Tris-HCl, final concentration 10 mM, pH 8.6, to which 4 mL of ice-cold CO_2-saturated water was added. The time required to achieve the same pH change was also noted when 10 units of carbonic anhydrase or a piece of *Udotea* thallus were added. The thallus had been cut the previous day so that wound healing would occur (41) and the enzyme being measured would be located on the thallus, rather than having leaked from the cytosol of the alga.

Thallus Surface pH

Udotea thalli sections cut the night before experimentation were placed into Petri dishes containing 40 mL unbuffered artificial seawater with 2 mM $NaHCO_3$ added. These sections were incubated in the growth chamber for 15 min, under a quantum irradiance of 5 μmol m^{-2} s^{-1}, after which time the thalli were moved to a fresh solution of 2 mM $NaHCO_3$ in artificial seawater. The thalli sections were then exposed to a quantum irradiance of 300 μmol m^{-2} s^{-1} (400-700 nm) while the pH of the thallus surface was recorded with a microelectrode (49). Measurements were made at various points on the thallus, and the change in the pH of the water from the beginning of the thallus measurements until the end was also recorded. Thallus measurements were also made in the presence of 40 mM KI, 0.24 mM DIDS, and 1 mM vanadate, as well as in the dark, and for the water in the absence of thalli.

Chlorophyll Determination

Chlorophyll was determined by the method of Arnon (3). The thallus was ground at 4°C in a mortar and pestle in 2 mL 10 mM Tris-HCl, pH 7.3. A 0.2 mL aliquot of the homogenate was pipetted into 0.8 mL 100% acetone. This solution was incubated on ice, in the dark. After 15 min, 2 mL 80% acetone was added to the solution, which was incubated for another 15 min period on ice in the dark. The solution was then centrifuged at 3600 g for 5 min at room temperature. The absorbances of the clear solution at 645 and 663 nm were determined against a blank of 80% acetone. The equation for the calculation is: [(A663 x 0.00802) + (A645 x 0.0202)] x 5 (dilution factor) x 2 (total mL in grind) = total mg Chl in thallus.

Results

An examination of the structural components of the *Udotea* thallus indicated that the fresh weight of the thallus was about double the dry weight, and nearly 50% of the dry weight was composed of carbonate salts that could be removed by treatment with HCl (Table 2-1).

Table 2-1. Proportion of *Udotea* dry weight composed of carbonates. DW_A refers to the dry weight remaining after acid treatment.

Thallus	Fresh Weight	Dry Weight	FW/DW	Dry Weight After Acid	FW/DW_A	Carbonate Component of Skeleton
	g			g		%
1	0.97	0.44	2.20	0.26	3.73	41
2	1.59	0.75	2.12	0.36	4.42	52
3	1.72	0.73	2.36	0.40	4.30	45
4	1.07	0.49	2.18	0.25	4.28	49
5	1.03	0.50	2.06	0.25	4.12	50
Mean	---	---	2.18± 0.11	---	4.17± 0.27	47± 4

The total amount of O_2 evolved during photosynthesis by *Udotea* at 2 mM DIC in the absence of $CaCl_2$ was similar to that with $CaCl_2$ present, although with 5 mM DIC in the medium, 22% more O_2 was evolved during the same time period when $CaCl_2$ was included in the photosynthetic reaction mixture (Table 2-2). However, a noticeable difference occurred with regard to the net change of the total inorganic carbon in the medium when $CaCl_2$ was omitted from the medium. The presence of the $CaCl_2$ seemed necessary for inorganic carbon to be removed from solution, as in its absence, more DIC was present at the end of the 15 min photosynthetic period than at its beginning. In the presence of $CaCl_2$, the quantity of inorganic carbon removed by the thallus section in 5 mM DIC was 6-fold greater than the amount removed in 2 mM DIC. When $CaCl_2$ was absent, about twice the amount of inorganic carbon was present after photosynthesis in the chamber which started with 2 mM DIC as compared to the chamber with 5 mM DIC.

The species of inorganic carbon used for photosynthesis was investigated (Fig. 2-1). By using a method modified from a study of Cooper *et al.* (44) on isolated enzymes, whole-thallus photosynthesis was carried out at 9°C so as to slow the equilibration of the carbon species added to the reaction medium. The experiment was performed at pH 8.2. When DIC was added as virtually all CO_2, the photosynthetic rate was five-fold higher than when the DIC was added so that 90% of the carbon was present as HCO_3^-. When CA was added along with HCO_3^-, no stimulation of photosynthesis was observed. When CA was added with CO_2, the photosynthetic rate dramatically decreased by five-fold, to the level attained in the presence of HCO_3^- alone.

In a pH drift experiment, where intact *Udotea* thalli were incubated for six hours under a quantum irradiance of 200 μmol m^{-2} s^{-1} (400-700 nm), the final pH attained by the plants was approximately 8.3 (Table 2-3). Of the total DIC present at the conclusion of the experiment, the CO_2 component was 5 μM, while nearly 88% of the

Table 2-2. Effect of 10 mM $CaCl_2$ on *Udotea* photosynthesis at pH 8.2. Time elapsed during photosynthetic measurement was 15 min. Values reported are the mean of 2 measurements ± SD.

DIC Concentration	With $CaCl_2$	Without $CaCl_2$	With $CaCl_2$	Without $CaCl_2$
	Total O_2 evolved		Net Change in total DIC	
mM		mmol g^{-1} FW		
2	0.11 ± 0.03	0.10 ± 0.06	-0.23	2.17
5	0.14 ± 0.01	0.11 ± 0.03	-1.30	1.10

Note: A positive value indicates that more inorganic carbon was present in the chamber after the photosynthesis measurement was made than at the start.

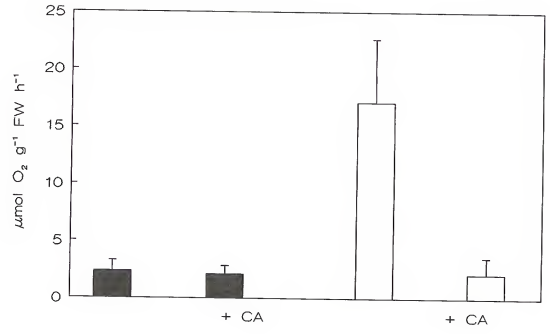

Figure 2-1. Examination of inorganic carbon substrate used by *Udotea* for photosynthesis. DIC was added as mostly HCO_3^- (■) with and without CA by adding $NaHCO_3$ solution to the reaction mixture. Of the 5 mM DIC present, 4.49 mM was HCO_3^- and 0.03 mM was CO_2. DIC was added as CO_2 (□) with and without CA at a concentration of 5 mM by acidifying $NaHCO_3$ solution with HCl in a syringe prior to adding it to the reaction mixture.

Table 2-3. Final pH of three replicates of *Udotea* following a pH drift experiment in 200 μmol quanta m^{-2} s^{-1} for 6 hours at 32°C. Values reported are the mean of 3 replicates ± SD.

Mean Final pH	Total DIC	Final CO_2	Final HCO_3^-	HCO_3^- Dehydration Rate
		μM		μmol min^{-1}
8.26 ± 0.40	1000 ± 464	5 ± 2	877 ± 407	0.29

inorganic carbon was present as HCO_3^-. At this pH, CO_2 was produced from HCO_3^- at the rate of 0.29 μmol min^{-1}. In another pH drift experiment, where the amount of DIC present at the start of the incubation period was only that added as a result of bubbling the artificial seawater with air for 0.5 h, the final pH reached was 8.95 ± 0.42 for 15 samples.

The manner in which pH affects photosynthesis was investigated (Fig. 2-2). For similar CO_2 concentrations, the additional HCO_3^- available at higher pH values was able to increase photosynthesis. At pH 9.0, 0.06% of the total DIC is CO_2 and 59.6% is HCO_3^-, at pH 8.2, 0.6% is CO_2 and 89.8% HCO_3^-, and at pH 7.7, 2.0% is CO_2 and 94.8% HCO_3^-. This higher photosynthetic rate suggested that some HCO_3^- was being employed for photosynthesis in addition to the CO_2, although the preferred species was CO_2 (Fig. 2-1). It can also be seen that even though 30 mM DIC was added at pH 8.2 and 50 mM DIC at pH 9.0, the photosynthetic rate still was not saturated due to the small proportion of inorganic carbon present as CO_2.

The rate of CO_2 production from HCO_3^- was calculated for this system using the equation of Johnston (47) (Table 2-4). If the rate of photosynthesis was greater than the rate of spontaneous CO_2 production from HCO_3^-, then the evidence suggests that the additional photosynthetic rate was supported by HCO_3^- utilization (47). At both 1 and 2 mM DIC, the measured photosynthetic rate for *Udotea* was greater than the rate predicted from spontaneous HCO_3^- dehydration (Table 2-4).

Udotea thalli were investigated to determine whether any external CA activity was present. The time for spontaneous HCO_3^- dehydration was 13 s, and adding 10 units of CA decreased the time by nearly 50% (Table 2-5). However, the presence of the *Udotea* thallus actually slowed the rate to 19 s, thus suggesting that no external CA was present on the thallus.

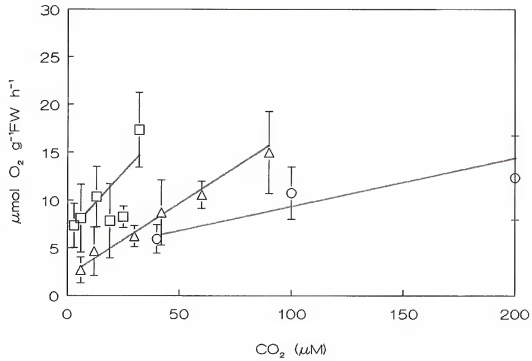

Figure 2-2. Measurement of photosynthesis in reaction mixtures of pH 7.7 (○), 8.2 (△), and 9.0 (□) with varying concentrations of CO_2.

Table 2-4. Comparison of photosynthetic rates for *Udotea* thallus sections measured at pH 8.2 and 300 μmol quanta m^{-2} s^{-1} and the predicted rates dependent upon the spontaneous rate of CO_2 production. The predicted rates were calculated according to Johnson (76). Measured photosynthetic rates are the mean of 4 replicates ± SD.

DIC	O_2	Photosynthetic Rate	
		Measured	Predicted
mM	%	μmol O_2 h^{-1}	
1	21	0.37 ± 0.08	0.29
	2	0.57 ± 0.24	
2	21	0.44 ± 0.10	0.58
	2	0.78 ± 0.07	
5	21	0.80 ± 0.25	1.46
	2	1.18 ± 0.17	

Table 2-5. Measurement of hydration time for CO_2 at 10-12°C, recorded as a pH change of 2 units. Values reported were the mean of four or five replicates ± SD. The net photosynthetic rate at 2 mM DIC for the thalli examined for the presence of external CA was 26.47 ± 5.77 μmol O_2 g^{-1} FW h^{-1}.

Condition	Time for Reaction
	sec
Spontaneous	13 ± 3
With 10 units CA	8 ± 1
With *Udotea* intact thallus	19 ± 2

Udotea photosynthesis was examined in the presence of several potential effectors of HCO_3^- use. In the presence of 40 mM KI, where the I^- may interfere with HCO_3^- uptake, photosynthesis was inhibited 26 to 35%, and the inhibition increased with increasing HCO_3^- concentration (Fig. 2-3). These measurements were made without any pre-incubation of the thallus in KI.

The photosynthetic rate was also inhibited in the presence of 0.24 mM DIDS, (Fig. 2-4), which inhibits transport by the band three anion transporter in red blood cells. The inhibition ranged from 13% at 3.7 mM HCO_3^- to 33% at 0.5 mM HCO_3^-.

Vanadate halts ATP synthesis by interfering with phosphate binding at plasma membrane ATPases (35). Each bar in Fig. 2-5 represents four alga pieces incubated for a period of 2 h in 0.01 mM vanadate solutions prepared by different methods. Several solution preparations were used to determine whether the vanadate ion species present in a particular solution was more effective at inhibiting the ATPase, if it were present. Photosynthesis was inhibited only 3% after 5 min incubation in solution A (Fig. 2-5), but this inhibition increased to 34% inhibition after a 2 h incubation period. Incubation in solution B did not appear to inhibit photosynthesis of *Udotea* thalli. For thalli incubated in solution C, photosynthesis was inhibited 19% after just 5 min, but no further inhibition resulted after prolonged incubation.

Surface pH measurements of *Udotea* thalli exposed to a quatum irradiance of 300 μmol m^{-2} s^{-1} were made on thallus pieces incubated in unbuffered, artificial seawater containing 2 mM DIC at 25 to 30°C. With no additions to the medium, the thallus pH was 0.1-0.2 units lower than the surrounding water (Table 2-6). During the course of the measurements, the water pH dropped 0.1 unit in the light. In the presence of 40 mM KI, the thallus surface was up to 1.4 pH units lower than the surrounding water. Apparently, the presence of the KI stimulated H^+ extrusion; the water pH dropped 0.4 units in the same

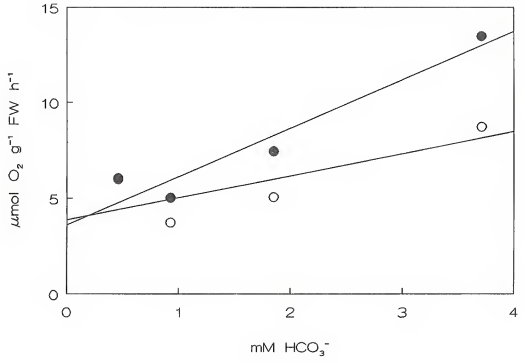

Figure 2-3. Effect of 40 mM KI on photosynthetic rate of *Udotea* thalli at pH 8.0. (●) control, (o) 40 mM KI added.

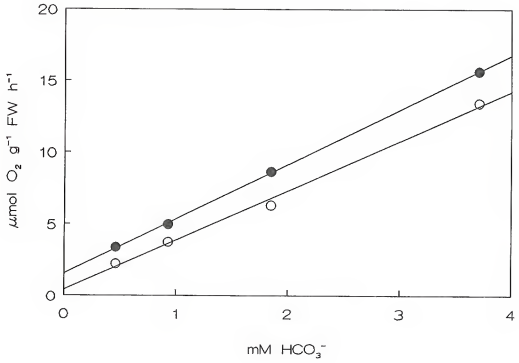

Figure 2-4. Effect of DIDS on photosynthetic rate of *Udotea* thalli at pH 8.0. (●) control, (o) 0.24 mM DIDS added.

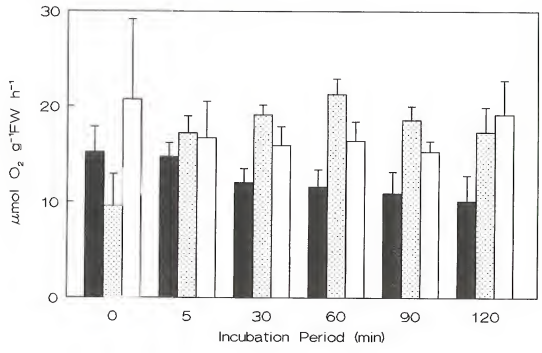

Figure 2-5. Effect of vanadate on photosynthesis of *Udotea* thalli. The vanadate solutions were prepared according to three different methods, as indicated in Materials and Methods. The pH of each reaction mixture with the vanadate solutions A, B, and C added, respectively, was different: 7.93 (■), 7.86 (▒), or 7.98 (□).

Table 2-6. Surface pH measurements of *Udotea* thalli under 300 μmol m^{-2} s^{-1} irradiation (400-700 nm), except as noted, at 25°C. The incubation medium for each was artificial seawater with 2 mM DIC added. The two pH values reported for the water were at the beginning and end of the experiment. Each set of values reported was for eight to ten measurements on one piece of thallus. The tip values were recorded at the natural apical end of the thalli.

Conditions	Water	Thallus Tip	Thallus Center
		pH	
No additions	8.73	8.32 ± 0.06	8.21 ± 0.08
	8.61	8.47 ± 0.06	8.58 ± 0.10
		8.47 ± 0.09	8.55 ± 0.06
+ 40 mM KI	8.59	8.34 ± 0.09	7.18 ± 0.68
	8.22	7.42 ± 0.16	6.99 ± 0.30
+ 0.24 mM DIDS	8.79	8.05 ± 0.83	8.31 ± 0.08
	8.64	8.27 ± 0.13	8.29 ± 0.10
+ 1 mM Vanadate	7.54	7.61 ± 0.14	7.44 ± 0.03
	7.48	7.23 ± 0.12	7.42 ± 0.02
No plant	8.90	---	---
	8.77		
Dark	8.80	8.43 ± 0.09	8.39 ± 0.09
	8.84	8.41 ± 0.19	8.42 ± 0.04
Dark, No plant	8.92	---	---
	8.90		

period. In the presence of 0.24 mM DIDS, the thallus surface was 0.4-0.6 pH units lower than the water, and the water also dropped 0.2 units during the readings. The presence of 1 mM vanadate lowered the water pH; however, the pH of the water did not change during the course of the measurements, and the thallus pH remained similar to that of the water. When no thallus was present in the water in the light, the pH dropped by about 0.1 unit over a 15 min period. In the dark, without a thallus piece, the water pH remained essentially unchanged. When a piece of thallus was incubated and measured in the dark, the pH of the water remained about the same, while the pH of the thallus was 0.4 pH units lower than the surrounding water, thus indicating that the reduced pH of the *Udotea* thallus surface, perhaps caused by H^+ extrusion, was not dependent on light or photosynthesis.

The effect of O_2 on photosynthesis at pH 8.2 was examined for the *Udotea* thalli (Table 2-7). The photosynthetic rate was inhibited 35 to 40% by 21% O_2 as compared to 1% O_2 in the gas phase. However, increasing the DIC had no effect on the degree of O_2 inhibition of photosynthesis, thus suggesting that the O_2 inhibition was not a photorespiratory phenomenon.

Discussion

The photosynthetic studies of *Udotea* thalli indicated that although CO_2 was used more readily for photosynthesis, there appeared to be some capacity for using HCO_3^-. The CO_2 could enter *Udotea* siphons by diffusing across the plasma membrane or it could be transported across, as hypothesized for the marine macroalga *Stichococcus bacillaris* (102), the green microalgae *Chlorella ellipsoidea* (127) and *C. saccharophila* (126), and the cyanobacterium *Synechococcus* sp. (7, 52). The CO_2 pump in the colonial green alga *Scenedesmus obliquus*, grown on high CO_2 and then adapted to air levels of CO_2, is accompanied by plasma membrane CA formation (143). Other species in the Chlorophyta, such as *Ulva lactuca* and *U. fasciata*, appear to take up HCO_3^- directly (6, 94), possibly by a

Table 2-7. Effect of oxygen concentration on photosynthesis in *Udotea* at pH 8.2 and 300 μmol quanta m^{-2} s^{-1}. Values reported are the mean of 4 replicates ± SD.

DIC	CO_2	HCO_3^-	O_2	Photosynthetic Rate	O_2 Inhibition
mM	μM	mM	%	μmol O_2 g^{-1} FW h^{-1}	%
1	9.84	0.93	21	4.85 ± 1.62	---
			2	7.80 ± 4.19	38
2	19.68	1.85	21	6.23 ± 0.55	---
			2	10.43 ± 1.42	40
5	49.20	4.64	21	10.40 ± 2.02	---
			2	16.11 ± 4.22	35

HCO_3^-/OH^- antiport system (12). In the green unicell *Chlamydomonas reinhardtii*, cells adapted to air levels of CO_2 after growth at 5% CO_2 reportedly utilize HCO_3^- in a DIC concentrating mechanism (39, 103). This mechanism also includes an appearance of external CA activity. Thus, CA may function as a component of either CO_2 or HCO_3^- utilization systems.

Carbon dioxide use in *Udotea* would have to be by diffusion or a CO_2 pump that does not require external CA activity, as external CA activity was not measurable on *Udotea* thalli. Bicarbonate use in two of the *Ulva* species is hypothesized to occur by a HCO_3^-/OH^- antiport, but the pH of the *Udotea* thalli did not support the occurrence of OH^- extrusion. External CA activity is also a component of some HCO_3^- utilization mechanisms, but this activity was lacking in *Udotea*. Thus, DIC utilization in this alga probably does not occur via any of these mechanisms.

The experiment modified from Cooper *et al.* (44) of investigating which species of DIC was used for photosynthesis indicated that CO_2 use resulted in the most rapid photosynthetic rate. This experiment was predicated on a lack of external CA on the *Udotea* thallus. The experiment to determine the inorganic carbon substrate for photosynthesis was performed at pH 8.2 at 9°C to slow the equilibration of the various carbon species. The reduced temperature also slowed the photosynthetic rate. When the inorganic carbon was added as largely HCO_3^-, even adding exogenous CA to the system did not result in a rapid enough production of CO_2 to raise the photosynthetic rate above that achieved when HCO_3^- alone was present. Carbonic anhydrase facilitates the rapid establishment of the equilibrium among the various carbon species for a given pH. When most of the DIC was added as CO_2, adding CA resulted in a rapid shift of most of the inorganic carbon to HCO_3^-, the species that predominates at pH 8.2, and this reduced the photosynthetic rate substantially. Thus, it appeared that the

photosynthetic rate dependended on the low CO_2 concentration, as Fig. 2-2 indicated that 0.03 mM CO_2 could support the same rate observed in this experiment. If little or no HCO_3^- use occurred, then the low concentration of CO_2 present in seawater in equilibrium with air (10 μM) is a major factor for *Udotea* photosynthesis in the environment. The alga must have a mechanism other than HCO_3^- utilization to elevate the internal carbon concentration above that in the surrounding water.

Although in a number of species of red, brown, and green micro- and macroalgae, external CA activity has been found (15, 63, 138, 141), Giordano and Maberly (61), in a survey of 34 species of macroalgae, were unable to find any correlation between the presence of CA activity and the relative ability to use HCO_3^- for photosynthesis, indicating that external CA activity is not always essential for HCO_3^- utilization. However, CA activity does play a role in some HCO_3^- use mechanisms, including that in the red alga *Gracilaria tenuistipitata* (63), where the external CA facilitates the conversion of HCO_3^- in the medium to CO_2 which then diffuses across the plasma membrane. Conflicting reports have appeared for the red alga *Chondrus crispus*. Smith and Bidwell (138) reported the presence of external CA, while Giordano and Maberly (61) did not find it to be present. The brown alga *Ascophyllum nodosum* uses HCO_3^- and lacks external CA activity (78). In contrast, external CA activity was found in some brown algae of the Fucales and Laminariales (141). A difference exists with regard to the presence of CA in the green macroalgal genus *Ulva*. Björk *et al.* (15) report the presence of CA in *U. rigida* as do Giordano and Maberly (61) for *U. lactuca*, although the activity is low. In contrast, Drechsler and Beer indicate they found no external CA activity for *U. lactuca* (47).

No external carbonic anhydrase activity could be detected on the *Udotea* thalli by direct measurement. Thus, it is unlikely that a DIC utilization mechanism, if present, would have external CA activity as a component. Reiskind *et al.* (123) measured high levels of internal CA

activity in *Udotea*, not associated with the membranes, and thus presumably soluble. Their data suggest that CA is located in the chloroplasts, but the concurrent activity in the cytosol cannot be excluded. Activity of CA in the cytosolic compartment could play a role in maintaining a sufficient CO_2 supply for the PEPCK enzyme that appears to be located in the cytosol (122,123) if HCO_3^- be transported across the plasma membrane into the cytosol.

The final pH values attained in a pH drift experiment were 8.3 and 8.95, which are in the range of CO_2-only users reported by Maberly (94). A low pH compensation point, the pH at which no net carbon exchange occurs, has been observed for sublittoral algae within each division, and this may be related to the growth conditions of these algae (6). Similarly, the low pH compensation point observed for *Udotea* as compared to the other algae examined by Maberly (94) may be related to the sublittoral growth conditions of *Udotea*. Maberly (94) indicates that the ability of a species to raise the pH and deplete the total available inorganic carbon varies with the habitat where the species grows. A major contrast exists between the macroalgae that grow in rockpools, which are very effective at removing inorganic carbon and those that are found subtidally in relatively low light, most of which have a more limited ability to use HCO_3^-.

The final CO_2 concentration attained by *Udotea conglutinata* of 5 μM was 25-fold higher that previously measured CO_2 compensation points of 7 μL CO_2 L^{-1} (0.2 μM) for *Udotea flabellum* (123), which also exhibits C_4-like photosynthetic features. The pH drift experiment began with 2 mM equivalent to 0.12 mmol DIC present in the incubation bottles. Based on a HCO_3^- dehydration rate of 0.29 μmol min^{-1}, a total of 0.104 mmol CO_2 would have been produced in 6 h in the 60 mL incubation bottles, and assuming all the CO_2 produced was used for photosynthesis, 0.016 mmol DIC would have remained at the end of that time period. However, the DIC measurements at the end of the incubation indicated that 1000 μM or

0.06 mmol DIC remained in solution. Thus, as the total DIC in the bottle became too low for the alga to photosynthesize, some of the carbon from its $CaCO_3$ skeleton may have been utilized as a source of carbon to be reduced, perhaps avoiding potentially lethal photoinhibition.

At the end of the incubation period, 2 of the 3 replicates showed an increase in the alkalinity of the artificial seawater, from 1.36 at the start to 1.93 when a final pH of 8.21 was attained, and 2.58 when the final pH reached 7.89. This phenomenon has also been reported for other macroalgae in pH drift experiments, including *Dilsea carnosa*, *Polysiphonia nigrescens*, and *Ceramium rubrum*, all red algae (6). These species grow sublittorally, as does *Udotea*. It has been suggested that an increase in the alkalinity of the seawater was responsible for the excretion of inorganic carbon into the medium by the red algae (6). Such an increase in alkalinity of the water surrounding the thallus could have been caused by the reduction of an internal pool of nitrate (6, 70).

Photosynthetic rates for *Udotea* at pH values of 7.7, 8.2, and 9.0 demonstrated "classic" HCO_3^- utilization by the alga (42, 77). Photosynthetic rates in solutions of different pH with the same concentrations of free CO_2 and varying amounts of HCO_3^- and CO_3^{2-} were plotted versus CO_2 concentration. As CO_3^{2-} is not used by plants for photosynthesis (93), the increasing concentration of HCO_3^- relative to CO_2 with pH was important. For a given DIC concentration, the proportion of the total DIC present as CO_2 decreases with increasing pH. However, at the higher pH values, the photosynthetic rates were higher than measured at a lower pH for the same DIC concentration, thereby strongly suggesting that the HCO_3^- present was contributing to the increased photosynthetic rate observed.

Even though there was evidence for some HCO_3^- use in *Udotea*, the question must still be answered whether the ability of the alga to use

HCO_3^- in addition to CO_2 from the surrounding seawater is able to explain the observed C_4-like photosynthetic features. The crucial part of this question is whether the alga is able to concentrate internal inorganic carbon above the level of the ambient solution so as to be able to shift the reaction of Rubisco to favor carboxylation and the photosynthetic carbon reduction cycle over oxygenation and photorespiration. To concentrate inorganic carbon internally requires the expenditure of energy (40) due to the thermodynamic constraints of the system. Photosynthesis in species that can use HCO_3^- is substantially more than half-saturated with air-equilibrium DIC concentration, i.e., 10 μM CO_2 and 2 mM HCO_3^-, while those restricted to using CO_2 are saturated to a lesser degree at the same DIC concentrations (94). Thus, the degree of saturation for the photosynthetic rate at ambient DIC concentration can be used as a guide to indicate whether a carbon concentrating mechanism is operational. In the red alga *Gracilaria conferta*, photosynthesis saturates at a DIC concentration close to ambient and exhibits O_2-insensitive photosynthesis, thus suggesting the operation of some sort of carbon concentrating mechanism, perhaps HCO_3^- utilization (73). Although internal DIC concentrations were not measured directly, the lack of saturation of photosynthesis in *Udotea* at ambient DIC concentration suggested that the alga was using primarily CO_2 for photosynthesis.

The data obtained from the effect of 40 mM KI on photosynthesis provided more clues as to whether *Udotea* can use HCO_3^-. It is possible that the K^+ ion interfered with a Na^+/HCO_3^- symporter in the plasma membrane, the same sort of transporter reported to be operating in the marine diatom *Phaeodactylum tricornutum* (46). Potassium iodide did not exhibit an inhibitory effect until the concentration was increased to 40 mM, but the same concentration also was used in *Ulva lactuca* to inhibit photosynthesis at pH 8.2 (47). This is a high concentration, but if it was competing with Na^+, the concentration of Na^+ in the bathing medium

was 450 mM, so potentially an inhibitory effect occurred at one-tenth the concentration of the important ion. Another possibility is that the I^- ion was in competition with HCO_3^- for transport on a membrane translocator. This is an unlikely scenario, as the Cl^- concentration was greater than 450 mM, so it would be more likely to interfere with HCO_3^- than I^-. Also, HCO_3^- was not able to reduce the inhibition. It cannot be ruled out that the I^- concentration inside the siphons may have interfered with various cellular processes. In the presence of 40 mM KI, the pH of the thallus surface was 1.0-1.5 pH units lower than the control, where thalli were immersed in 2 mM DIC in unbuffered artificial seawater, indicating that the KI increased H^+ extrusion or OH^- uptake by the alga.

The pH microelectrode used for these measurements was placed in contact with the thallus, but *Udotea conglutinata* has a sheath external to the plant cell wall, and the role and chemical composition of this sheath are unknown (24). Thus, the pH electrode could not be placed immediately next to the cell wall. Nonetheless, the pH data indicated that the thallus was performing either H^+ extrusion or OH^- uptake at the surface. This acidification did not appear to be localized to particular regions, as the lower pH was found all over the whole thallus and on both sides. Polarity with respect to pH, as exhibited by the submerged aquatic angiosperm *Potamogeton lucens* on opposite sides of the leaves (139), or the green alga *Chara* in different regions of the cell wall (155) could not be detected. One caveat is that the size of the microelectrode tip (1.5 mm diameter) would preclude the detection of acid/alkaline banding patterns that were smaller than about 1 mm in width. In contrast to these *Udotea* data, measurements of surface pH of *Ulva* have indicated that this thallus has a much higher pH of 10, but it is also uniform with no detectable zones of acidification or alkalinization (12). Clearly, *Ulva* is not extruding H^+.

The contrast in thallus pH measurements between *Udotea* and *Ulva* suggest a difference in the DIC utilization mechanisms. The H^+ extrusion at the *Udotea* surface could cause HCO_3^- in the boundary layer to be converted to CO_2, which could then either diffuse into the cytosol or be actively transported across the plasma membrane into the cytoplasm. *Ulva*, in contrast, is likely to be transporting HCO_3^- across the plasma membrane into the cytosol via a HCO_3^-/OH^- antiport, which would be accompanied by an increase in pH on the outside of the thallus (12).

Calcification (100) or a Na^+/H^+ antiport system, as reported for *Dunaliella salina* (82) could be causing the H^+ release . However, when a section of *Udotea* thallus was incubated in the dark for 15 min, the plant surface was 0.4 pH units lower than the seawater in the incubation medium. Thus, photosynthesis or even the presence of light was not essential for the putative extrusion of H^+. The pH change at the algal surface caused the artificial seawater pH to decrease by 0.4 units during the time the thallus pH was being measured. In the case where no plant was present and the artificial seawater was incubated in the light, the water pH dropped by 0.1 unit over a 15-min period, probably due to a temperature increase in the water, so most of this acidification of the external water could be attributed to the presence of the macroalga.

The inhibition of photosynthesis in *Udotea* that occurred in the presence of DIDS suggested the presence of an anion exchanger in the plasma membrane. In red blood cells, a protein located in the plasma membrane called the band 3 anion transporter (anion exchanger) facilitates HCO_3^- transport, but this is not an active transport system, and thus does not require expenditure of ATP energy (53, 135). In red blood cells, this protein catalyzes the transmembrane exchange of one HCO_3^- for one Cl^-. The inhibitor DIDS, used in this study of *Udotea*, competes quite specifically with Cl^- for binding at a lysine residue in

the vicinity of the outward-facing transport site and inhibits inward-facing sites by shifting their conformation to that of the outward-facing site (53). This band 3 anion transporter is also located in the plasma membrane of *Ulva*, as DIDS was able to reduce the photosynthetic rate when HCO_3^- but not CO_2 was available as the external DIC species to be taken up by the alga (47). In the presence of DIDS, the surface pH of the alga was 0.2 to 0.3 units more acidic as compared to the control, although H^+ translocation is not reported as a function of the anion exchanger.

Based on data from thallus incubation with vanadate, ATP may be necessary for utilization of HCO_3^-, as after 2 h incubation in 5 mM Na_3VO_4, photosynthesis was inhibited 34%. For intact cells of *Dunaliella parva*, where a plasma membrane ATPase plays a role in photosynthesis, 77% of the ATPase activity was inhibited after 3 h incubation in vanadate (60). For intact *Scenedesmus* and *Chlamydomonas* cells, vanadate inhibited plasma membrane ATPase activity after 90 min incubation (114). In the presence of vanadate, *Udotea* thallus surface pH remained unchanged over time, and the pH of the water did not decrease, suggesting that the putative H^+ extrusion was eliminated. These data may lend further support for the presence of a plasma membrane H^+ translocating ATPase. If the ATP synthesis is halted, no proton movement occurs, as the two processes are intimately tied together, according to the chemiosmotic hypothesis. Thus, if a HCO_3^- translocator is operating in *Udotea*, it appears to require ATP for the transport and so be able to accumulate DIC inside the cell at a concentration higher than that found in the surrounding medium. However, after the 2 h incubation with vanadate, photosynthesis was decreased only 34%, thus suggesting that other DIC utilization mechanisms were operating to maintain the photosynthetic rate.

A comparison was made between the measured rate of photosynthesis and that predicted if photosynthesis was limited by the rate of CO_2

production from the spontaneous dehydration of HCO_3^-. This analysis is complicated by the process of calcification that occurs in *Udotea conglutinata*. In *Chara*, it has been demonstrated that photosynthesis and calcification occur in about a 1:1 ratio (99). Using O_2 evolution as a measure of carbon metabolism in photosynthesis assumes that for every mole of inorganic carbon fixed, one mole of O_2 is evolved. But when considering the effect of calcification in this picture, it must be considered that when the alga is photosynthesizing, each photosynthesis "event" requires the uptake of 1.25 moles of inorganic carbon: one is fixed by Rubisco in the chloroplast and after four fixations, precipitation occurs at the surface with Ca^{2+} to form carbonate (23). Inorganic carbon use in *Udotea* in light of these two processes must then be considered. At 2 mM DIC and pH 8.2, the ambient conditions found in natural seawater, 0.58 μmol of CO_2 was produced per hour in the closed system of the O_2 electrode chamber based on the kinetics of HCO_3^- dehydration. In 21% O_2, the photosynthetic rate was 0.44 μmol h^{-1}, indicating that CO_2 was supplied at a rate that exceeded the uptake rate. If calcification is considered in addition to the measured O_2 evolution, then the carbon really used by the alga for photosynthesis was 0.55 μmol h^{-1}. The CO_2 supply rate of 0.58 μmol h^{-1} still met the inorganic carbon requirements of the algae. At 2 mM DIC and 2% O_2, the photosynthetic rate was 0.78 μmol h^{-1}. Under these conditions, CO_2 could not be produced fast enough to meet the photosynthetic requirement, so HCO_3^- use may have made up the deficit. In 1 mM DIC with a HCO_3^- dehydration rate of 0.29 μmol h^{-1}, under both 21% and 2% O_2, HCO_3^- would have to be used to meet the requirement for photosynthetic carbon and then additional HCO_3^- used for calcification. When the alga was placed in 5 mM DIC, more than twice the concentration the plant is exposed to in nature, CO_2 was supplied from HCO_3^- dehydration at 1.46 μmol h^{-1}, a rate higher than the O_2 evolution in both 21% and 2% O_2, thus indicating that the CO_2 supply was sufficient for both carbon fixation

and calcification. Thus, it appears that *Udotea* does have some capacity for HCO_3^- utilization above and beyond the use of free CO_2.

Although O_2 inhibited the photosynthesis of *Udotea*, it was unlike the phenomenon observed in C_3 plants. The photosynthetic characteristics of *Udotea flabellum* clearly indicate that its metabolism is C_4-like in nature (123), and some earlier work on *U. conglutinata* indicated the same metabolism as the other species (Reiskind & Bowes, unpublished). The apparent O_2 sensitivity of photosynthesis may be attributed to other O_2 effects, such as the Mehler reaction, mitochondrial respiration, or the glycolate pathway, similar to that found in the red alga *Chondrus crispus*, where O_2 inhibition is relatively insensitive to CO_2 concentration and not completely reversed by high CO_2 (30).

Because *Udotea conglutinata* is a calcareous alga, the skeleton of carbonates plays a role in photosynthesis in addition to providing structural integrity for the intertwined siphons of the thallus. In species that calcify, the process does not occur until the cells are photosynthetically competent (24). In the presence of $CaCl_2$ at 2 mM DIC and 21% O_2, twice as much DIC was removed from the medium as O_2 was evolved. This proportion suggested that 2 moles of inorganic carbon were required to complete the whole photosynthetic process in *Udotea* of O_2 evolution and calcification. At 5 mM DIC, nearly 10 times more DIC was removed from the medium as O_2 was evolved, but the quantity of O_2 evolved was approximately equal to that in 2 mM DIC. A portion of this inorganic carbon could be used in calcification, but the reason for this difference is not known at this time. When $CaCl_2$ was withheld from the photosynthetic medium, photosynthesis was measurable as O_2 evolution in the O_2 electrode, but the amount of inorganic carbon in the medium actually increased during the course of the 15 min measuring period. Thus, it may be that the plant was excreting inorganic carbon at its

surface which normally would complex with Ca^{2+} to form $CaCO_3$ in the skeleton. *Chara* also does not calcify under low Ca^{2+} conditions (99).

Calcification in *Udotea* appears to occur by a mechanism similar to that in *Halimeda*, a closely related siphonaceous species from the same family (23). Calcium carbonate precipitates as aragonite crystals in the intercellular spaces which are separated from the external seawater. In *Halimeda*, swollen ends of the siphons, called utricles, cause this isolation and the sheath found outside the cell wall in *Udotea conglutinata* may serve a similar function. The model for *Halimeda* states that about 70% of the cell wall area faces these intercellular spaces. When CO_2 uptake occurs from the carbon in the intercellular spaces, the pH increases as does the concentration of CO_3^{2-} in these secluded spaces and Ca^{2+} from the surrounding medium moves through the cell walls to these areas, thereby facilitating $CaCO_3$ precipitation (23). The photosynthetic removal of carbon is greater than the resupply rate from the external seawater and cellular respiratory processes. The surface acidification in the presence of $CaCl_2$ in the seawater is a by-product of the precipitation of $CaCO_3$ (100).

Studies in *Chara* also have provided important information about the calcification process. Protons generated from the hydroxylation and precipitation of CO_2 allow the plant to manufacture twice the amount of CO_2 used in calcification (99). The model for *Chara* suggests that the inorganic carbon and Ca^{2+} for the process come from inside a heavily encrusted plant, and a Ca^{2+}/ATPase appears to be involved in part of the transport (99). The H^+ must be removed from the calcification site; perhaps H^+ are transported by cytoplasmic streaming and through a large, acidic vacuole to another part of the plant cell. In fact, H^+ generation may be the principal benefit of calcification (99). This precipitation occurs at an appreciable rate in nature, as 50% of the dry weight of the *Udotea* thalli was composed of carbonate salts, and a similar proportion occurs in Characeans (100).

Calcification in *Udotea* could occur in the intercellular spaces, which are really spaces between the siphons. As $CaCO_3$ precipitation occurred, the H^+ generated were translocated to the outer surface of the thallus, and this H^+ extrusion was recorded in this investigation. The calcification process was actually quite similar to that for *Chara*, with H^+ movement occurring across the same cell, or siphon in this case, except that only the acidification could be measured because the removal of H^+ occurred inside the thallus. However, in *Udotea*, some H^+ extrusion continued in the absence of photosynthesis.

The current hypothesis regarding inorganic carbon utilization in *Udotea* is that the alga preferentially uses CO_2 when it is available, but limited HCO_3^- use also occurs. The HCO_3^- is probably transported by a carrier protein in the plasma membrane in a facilitated manner, such that no energy expenditure is required, and thus internal accumulation of DIC does not occur above the external concentration. However, it also appears as if some ATPase is involved, but no external CA. ATPase may be involved in calcification or conversion of HCO_3^- to CO_2 by acidification and thus H^+ extrusion.

Thus, the model for photosynthesis in *Udotea* includes DIC uptake in the form of CO_2, which is produced in the boundary layer by H^+ extrusion associated with the calcification process. This uptake could occur via diffusion or active transport of the CO_2 across the plasmamembrane. Some HCO_3^- uptake across the plasmamembrane also occurs probably on an anion exchanger that operates via facilitated transport. As inhibition of these mechanisms inhibited photosynthesis by no more than 34%, the high phosphoenolpyruvate carboxykinase activity, reportedly located in the cytosol, is the key component of the photosynthetic mechanism in *Udotea* to concentrate inorganic carbon for Rubisco and thus, cause the macroalga to exhibit its C_4-like features.

CHAPTER 3
ROLE OF PHOSPHOENOLPYRUVATE CARBOXYKINASE IN THE PHOTOSYNTHESIS OF THE MARINE MACROALGA *UDOTEA*

Introduction

Udotea is a green, marine, macroalga which exhibits C_4-like photosynthetic characteristics, despite lacking the Kranz anatomy associated with terrestrial C_4 species. The thallus of this alga is composed of intertwined coenocytic siphons. Although a "primitive" plant, this alga appears to utilize a more "advanced" type of photosynthetic metabolism, initiated by the enzyme PEPCK, as when PEPCK is inhibited by MPA, the photosynthetic metabolism of this alga appears C_3-like (122). The focus of this investigation was to examine the kinetics of PEPCK in order to ascertain how this enzyme could be functioning as a component of the C_4-like metabolism. In some higher plants that utilize C_4 photosynthesis, PEPCK functions as a decarboxylase in the cytosol of bundle sheath cells (4). In the brown algae, PEPCK is hypothesized to function in an anapleurotic role to supply the cells with carbon skeletons for the synthesis of other compounds (159). PEPCK is also found in a variety of other organisms ranging from bacteria and yeast to diatoms and vertebrates. In the plants and diatoms, PEPCK uses ADP/ATP, while the enzyme in *Euglena* and vertebrates utilizes GDP/GTP for its activity (117, 152). In mammals, PEPCK is a critical enzyme in gluconeogenesis, involved in removing CO_2 from OAA to produce PEP for the eventual production of glucose.

Materials and Methods

Materials

The marine macroalga *Udotea flabellum* (Ellis and Solander) Lamouroux (division Chlorophyta) was collected during the summer on the north side of Marathon Key, Florida, in Florida Bay in water ranging

from 0.5-2.5 m in depth. After collection, the plants were kept outdoors for up to two days in a fresh seawater-fed and aerated tank until frozen in liquid nitrogen (LN_2).

Enzyme Extraction

For experiments on crude extract, 1-2 g of LN_2-frozen plant material was ground in a mortar and pestle with sand at 4°C in 3-6 mL of 50 mM Hepes-NaOH, 2 mM $MnCl_2$, 5 mM DTT, 1% (w/v) PVP-40, 1 mM PMSF, and 10 μM leupeptin at pH 7.0. The homogenate was centrifuged at 13,000 g for 2 min in a microfuge at 4°C. The supernatant was then desalted through either a 5 mL Sephadex G-25 or BioRad P-6 column with the same medium used for grinding, but without PVP-40. The column eluant collected just after the void volume was then used for subsequent enzyme assays.

For isolation of *Udotea* PEPCK, approximately 45 g of frozen plant material was powdered in LN_2 and then ground with a mortar and pestle and sand at 4°C in 150 mL of a medium containing 50 mM MES-NaOH, 5 mM $MnCl_2$, 5 mM $MgCl_2$, 5 mM DTT, 0.2 mM Na_2EDTA, 1 mM PMSF, and 1% (w/v) PVP-40 at pH 6.5. Following centrifugation at 4°C for 15 min at 12,000 g, the pellet was discarded, and the supernatant was used for protein isolation. Solid $(NH_4)_2SO_4$ was added slowly, with constant stirring, to the protein solution kept on ice. The protein that precipitated between 40 and 50% (w/v) $(NH_4)_2SO_4$ was pelleted at 3500 g and resuspended in 6 mL of the elution buffer, which consisted of 50 mM MES-NaOH, 5 mM $MnCl_2$, 5 mM $MgCl_2$, 5 mM DTT, and 1 mM PMSF at pH 6.5. The solution was then brought to 20% (v/v) glycerol.

Enzyme Purification

The protein solution was loaded onto a Sephacryl S-300 column (78 x 2.5 cm, 380 mL bed volume) and eluted at 4°C with the buffer described above. Fractions were analyzed for protein by measuring the absorbance at 280 nm in a spectrophotometer. Fractions were also analyzed for PEPCK, malate dehydrogenase (MDH), and Rubisco activities. Those

fractions containing high PEPCK activity and low MDH activity were loaded onto a Sepharose CL-6B column (25 x 1.5 cm, 40 mL bed volume) for ion exchange chromatography and eluted with a linear 0-0.3 M KCl gradient in the same buffer used for gel filtration. Fractions were analyzed for PEPCK, MDH, and Rubisco activities, and protein. The fractions containing highest PEPCK activity were pooled (total volume 35 mL), the protein concentration was determined, 2 mg mL^{-1} bovine serum albumin (BSA) was added, and the solution was frozen in LN_2 for further enzyme studies.

Enzyme Assays

Enzymes were assayed at 25°C (except where noted). The carboxylation activity of PEPCK was routinely measured spectrophotometrically at 340 nm by the MDH/NADH-coupled reaction (151). The standard assay mixture consisted of 50 mM PIPES-NaOH, 5 mM $MnCl_2$, 30 mM $NaHCO_3$, 5 mM DTT, 20 to 30 μL enzyme extract, 2 units MDH, 0.2 mM NADH, 3 mM ADP, and 10 mM PEP at pH 6.8 in a total volume of 0.5 mL. The reaction was initiated by adding ADP and followed for a period of 3 minutes during which the reaction proceeded at a linear rate. An absorption coefficient of 6.22 mM^{-1} cm^{-1} was used for NADH. The PEPCK carboxylation activity was also measured radiochemically in a standard assay of 50 mM PIPES-NaOH, 5 mM $MnCl_2$, 30 mM $NaH^{14}CO_3$ (2 μCi μmol^{-1}), 5 mM DTT, 20 to 30 μL enzyme extract, 2 units MDH, 0.2 mM NADH, 2 mM ADP, and 7 mM PEP at pH 6.8 in a total volume of 0.5 mL. The reaction was initiated with PEP and terminated after 6 min with 0.1 mL 6 N HCl saturated with 0.13 M dinitrophenylhydrazine. After drying at room temperature to allow unreacted $NaH^{14}CO_3$ to escape, the sample was rehydrated with 0.4 mL deionized water, one drop of 6 N NaOH, and 4 mL liquid scintillation cocktail (RPI 3a70). The capped vials were then vortexed. The acid-stable products were counted in a liquid scintillation counter.

The decarboxylation activity of PEPCK was measured spectrophotometrically at 340 nm by the MDH/NADH-coupled reaction modified from Burnell (33). The assay mixture consisted of 50 mM Bicine-NaOH, pH 7.8, 5 mM $MnCl_2$, 20 to 30 μL PEPCK enzyme extract, 0.25 mM NADH, 1 unit lactate dehydrogenase, 2 units pyruvate kinase, 0.5 mM ATP, and 0.5 mM OAA, at pH 7.8, also in a total volume of 0.5 mL. The reaction was initiated with OAA and followed for 3 min, during which time the reaction proceeded at a linear rate.

The activity of MDH was assayed spectrophotometrically at 340 nm by measuring NADH oxidation in a method modified from Yueh *et al.* (161). The assay mixture was composed of 50 mM Bicine-NaOH, 1 mM Na_2EDTA, 0.2 mM NADH, 10 μL enzyme extract, and 0.5 mM OAA at pH 8.0. The reaction was initiated with OAA.

The activity of Rubisco was measured radiochemically in an assay mixture consisting of 50 mM Bicine-NaOH, 10 mM $MgCl_2$, 50 μL enzyme extract, 5 mM DTT, 5 mM isoascorbate, 10 mM $NaH^{14}CO_3$ (0.5 μCi μmol^{-1}), and 1 mM RuBP at pH 8.0. The enzyme was activated for 5 min at 30°C in the assay mixture without RuBP present (128). The reaction was initiated with RuBP, performed at 30°C, and terminated after 30 s with 6 N HCl. After drying in a 70°C oven and rehydrating the samples, the radioactivity of the acid-stable products were measured as described above.

Protein Assay

During elution of the columns, protein concentration was determined by measuring the absorbance of the protein solution at 280 nm, but in all other instances, it was determined by the method of Bradford using bovine Γ-globulin as standard (29).

Enzyme Storage Conditions

Following purification, aliquots of PEPCK were stored for a period of 5 weeks as enzyme solution in elution buffer, with and without 2 mg mL^{-1} BSA, or as the precipitate of 65% $(NH_4)_2SO_4$ in the refrigerator

(4°C), freezer (-20°C), or in LN_2 (-196°C). The carboxylation activity of the aliquots was measured after 2 weeks and again after 5 weeks of storage.

Enzyme Kinetic Analyses

The inorganic carbon species utilized for carboxylation by *Udotea* PEPCK was determined by the method of Cooper *et al.* (44) at 12°C so as to slow equilibration among the inorganic carbon species. The DIC was added at a concentration of 8 mM as either HCO_3^- or CO_2 to initiate the reaction in the presence or absence of CA. To provide predominantly HCO_3^- to the enzyme, a solution of 0.5 M $NaHCO_3$ was added directly from a Hamilton syringe into the assay mixture in the cuvette. However, to provide predominantly CO_2, $NaHCO_3$ solution was drawn up into a Hamilton syringe followed by an equal volume of 0.5 N HCl. After dissolved CO_2 was produced in the syringe, the solution was dispensed into the cuvette where the reaction was to occur. The reactions were performed at pH 8.0. All solutions, except $NaHCO_3$, were prepared CO_2-free by bubbling with N_2. This bubbling was continued after the mixture components, except for the DIC, were combined in the cuvette, so that the assays were performed under CO_2-free conditions. The DIC was added last to initiate the reaction. The reaction was followed for only one minute in the spectrophotometer so that the measured rate would be dependent upon the inorganic carbon species initially added to the reaction mixture.

The affinity of PEPCK for the carboxylation substrates, DIC, ADP, and PEP and the decarboxylation substrates, OAA and ATP was examined. The effect of Mn^{2+} was investigated for both reactions. The concentration of the substrate in question was varied while the other reaction mixture components were held constant at saturating concentrations. The constants were calculated from Eadie-Hofstee plots. The computer program Enzfitter was also used to calculate Michaelis-Menten constants.

The carboxylation reaction was performed in the presence of ADP, GDP, or IDP, and the decarboxylation reaction was run with ATP, GTP, or ITP to determine how these components affected the reaction.

The effects of 0.5 mM OAA and 0.5 mM ATP on the carboxylation reaction and 1 and 3 mM DIC, 0.02 mM ADP, and 4 mM PEP on the decarboxylation reaction were examined. For both carboxylation and decarboxylation, the effect of 100 μM MPA on *Udotea* PEPCK was investigated. The effects of the intracellular metabolites malate, aspartate, F6P, F-1,6-BP, 3-PGA, and dihydroxyacetone phosphate (DHAP) were examined for both reactions. These potential effectors were added at 4 mM over a range of subsaturating concentrations for one reaction component at a time. Other substrates were present in saturating concentrations.

The carboxylation reaction was run at subsaturating DIC concentrations and the decarboxylation reaction at subsaturating OAA concentrations in 0, 21, and 100% gas phase O_2, (0, 0.46, and 2.18 mM O_2 in solution) to determine whether O_2 was an effector of either the carboxylation or decarboxylation reactions.

Results

In initial experiments, assays of PEPCK activity in both the carboxylating (pH 6.8) and decarboxylating (pH 7.8) directions were performed with crude extracts of *Udotea* thalli subject only to gel filtration through a 5 mL column of Sephadex G-25. The V_{max} values from the preparations ranged from 0.69 to 1.32 μmol NADH mg^{-1} protein min^{-1} and 0.51 to 0.98 μmol NADH mg^{-1} Chl min^{-1} for the carboxylation reaction, but were approximately four- to five-fold lower for the decarboxylation reaction, ranging from 0.14 to 0.34 μmol NADH mg^{-1} protein min^{-1} and 0.10 to 0.25 μmol NADH mg^{-1} Chl min^{-1}. The K_m values for the various substrates are listed in Table 3-1. In the carboxylating direction, the enzyme exhibited an almost 100-fold concentration difference in K_m values, with the lowest K_m being for ADP and the highest for dissolved

Table 3-1. K_m values for PEPCK activity in crude extracts of *Udotea thalli*. The values were derived from Eadie-Hofstee plots.

Substrate	K_m
	mM
Carboxylating Direction	
ADP	0.075
PEP	0.920
DIC	7.326
Decarboxylating Direction	
ATP	0.023
OAA	0.028

inorganic carbon. In contrast, the affinities of the substrates ATP and OAA for decarboxylation were similar and comparable to the low K_m(ADP) for carboxylation.

In an experiment where the same concentration (5 mM) of GDP or IDP was substituted for ADP, carboxylation proceeded at less than 20% of the ADP-catalyzed rate (Table 3-2). Similarly, for the decarboxylation reaction, the rate with 0.4 mM GTP or ITP was considerably reduced when compared to the rate with the same concentration of ATP. The nucleotide preference of the decarboxylation reaction was less specific than that of the carboxylation reaction, as the decarboxylation rate proceeded more rapidly when other nucleotides were substituted for ATP.

An examination of the metal ion requirement for PEPCK in crude extracts indicated that Mn^{2+} was essential for maximum catalytic activity in the carboxylation direction (Fig. 3-1). When Mg^{2+} was supplied at the same concentration as Mn^{2+}, catalysis was only 10 to 25% of the rate with Mn^{2+}; thus, Mg^{2+} alone could not substitute for Mn^{2+}. If both species were present at the same concentration, Mg^{2+} inhibited the rate obtained in the presence of only Mn^{2+} by 5% and 44% at 2 and 5 mM ion concentration, respectively.

Udotea PEPCK was purified in a three-step procedure involving $(NH_4)_2SO_4$ precipitation, which removed a portion of the extraneous cellular proteins, followed by separation of the proteins of interest according to molecular weight using gel filtration, and finally an ion-exchange column. Protein was measured by reading the absorbance at a wavelength of 280 nm, and the presence of PEPCK was detected by its carboxylation activity. Two other enzymes, MDH and Rubisco, were also detected by assay of their activity in various fractions. The gel filtration step separated PEPCK from most of the MDH, but some MDH activity remained (Fig. 3-2). This step also eliminated the remainder of the Rubisco activity associated with the PEPCK. For the next step in the purification procedure, only the PEPCK fractions preceding the first

Table 3-2. Effect of various nucleotides on crude PEPCK activity. The carboxylation rate was 0.642 ± 0.018 μmol NADH mg^{-1} protein min^{-1} with ADP, and the decarboxylation rate was 0.299 ± 0.021 μmol NADH mg^{-1} protein min^{-1} with ATP.

	Relative Reaction Rate	
Substrate	Carboxylation	Decarboxylation
	%	
ADP	100	---
GDP	17	---
IDP	10	---
ATP	---	100
GTP	---	38
ITP	---	55

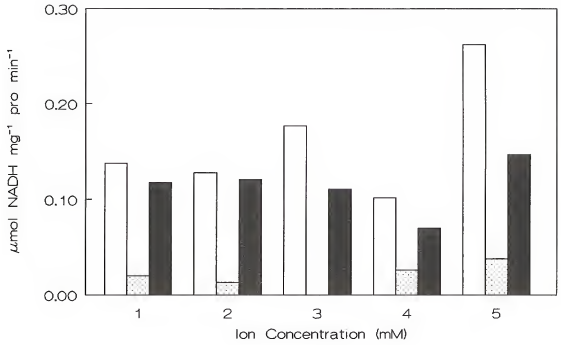

Figure 3-1. Effect of either Mn^{2+} (□) or Mg^{2+} (▤) or both ions present together at equal concentrations (■) on PEPCK carboxylation activity from crude extracts.

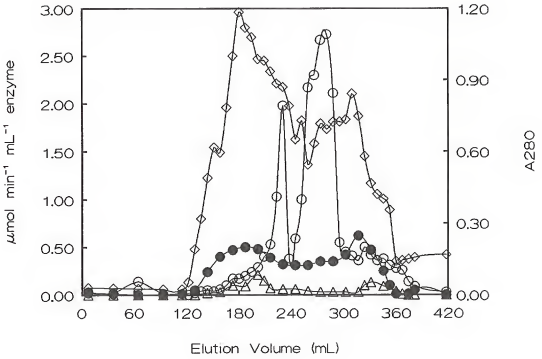

Figure 3-2. Elution profile of the proteins PEPCK (●), MDH (○), and Rubisco (▵) according to molecular weight from the Sephacryl S-300 column. Protein concentration (◊) was measured at wavelength 280 nm as the fractions eluted from the column.

major MDH peak (i.e., elution volume 130 through 210 mL) were selected. These fractions with high PEPCK activity were pooled and loaded onto the ion exchange column. After rinsing with buffer lacking KCl, elution was accomplished with a 0-0.3 M linear KCl gradient in the elution buffer. Ion exchange reduced the proportion of MDH in the PEPCK fraction such that the pool of the most active PEPCK had an average activity ratio of 7 units PEPCK to one unit of MDH (Fig. 3-3). This step also separated the remaining Rubisco activity from the PEPCK. After gel filtration and ion exchange chromatography, PEPCK was purified 12.6-fold, resulting in a specific activity of 18.52 μmol NADH mg^{-1} protein min^{-1} (Table 3-3).

To test its stability and determine optimum storage conditions, the isolated enzyme was stored under a variety of conditions for up to five weeks. Three temperatures were utilized (4, -20 and -196°C) and the enzyme was maintained in the ion exchange elution buffer or with 2 mg mL^{-1} BSA, or as precipitate in 65% (w/v) $(NH_4)_2SO_4$ (Table 3-4). After 2 weeks, the enzyme stored as a solution in buffer or as a precipitate with $(NH_4)_2SO_4$ at 4 and -20 °C lost nearly all activity, whereas that kept in LN_2 at -196°C still retained about one-third of the initial activity. The enzyme stored with BSA retained between 70-90% of its initial activity at all the temperatures. After 5 weeks, the enzyme stored with BSA at -20°C had lost half of its original activity, while the samples stored at 4 and -196°C retained 66% of the initial activity. Based on these experiments, the purified enzyme was routinely stored at -196°C after adding 2 mg mL^{-1} BSA to the solution, and this solution was utilized to characterize the purified enzyme.

When measured as a function of pH, the carboxylating and decarboxylating activities of isolated PEPCK exhibited peaks of activity ranging from 6.0 to 7.5 and 7.5 to 8.0, respectively (Fig. 3-4). At pH 7.6, the rates of the two activities were equivalent, but at its optimum pH of 6.8, the carboxylation rate was 136% of the decarboxylation rate at its optimum of pH 7.8.

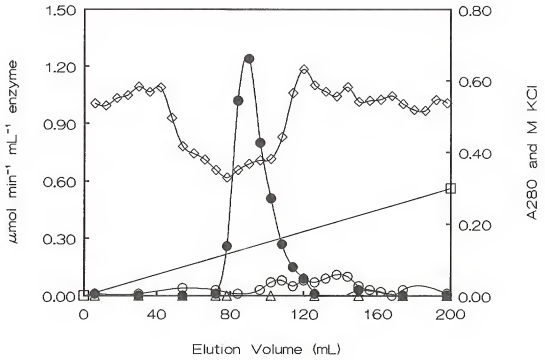

Figure 3-3. Elution profile of the proteins PEPCK (●), MDH (○), and Rubisco (△) according to charges on the molecules from the Sepharose CL-6B column. Proteins were eluted with a 0 to 0.3 M KCl gradient (□). Protein concentration (◇) was measured at wavelength 280 nm as the fractions eluted from the column.

Table 3-3. Isolation of PEPCK from *Udotea*.

Purification Step	Volume	Protein	Enzyme Units	Specific Activity	Recovery	Purification
	mL	mg	μmol min^{-1}	units mg^{-1}	%	-fold
Crude	162	57.51	84.54	1.47	100	---
40-50% $(NH_4)_2SO_4$ pellet, resuspended	6	---	148.36	---	---	---
Sephacryl S-300	74	23.75	12.43	0.52	15	0.35
Sepharose CL-6B	38	0.46	8.52	18.52	10	12.6

Table 3-4. Effect of storage conditions on purified PEPCK carboxylation activity. The initial activity was 15.17 μmol NADH mg^{-1} pro min^{-1}.

Storage Conditions				
Temperature	Time	Addition	Activity Remaining	
°C	Weeks		μmol NADH mg^{-1} pro min^{-1}	%
4	2	Buffer	0.42	3
		+ BSA	13.83	91
		+$(NH_4)_2SO_4$	0.67	4
4	5	Buffer	0.12	1
		+ BSA	10.00	66
		+ $(NH_4)_2SO_4$	0.32	2
-20	2	Buffer	1.69	11
		+ BSA	10.42	69
		+ $(NH_4)_2SO_4$	0.77	5
-20	5	Buffer	0.60	4
		+ BSA	7.68	51
		+ $(NH_4)_2SO_4$	1.43	9
-196	2	Buffer	4.88	32
		+ BSA	13.42	88
		+ $(NH_4)_2SO_4$	4.21	28
-196	5	Buffer	1.84	12
		+ BSA	9.86	65
		+ $(NH_4)_2SO_4$	3.37	22

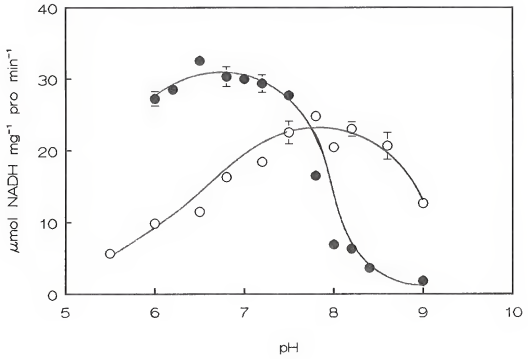

Figure 3-4. Effect of pH on the carboxylation (●) and decarboxylation (o) activities of purified PEPCK at 25°C.

The carboxylating and decarboxylating reactions of PEPCK exhibited a similar optimum temperature of 35°C when measured at their respective pH optima (Fig. 3-5). The carboxylation reaction for the purified enzyme was measured as a function of DIC concentration at the optimum pH for carboxylation, 6.8, and at the optimum pH for decarboxylation, 7.8 (Fig. 3-6). The curve at pH 7.8 is flatter than that at 6.8; however, at both pH values, the reaction was saturated at 30 mM DIC with a $K_{0.5}$(DIC) of 7.8 mM at pH 6.8 and 15.5 mM at pH 7.8. In solution, DIC exists as free CO_2, H_2CO_3, HCO_3^-, and CO_3^{2-} with the relative proportions dependent upon the pH and temperature of the solution. The relative species proportions were calculated from the Henderson-Hasselbach equation. The pK_{a1} of 6.36 for carbonic acid (H_2CO_3) in freshwater at 25°C was used for the calculations (146). At pH 6.8, 0.273 of total DIC is CO_2 and 0.727 is HCO_3^-, and at pH 7.8, 0.035 of total DIC is CO_2 and 0.965 is HCO_3^-. At these pH values, the proportion of CO_3^{2-} was negligible. Using these proportions, it was possible to calculate the $K_{0.5}$ values for CO_2 and HCO_3^- at the two pH values used in the assay. At pH 6.8, using a Michaelis-Menten plot (Enzfitter program), the $K_{0.5}(CO_2)$ was calculated to be 2.1 mM and the $K_{0.5}(HCO_3^-)$ was 5.6 mM, while at pH 7.8 the $K_{0.5}(CO_2)$ was 0.5 mM and the $K_{0.5}(HCO_3^-)$ was 15.0 mM. Thus, the $K_{0.5}(CO_2)$ at pH 7.8 was four-fold lower than at pH 6.8, whereas the $K_{0.5}(HCO_3^-)$ was 2.5-fold lower at pH 6.8.

Further investigation of the carboxylation reaction showed that it proceeded most rapidly when free CO_2 rather than HCO_3^- was provided to the enzyme (Table 3-5). This assay was run at 12°C to reduce the rate of spontaneous equilibration between CO_2 and HCO_3^-, and the reaction rates were lower as a result of the decreased temperature. Adding CA to speed the equilibration between CO_2 and HCO_3^- decreased the carboxylation rate by 36% when CO_2 was the inorganic carbon source. When HCO_3^- was the predominant form of C_i supplied to the enzyme, the reaction rate was just 28% of that in the presence of CO_2. Adding CA in

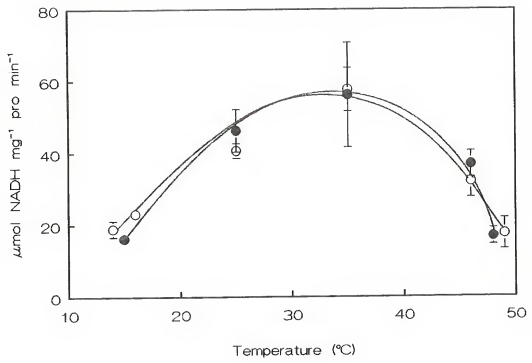

Figure 3-5. Effect of temperature on purified PEPCK carboxylation activity (●) at pH 6.8 and decarboxylation activity (○) at pH 7.8.

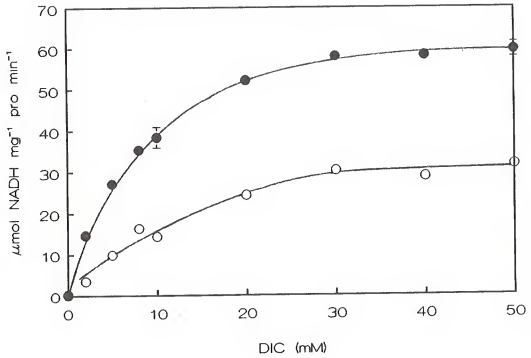

Figure 3-6. Influence of DIC concentration on PEPCK carboxylation activity at the carboxylation optimum pH of 6.8 (●) and the decarboxylation optimum pH of 7.8 (○).

Table 3-5. Form of dissolved inorganic carbon utilized by *Udotea* PEPCK for carboxylation. The reaction was performed at 12°C to slow the equilibration between CO_2 and HCO_3^- in solution.

Treatment	Rate of PEPCK Reaction	
	With CO_2	With HCO_3^-
	μmol NADH mg^{-1} pro min^{-1}	
Without CA	9.47 ± 0.51	2.66 ± 0.81
With CA	6.06 ± 0.32	7.44 ± 0.56

the presence of HCO_3^- increased the rate to 79% of the CO_2 rate. These data indicate that *Udotea* PEPCK uses CO_2 rather than HCO_3^- as the inorganic carbon substrate for carboxylation.

The K_m values for the substrates of carboxylation and decarboxylation are summarized in Table 3-6 for the isolated PEPCK by way of comparison with the crude extract data (Table 3-1). For the carboxylation reaction, the K_m(DIC) of 7.7 mM for the isolated enzyme at pH 6.8 was similar to the value obtained with the crude enzyme extract. For the other substrates of the carboxylation reaction, the K_m values found with the isolated enzyme were comparable to those observed with the crude extract. However, in the decarboxylation reaction, the K_m(ATP) of 2 μM for the isolated enzyme was ten-fold lower than that of the crude extract. A comparison of K_m values for both reactions indicated that the affinity of *Udotea* PEPCK for the substrates of the decarboxylation reaction was higher than for the substrates of the carboxylation reaction.

Since CO_2 appeared to be the inorganic carbon substrate for PEPCK, the reactions were examined at several O_2 levels to investigate whether O_2 was a competitive inhibitor with respect to CO_2 as occurs with Rubisco (26, 90). The carboxylation reaction was examined with a range of DIC concentrations from subsaturating to saturating with 0, 21 and 100% O_2 in the gas phase (Table 3-7). No inhibitory effect of O_2 was observed at any of the DIC or O_2 concentrations employed. Similarly, the decarboxylation reaction was insensitive to O_2 at saturating and subsaturating OAA concentrations (Table 3-7).

3-Mercaptopicolinic acid has been reported to be a specific inhibitor of PEPCK isolated from mammalian livers and kidneys (120) and from the liver fluke (88). In regard to *Udotea*, MPA inhibited both reactions competitively: with respect to PEP for carboxylation (Fig. 3-7) and with respect to OAA for decarboxylation (Fig. 3-8). In the presence of 100 μM MPA, the apparent K_m(PEP) increased seven-fold, from

Table 3-6. K_m values for substrates of isolated PEPCK at optimal pH for the reactions determined from Eadie-Hofstee plots. The K_m values for CO_2 and HCO_3^- at each pH were calculated based on the Henderson-Hasselbach equation using the pK_{a1} of 6.36 for carbonic acid in freshwater at 25°C (146).

Reaction	Substrate	pH	K_m
			mM
Carboxylation	DIC	6.8	7.70
	CO_2	6.8	2.10
	HCO_3^-	6.8	5.60
	DIC	7.8	16.62
	CO_2	7.8	0.58
	HCO_3^-	7.8	16.04
	PEP	6.8	1.66
	ADP	6.8	0.03
	Mn^{2+}	6.8	0.88
Decarboxylation	OAA	7.8	0.035
	ATP	7.8	0.002
	Mn^{2+}	7.8	1.67

Table 3-7. Effect of oxygen in the gas phase on the carboxylation and decarboxylation activities of isolated PEPCK at various DIC and OAA concentrations.

Reaction and Substrate Concentration	Rate of PEPCK Reaction		
	0% O_2	21% O_2	100% O_2
mM	μmol NADH mg^{-1} pro min^{-1}		
Carboxylating (DIC)			
2	1.61 ± 0.07	2.53 ± 0.55	3.44 ± 0.14
5	5.81 ± 0.41	4.84 ± 0.56	5.01 ± 0.95
8	8.66 ± 1.12	8.55 ± 1.10	8.42 ± 0.57
20	13.18 ± 1.12	13.85 ± 0.41	14.06 ± 1.45
30	17.14 ± 0.76	16.02 ± 0.59	18.36 ± 0.97
Decarboxylating (OAA)			
0.05	10.50 ± 0.42	---	11.07 ± 1.44
0.5	15.37 ± 1.62	---	15.77 ± 1.57

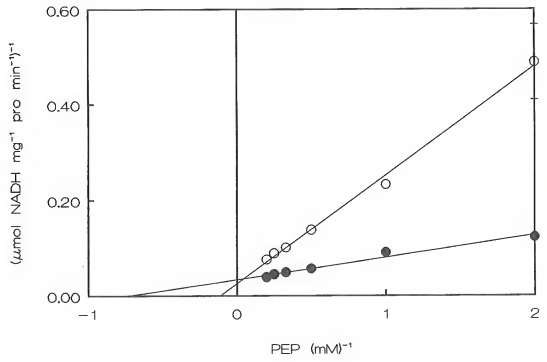

Figure 3-7. Competitive inhibition of PEPCK carboxylation activity by 100 μM MPA with respect to PEP. (●) no MPA present, (○) with MPA present.

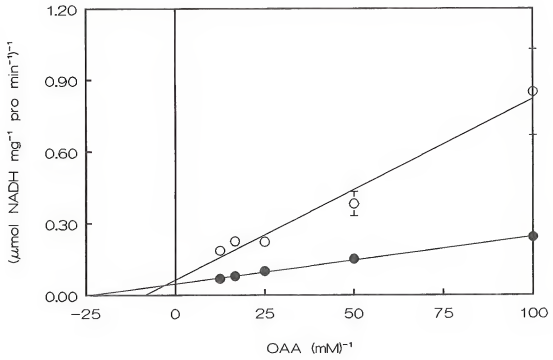

Figure 3-8. Competitive inhibition of PEPCK decarboxylation activity by 100 μM MPA with respect to OAA. (●) no MPA present, (o) with MPA present.

1.6 to 9.0 mM, while the apparent K_m(OAA) increased 3.5-fold, from 41 to 114 μM.

A number of cellular metabolites were also examined as potential effectors of the carboxylation and/or decarboxylation reactions of *Udotea* PEPCK (Table 3-8). The C_4 acids malate and aspartate had only a minor inhibitory effect on either reaction, of no more than 10%, but malate decreased the K_m(DIC) from 5.91 mM to 2.97 mM (Fig. 3-9). Malate also lowered the V_{max} by 60%. The PCR cycle intermediates DHAP and 3-PGA inhibited PEPCK carboxylation at subsaturating DIC but not at subsaturating PEP. The K_m(DIC) was decreased by DHAP from 5.91 mM to 3.15 mM, and the V_{max} was decreased by 45% (Fig. 3-10). With respect to DIC, carboxylation activity was inhibited non-competitively by 4 mM 3-PGA, and the V_{max} of the reaction decreased 45% in its presence (Fig. 3-11). Two 6-carbon sugar phosphates of the PCR cycle, F6P and F-1,6-BP, also affected the PEPCK reactions. Fructose-6-P inhibited decarboxylation by 30% at subsaturating OAA concentrations while it slightly stimulated carboxylation, by 14%, at subsaturating levels of PEP. At a concentration of 4 mM, it also doubled the K_m(OAA) from 41 μM (●) to 89 μM (Fig. 3-12). Both reactions were stimulated by F-1,6-BP, but carboxylation was stimulated to a greater extent at subsaturating PEP concentrations, and the K_m(PEP) was decreased three-fold in the presence of F-1,6-BP (Fig. 3-13). However, carboxylation at subsaturating levels of DIC was inhibited 27% by F-1,6-BP in an uncompetitive manner (Fig. 3-14). The photorespiratory compound glycolate inhibited carboxylation by less than 10% when PEP concentrations were below saturation. Decarboxylation was inhibited by substrates of the carboxylation reaction, PEP and DIC, but ADP appeared to stimulate decarboxylation at subsaturating ATP concentrations. The decarboxylation rate was decreased by 50% in the presence of 4 mM PEP, and the K_m(OAA) was halved (Fig. 3-15), while 20 μM ADP decreased the K_m(ATP) nearly three-fold (Fig. 3-16). In contrast, ATP inhibited

Table 3-8. Influence of metabolites on PEPCK reactions. All reaction components were present at saturating concentrations for each reaction, except the effect of the metabolite on the reaction for a given substrate was measured at subsaturating concentrations of that particular substrate. Inhibition is reported vs. 1 mM substrate concentration for carboxylation and vs. 0.02 mM substrate for decarboxylation (unless noted differently).

Metabolite	Metabolite Concentration	Degree of Stimulation or Inhibition				
		Carboxylation			Decarboxylation	
		PEP	DIC	ADP	OAA	ATP
	mM	%				
Malate	4	0	-7	---	-10	---
Aspartate	4	-9	-4	---	-7	---
DHAP	4	-4	-31	---	-3	---
3-PGA	4	-6	-61	---	-2	---
F6P	4	14	-6	---	-30	---
F-1,6-BP	4	34	-27	---	7	---
Glycolate	4	-8	---	---	---	---
PEP	4	---	---	---	-37	---
DIC	1	---	---	---	-10	---
	3	---	---	---	-22	---
ADP	0.02	---	---	---	---	21*
ATP	0.4	---	---	-68**	---	---

Note: A negative value indicates inhibition of the reaction.
*Substrate concentration was 0.004 mM.
**Substrate concentration was 0.05 mM.

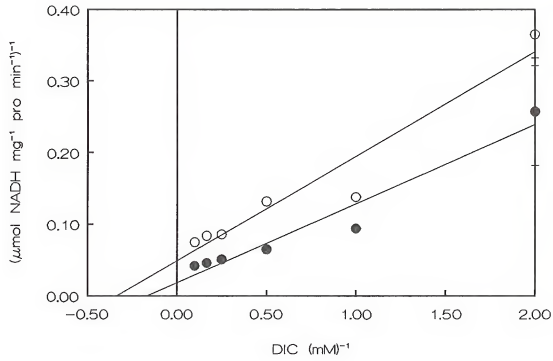

Figure 3-9. Effect of of 4 mM malate on the K_m(DIC) for PEPCK carboxylation. (●) no malate present, (○) with malate present.

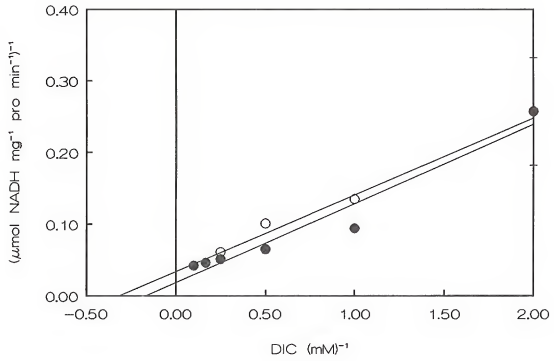

Figure 3-10. The effect of 4 mM DHAP on K_m(DIC) for PEPCK carboxylation. (●) no DHAP present, (○) with DHAP present.

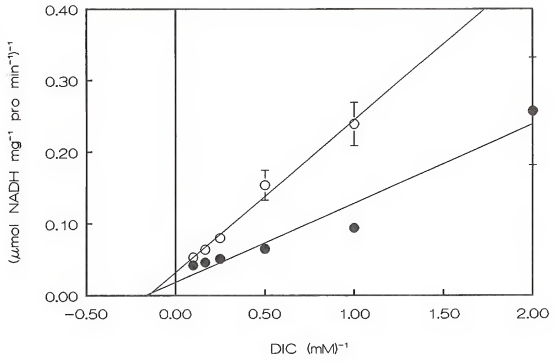

Figure 3-11. Effect of 4 mM 3-PGA on PEPCK carboxylation with respect to DIC concentration. (●) no 3-PGA present, (○) with 3-PGA present.

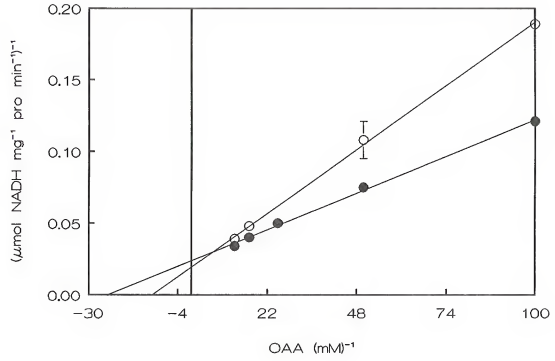

Figure 3-12. Effect of 4 mM F6P on the K_m(OAA) for PEPCK decarboxylation. (●) no F6P present, (○) with F6P present.

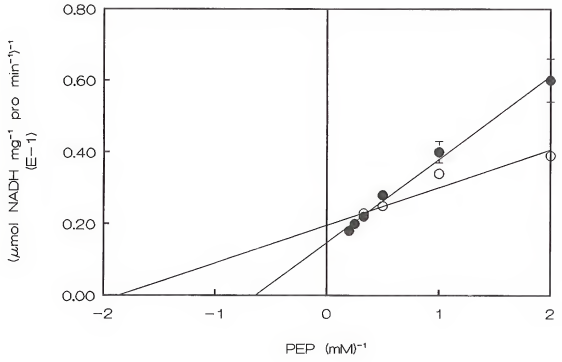

Figure 3-13. Effect of 4 mM F-1,6-BP on the K_m(PEP) for PEPCK carboxylation. (●) no F-1,6-BP present, (o) with F-1,6-BP present.

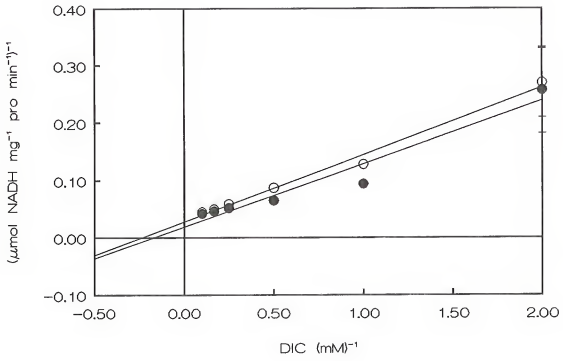

Figure 3-14. Effect of 4 mM F-1,6-BP on K_m(DIC) for PEPCK carboxylation. (●) no F-1,6-BP present, (○) with F-1,6-BP present.

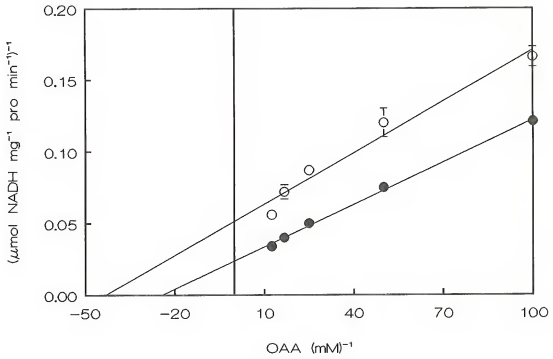

Figure 3-15. Effect of 4 mM PEP on the K_m(OAA) for PEPCK decarboxylation. (●) no PEP present, (○) with PEP present.

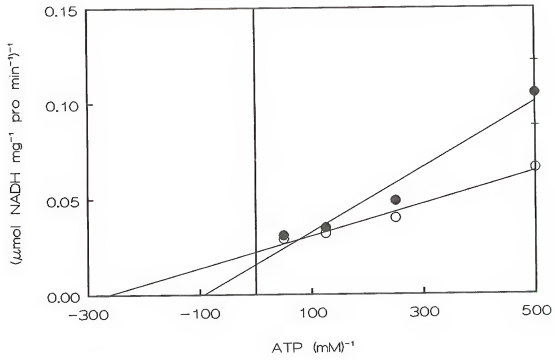

Figure 3-16. Effect of ADP on the K_m(ATP) for PEPCK decarboxylation. (●) no ADP present, (o) with ADP present.

carboxylation by 68% at subsaturating levels of ADP. In the presence of 4 mM ATP, the K_m(ADP) for PEPCK carboxylation was doubled and the V_{max} decreased by one-third (Fig. 3-17).

Although the spectrophotometric method is a rapid and easy technique to use for most measurements of PEPCK, it does have its drawbacks. The PEPCK carboxylation spectrophotometric assay is coupled to MDH and NADH so that a change in absorbance at 340 nm wavelength occurs in a one to one ratio with the production of OAA. As soon as the carboxylation product OAA appears, it is reduced by MDH with NADH to yield malate. The decrease in absorbance is a direct measure of the oxidation of NADH and an indirect measure of OAA production. Because of this coupled assay method, the rate of carboxylation cannot be measured spectrophotometrically in the absence of MDH and NADH. The coupled assay method also precludes examining a direct effect of OAA on the carboxylation reaction, as any exogenously added OAA would be consumed by the MDH and NADH at a rapid rate, thus resulting in an artificially high oxidation rate of NADH. The ^{14}C method, although more time-consuming and less flexible, does produce a direct measure of OAA formation. Using this technique, the presence of MDH and NADH in the reaction mixture was found to increase the reaction rate by six-fold (Table 3-9). Malate inhibited the reaction with or without MDH and NADH present by 25-30%, and this was a greater effect than observed with the spectrophotometric assay, where it resulted in only 10% inhibition (Table 3-8). The decarboxylation substrate ATP inhibited the reaction with MDH and NADH present by only half as much as the reaction measured when MDH and NADH were absent. Both of the radiochemical assays, with and without MDH and NADH present, were affected less than the spectrophotometric assay, which was inhibited 68% by ATP. The reaction in the presence of MDH and NADH was inhibited 33% by OAA, but in contrast, OAA appeared to stimulate the reaction by nearly three-fold when MDH and NADH were absent.

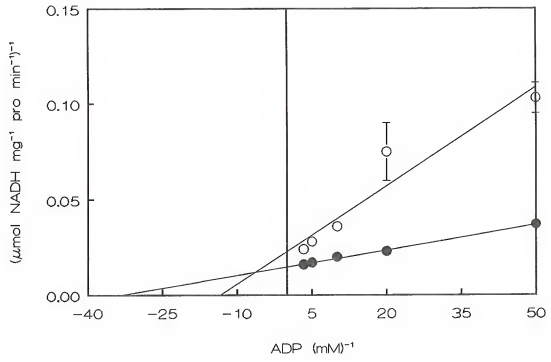

Figure 3-17. Effect of 4 mM ATP on the K_m(ADP) for PEPCK carboxylation. (●) no ATP present, (○) with ATP present.

Table 3-9. Influence of various metabolites and MDH/NADH on the rate of PEPCK carboxylation measured as $^{14}CO_2$ uptake.

Effector	PEPCK Carboxylation Reaction			
	Rate Without MDH/NADH	Stimulation or Inhibition	Rate With MDH/NADH	Stimulation or Inhibiton
	μmol $^{14}CO_2$ mg^{-1} pro min^{-1}	%	μmol $^{14}CO_2$ mg^{-1} pro min^{-1}	%
None	3.94 ± 0.09	---	23.62 ± 0.98	---
Malate	2.94 ± 0.29	-25*	16.55 ± 0.27	-30
ATP	2.87 ± 0.05	-27	19.98 ± 1.01	-15
OAA	11.22 ± 0.30	285	15.71 ± 0.14	-33

Note: A negative value indicates inhibition of the reaction.

Discussion

Earlier photosynthetic work with *Udotea* indicated that the alga has several C_4-like characteristics including photosynthesis that is largely O_2-insensitive, a low photorespiration rate, low labeling of photorespiratory compounds, and C_4 acids that appear early and turn over rapidly rather than accumulating as end-products (122, 123). In an examination of enzymes capable of C_4 acid production, the only one that was found with activity comparable to that of Rubisco and the photosynthetic rate was PEPCK (123). Furthermore, in the presence of the PEPCK inhibitor MPA, photosynthesis of the *Udotea* thallus exhibited C_3-like characteristics, in that photosynthesis was inhibited by O_2, the labeling of photorespiratory compounds increased, and the production of C_4 acids as early products was reduced (122, 123). These studies have provided good evidence that PEPCK functions in *Udotea* as a light-dependent carboxylase for photosynthesis. However, they do not indicate what drives the reaction in the carboxylation direction, given that in those higher plants where it has a photosynthetic role, the enzyme operates as a decarboxylase.

This enzyme is found in a variety of organisms and is responsible for a number of quite different metabolic functions. In *Udotea*, PEPCK appears to be similar to the E.C. 4.1.1.49 enzyme as found in higher plants, yeast, bacteria and parasitic protozoa (33, 147, 150) because the enzyme utilizes the adenine nucleotide. Furthermore, it is an oligomer (Reiskind *et al.*, unpublished data). This contrasts with the E.C. 4.1.1.32 enzyme found in vertebrates, *Euglena*, and helminths, which uses the guanine or inosine nucleotide for its reaction and is a monomer (116, 117, 130). A difference between the two forms of the PEPCK enzyme is indicated by the monomeric PEPCK enzymes' sharing a 62-64% amino acid sequence similarity, but no significant similarities to the yeast gene sequence and the sequences from the corresponding enzymes of rat liver

or chicken (50). Thus, though the two enzymes catalyze essentially the same reaction, the two proteins are quite dissimilar.

Carboxylation by the *Udotea* PEPCK enzyme is similar to that of the higher plant *Panicum* which has a pH optimum of 6.8 and a K_m(PEP) of 1.46 mM (151). The *Udotea* $K_m(CO_2)$ is similar to that from *Urochloa*, at 2.5 mM (74). In this investigation of *Udotea*, MPA inhibited the carboxylation activity of the purified enzyme in a competitive manner. The PEPCK from *Panicum maximum* is also inhibited by MPA (120), as is the enzyme from *Urochloa*, but here the inhibition is noncompetitive with regard to OAA (33). The K_m(ADP) also was comparable to the cytoplasmic PEPCK of the brown alga *Ascophyllum* (78). *Udotea* PEPCK interaction with other substrates is also similar to the enzyme from *Phaeodactylum* which has a K_m(PEP) and (ADP) of 2.2 and 0.048 mM, respectively, at the optimum pH of 6.2 (72). The $K_m(HCO_3^-)$ for *Udotea* compares with that of PEPCK from the diatom *Phaeodactylum* (72) and the helminth *Ascaris* (116). It is also similar to that for both the autotrophic and heterotrophic forms of *Euglena* enzyme (117), although that enzyme uses GDP rather than ADP. The K_m(ADP) also was comparable to that from the PEPCK of the cytoplasm of chicken liver (130).

For decarboxylation, the K_m(OAA) was the same as that determined for *Chloris* at 0.035 mM (67) and similar to *Panicum* at 0.025 mM (33) and *Trypanosoma* at 0.027 mM (150). However, the K_m(ATP) of 2 μM for the *Udotea* enzyme is approximately ten-fold lower than any values reported in the literature for the higher plant enzyme (33, 67, 151).

The enzyme from *Udotea* is not unique among PEPCK enzymes. It shares kinetic characteristics with PEPCK enzymes from C_4 plants, unicellular algae, brown algae, a protozoan, and a roundworm. Among these organisms, PEPCK functions as a carboxylase in some and a decarboxylase in others. The question to be answered is how this enzyme plays a role in the C_4-like photosynthetic metabolism observed in *Udotea*.

This examination of the interaction of *Udotea* PEPCK with its substrates indicates that the enzyme has a greater affinity for the substrates of the decarboxylation reaction, OAA and ATP, than for the carboxylation substrates. If this were the only basis for consideration, it might be reasonable to conclude that *Udotea* PEPCK functions predominantly as a decarboxylase. In this study, MPA inhibited PEPCK decarboxylation in a competitive manner with respect to OAA. In contrast, in mammalian systems, MPA inhibition of PEPCK is noncompetitive with respect to the GTP-dependent decarboxylation of OAA, which halts gluconeogenesis (80).

Earlier enzyme investigations in *Udotea* showed that the only carboxylase/decarboxylase enzyme normally associated with C_4 photosynthesis which had substantial activity in the alga was PEPCK (123). In the terrestrial C_4-PEPCK plants, the initial carboxylation is carried out by PEPC with the subsequent decarboxylation step catalyzed by PEPCK. However, PEPC activity in *Udotea* extracts was minimal (123). There are three major differences between *Udotea* PEPCK and the PEPC of higher plants: PEPCK uses CO_2 as its inorganic carbon substrate while PEPC uses HCO_3^- (4), the metal ion cofactor needed by PEPCK is Mn^{2+} while PEPC requires Mg^{2+} (4), and PEPCK carboxylation activity requires ADP while PEPC does not (4). An attempt to detect carboxylation activity in *Udotea* crude extract with only Mg^{2+} as the metal ion or in the absence of ADP did not result in any OAA production (123). Thus the evidence strongly indicated that the enzyme from the extract operating in carboxylation was PEPCK and not PEPC. However, for C_4 photosynthesis to operate, there must be an initial carboxylation reaction followed by a decarboxylation which provides a higher concentration of CO_2 for Rubisco in the chloroplast. In the absence of good evidence for other decarboxylase enzymes, it was hypothesized that perhaps PEPCK operated in *Udotea* in both the carboxylating and decarboxylating directions. For this to occur without futile metabolite and energy cycling, there would

have to be a separation of the carboxylation and decarboxylation reactions. The working hypothesis was that one isozyme of PEPCK might be operating in the cytosol as a carboxylase while a second isozyme, located in the chloroplast, might operate in the decarboxylating mode to provide the CO_2 for Rubisco (122, 123).

In terrestrial C_4 plants, the separation of carboxylation and decarboxylation functions is achieved through Kranz anatomy (48), but in CAM species, the separation of carboxylation and decarboxylation is temporal, between day and night, rather than spatial (112), while in low photorespiration-state *Hydrilla verticallata*, intracellular compartmentation of enzymes sparates carboxylation from decarboxylation (121). Thus, Kranz anatomy is not always essential for a plant to be able to utilize a form of C_4-metabolism for photosynthesis.

During the isolation of PEPCK from *Udotea*, only one activity peak was detected in the eluant from the weak anion exchange chromatography column, and this was consistently found in a number of preparations. In organisms where two isozymes are present, the two forms can usually be distinguished by ion exchange chromatography (58, 69). In addition, cellular fractionation of *Udotea* resulted in the detection of PEPCK in only the cytosolic fraction and not the chloroplast fraction (Jun and Reiskind, unpublished data). Thus, it appears there is only one isozyme of PEPCK in *Udotea*, located in the cytosol, which functions predominately as a carboxylase.

These data indicated that the working hypothesis required modification to consider that PEPCK may be functioning only as a carboxylase, with the subsequent decarboxylation performed by another enzyme, such as NAD-malic enzyme, which is also present in *Udotea* (123).

In the higher plants, the ATP-PEPCK functions in the species of one of the C_4 photosynthetic subgroups as a decarboxylase in the cytosol of bundle sheath cells to provide CO_2 for Rubisco in the chloroplasts of these cells (48). The enzyme is operating essentially to increase the

concentration of CO_2 in the vicinity of Rubisco so as to favor carboxylation over oxygenation with a concomitant decrease in the PCO cycle. In some of the brown algae, PEPCK operates in a light-independent carboxylating mode to provide the carbon skeletons for anapleurosis (78). In yeast, PEPCK functions to supply the cells with glucose from three- and four-carbon precursors (36). High activity of PEPCK is also found in *Ascaris*, a parasitic worm, where the enzyme operates as a glycolytic CO_2-fixing enzyme (116).

In the unicellular alga *Euglena* grown under heterotrophic conditions, GDP-PEPCK plays a role in anaerobic CO_2 fixation for synthesizing odd-numbered fatty acids via the methylmalonyl-CoA pathway (117). PEPCK is found in mammals as well, where it functions in replenishing depleted glucose levels in the blood through gluconeogenesis with the enzyme operating in the decarboxylating direction in humans (69), rats (31), and chickens (43).

Thus, PEPCK is involved in a number of different metabolic functions ranging from producing cellular energy in the form of ATP for marine diatoms in low light (72), to producing GTP during carboxylation for fatty acid synthesis (117) and glucose in gluconeogenesis (152), as well as providing a source of CO_2 for an enzyme in the next step of metabolism. Given this wide variety of metabolic functional roles, this investigation was carried out to determine the kinetic features of *Udotea* PEPCK to ascertain how this enzyme may play a role in the C_4-like photosynthetic metabolism of this marine alga.

The pH profiles for carboxylation and decarboxylation suggested that the pH of the environment to which the enzyme was exposed *in vivo* could play a role in determining the predominant direction of the reaction. If the cytosolic pH were in the range of 6.5 to 7.0, the carboxylation reaction could run up to two to three times more rapidly than decarboxylation. Even at a pH of 7.0, carboxylation proceeded at a rate 1.5-fold greater than decarboxylation. Assuming that the cytosol,

where PEPCK is believed to be located, has a pH close to neutral (47), then carboxylation by PEPCK would be favored. Increasing the pH from 6.8 to 7.8 increased the affinity for CO_2 by nearly four-fold as the $K_m(CO_2)$ of *Udo*tea PEPCK decreased with increasing pH. A similar situation has been reported for the diatom *Phaeodactylum tricornutum* (72), where the $K_m(CO_2)$ decreased eight-fold over the pH range 6.2 to pH 7.6 (72). In the diatom system, the PEPCK is also postulated to function as a carboxylase. However, this must be weighed against the decrease in the V_{max} of carboxylation rate as the pH rises above the optimum.

An examination of the inorganic carbon source for carboxylation indicated that *Udo*tea PEPCK utilized free CO_2, as has been found for PEPCK in organisms as diverse as the higher plant *Urochlo*a (74), the brown alga *Ascophyllum* (78), a bacterium (44), and a parasitic worm (150). However, the enzyme from *Phaeodactylum*, with which *Udo*tea PEPCK shares several characteristics, is reported to use HCO_3^- as the substrate (72). Because of its use of CO_2 rather than HCO_3^- as substrate, the possibility was considered that O_2 might act as a competitive inhibitor, in a manner reminiscent of the situation with Rubisco (26). The other major carboxylating enzyme, PEPC, is not sensitive to inhibition by O_2 (26), but its inorganic carbon source is HCO_3^- (4). The present study indicated that carboxylation by *Udo*tea PEPCK was not inhibited by O_2, even at 100% O_2 (gas phase) and subsaturating DIC concentrations, where a competitive effect would be maximized. This is, therefore, further evidence that PEPCK could play a similar role to PEPC in terrestrial C_4 plants which provides the initial CO_2 fixation step unhampered by inhibitory effects of dissolved O_2 in the vicinity.

An examination of the effect of OAA on the PEPCK carboxylation reaction using the ^{14}C method indicated that OAA appeared to stimulate carboxylation (Table 3-9), which seemed an unlikely occurrence. The

data can be explained by considering that a $^{14}CO_2$-OAA exchange reaction, also catalyzed by PEPCK, was occurring in the reaction mixture. The OAA added exogenously was becoming radioactive due to the exchange reaction, and this was in addition to the labeled OAA produced by the carboxylation reaction. Therefore, there were two reactions producing ^{14}C-OAA in the reaction vial. This exchange reaction proceeds 30 times faster than the carboxylation reaction and has been documented for PEPCK from pig liver (152) and chicken embryo liver (130). However, when the ^{14}C carboxylation reaction was performed in the presence of MDH and NADH, OAA inhibited the reaction. This result could come about either because the OAA was truly inhibiting the PEPCK carboxylation reaction or because the OAA was inhibiting the MDH catalyzed reduction of OAA. However, because the MDH reaction was operating at a capacity far in excess of PEPCK carboxylation, the former seems to be the more likely explanation, and this would be in accord with a build-up of product reducing the PEPCK carboxylation rate.

A question arises as to whether the exchange reaction was being measured in the spectrophotometric method for carboxylation instead of the true carboxylation reaction. The exchange reaction would not be measurable by the oxidation of NADH, which is used as a measure of the carboxylation rate in the spectrophotometer. Also, in the reaction mixture for that assay, the only OAA present was that produced as a result of the carboxylation of PEP. Because there is an abundance of MDH activity present, as soon as the OAA is produced, it can be reduced by the MDH with NADH to malate.

To understand further how PEPCK may be functioning *in vivo*, the effects of cellular metabolites on the enzyme activity were examined. The C_4 acid malate was an uncompetitive inhibitor of *Udotea* PEPCK, causing a slight decrease in the apparent K_m(DIC) and lowering the V_{max}. In *Phaeodactylum*, the C_4 acid aspartate had the opposite effect by increasing the reaction velocity (72). However, in other organisms, C_4

acids have been reported not to affect either the carboxylation or the decarboxylation reaction (72).

Of the phosphorylated compounds examined, ATP exerted the greatest effect on the *Udotea* carboxylation reaction with an inhibition of 68%. The inhibition was partially competitive with respect to ADP, and ATP lowered the V_{max} and increased the apparent K_m(ADP). Competitive inhibition by ATP of the carboxylation reaction has been reported in the brown alga *Laminaria*, which catalyzes a light-independent carboxylation (159), in the liver fluke *Fasciola* with respect to PEP (88), and in *Ascaris* with respect to PEP and IDP (116). ATP also inhibited carboxylation by PEPCK in yeast by 43% (147).

In regard to decarboxylation, reports of inhibition by ADP are fewer than for ATP in carboxylation, but in the higher plant *Panicum*, ADP is a competitive inhibitor of the decarboxylation reaction with respect to ATP (151), while in *Urochloa*, the combination of ADP and Mn^{2+} functions as a noncompetitive inhibitor with respect to ATP (33). In *Udotea*, ADP appeared to stimulate decarboxylation, but this could be attributed to the interaction of ADP with pyruvate kinase in the reaction mixture to increase the concentration of ATP for the reaction, rather than actually stimulating the decarboxylation reaction directly. Related to the substrate function of ADP for PEPCK carboxylation is its interaction with Mn^{2+} and the enzyme. Several inhibitor studies have indicated that the binding of $ADPMn^{-}$ to the active site of the enzyme protects the active thiols in the active site of yeast PEPCK against deactivation (36, 50). In addition to binding with the nucleotides, free Mn^{2+} must bind to a site on PEPCK to effect catalysis (33, 67, 152). For most enzymes, this Mn^{2+} is essential and cannot be replaced by any other divalent metal cation, including Mg^{2+} (33). In *Udotea*, the presence of Mg^{2+} along with Mn^{2+} inhibited the carboxylation reaction. The decarboxylation reaction in *Urochloa* is also inhibited by Mg^{2+} under similar conditions (33).

The phosphorylated organic acid 3-PGA inhibited decarboxylation by at least 50% in the enzyme from the higher plants *Chloris* (67) and *Urochloa* (33) and in the diatom *Phaeodactylum*, where the enzyme operates as a carboxylase (72). Likewise, 3-PGA inhibited carboxylation in *Udotea* by 61% in a noncompetitive manner. However, in an anaerobic bacterium of the human mouth, *Veillonella*, 3-PGA actually activates PEPCK for gluconeogenesis to produce PEP during lactate metabolism (38). Several other phosphorylated compounds influenced the decarboxylation reactions of the higher plant species. *Chloris* enzyme is inhibited by DHAP, F6P, and F-1,6-BP (67). *Urochloa* PEPCK is inhibited by F6P and F-1,6-BP, both against free Mn^{2+} (33). PEP functions as a noncompetitive inhibitor versus OAA for PEPCK decarboxylation in *Panicum* (151). In *Udotea*, both DHAP and F-1,6-BP inhibited carboxylation by approximately 30% with regard to DIC. However, F-1,6-BP stimulated carboxylation by 34% and decreased the apparent K_m(PEP) from 1.55 to 0.54 mM. Fructose-6P, on the other hand, slightly stimulated carboxylation while inhibiting decarboxylation versus OAA. At physiological concentrations, PEP and DIC inhibited decarboxylation, but PEP also halved the apparent K_m(OAA), from 0.04 mM to 0.02 mM. Decarboxylation was inhibited by DIC (data not shown), as also indicated for the interaction of CO_2 with the enzyme from higher plants (4).

One of the major metabolic pathways operating in the cytosol, where PEPCK appears to be located in *Udotea*, is glycolysis. However, PEPCK is hypothesized to be functioning in photosynthetic carbon assimilation, so the intracellular milieu at that time must be considered. As the function of glycolysis is to provide pyruvate to enter the tricarboxylic acid cycle for the subsequent generation of ATP, it is reasonable to assume that glycolysis is functioning at a minimal level because sufficient ATP is provided by the light reactions of photosynthesis. One of the control enzymes in glycolysis is phosphofructokinase, which is inhibited by ATP (148). Glycolysis does

occur in plant tissue, but its need for operation during photosynthesis is probably diminished. A major function of PEPCK in other organisms is in gluconeogenesis, where the pathway remobilizes glucose. As is the case for glycolysis, there is little need for gluconeogenesis to be functioning in actively photosynthesizing cells. Gluconeogenesis does occur in plants, both in non-photosynthetic tissue for the breakdown and remobilization of stored fats (148) and in the dark in all plant cells. Thus, a major source of cytosolic metabolites that could interact with PEPCK would be the chloroplast during photosynthesis. The DHAP transported out of the chloroplast can be isomerized in the cytosol to 3-phosphoglyceraldehyde (3-PGAl). The combination of DHAP and 3-PGAl produces the 6-carbon sugars. Since F6P and DIC inhibit the decarboxylation reaction while F-1,6-BP enhances it at subsaturating PEP concentrations, it may be that the metabolites in the cytosol during photosynthesis alter the kinetics of the reaction enough so that carboxylation can occur at an appreciable rate.

After OAA is produced in the carboxylation reaction, the high activity of cytosolic MDH, which has a high affinity for OAA with a K_m(OAA) of 0.06 mM (Rattray and Bowes, unpublished), may function to rapidly convert the OAA to malate. The removal of OAA may aid in pulling the reaction in the carboxylation direction. In the blood fluke *Leishmania*, high PEPCK activity is also accompanied by high MDH activity (105). In this organism, where PEPCK functions as a carboxylase, the high MDH activity may work to bring about succinate production in conjunction with fumarate reductase. Thus, here is an example of PEPCK and MDH working in concert to accomplish the metabolic task. The situation appears to be similar in *Udotea*, though the metabolic role is different.

Thus, although *Udotea* PEPCK appears to have a higher affinity for the substrates of the decarboxylation reaction, it is hypothesized that the microenvironment in the cytosol, where PEPCK is located, is such

that PEPCK is capable of carrying out the carboxylation of PEP to the extent that the subsequent metabolism of the OAA produced is able to provide a higher CO_2 concentration for Rubisco in the chloroplast. The cytosolic pH of approximately 7.2 (47) coupled with the high MDH activity facilitates the operation of PEPCK in *Udotea* in the carboxylating direction. Enhancing the carboxylation of RuBP relative to its oxygenation is apparent in *Udotea* from the low CO_2 compensation point, low photorespiration rate, low concentrations of photorespiratory compounds, and low sensitivity of photosynthesis to O_2, as well as the early appearance of C_4 acids which rapidly turn over (123). The important role of PEPCK in initiating this metabolism was clearly demonstrated when *Udotea* thalli were treated with MPA. When PEPCK was inhibited, the photosynthetic characteristics of the alga were very C_3-like: photosynthesis became O_2-sensitive, an increase in photorespiration occurred as evidenced by an increase in the ^{14}C-labeled photorespiratory intermediates detected, and the early production and subsequent turnover of C_4 acids disappeared (123).

The current working hypothesis of the photosynthetic metabolism in *Udotea* is presented in Fig. 3-18. According to this scheme, CO_2 would be fixed by PEPCK in the cytosol to OAA, which is then reduced by MDH and NADH to malate. Not only would this step stabilize the C_4 acid, it would also serve as a mechanism for re-oxidizing NADH as also suggested for *Chloris* (66). The malate produced in the cytosol would be transported to the chloroplast where the decarboxylation event would occur by an enzyme that remains to be determined. One possible enzyme that could catalyze this reaction is NAD-malic enzyme. In terrestrial C_4 species, this enzyme is located in the mitochondria of bundle sheath cells, but in the marine diatom *Phaeodactylum*, this enzyme is reportedly present in the chloroplasts (72). If NAD-malic enzyme also be present in the chloroplasts of *Udotea*, the CO_2 released could be fixed into the PCR cycle by Rubisco, while the pyruvate could be used to regenerate PEP

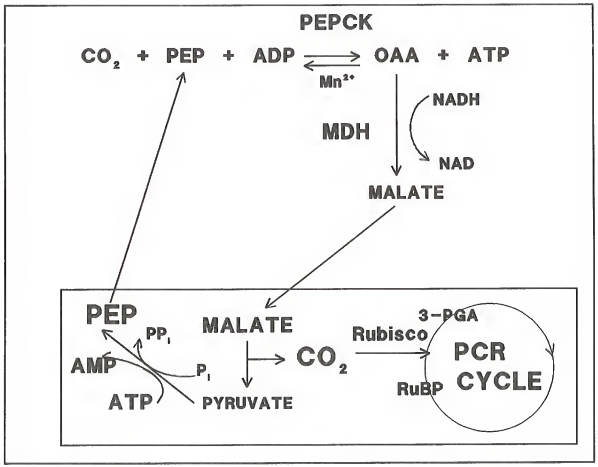

Figure 3-18. Proposed scheme for photosynthetic carbon metabolism in *Udotea*. Carboxylation of PEP occurs by PEPCK in the cytosol. The OAA produced is rapidly reduced to malate by cytosolic MDH, thereby pulling the PEPCK reaction in the carboxylation direction. Malate moves to the chloroplast where it is decarboxylated, and the released CO_2 is refixed by Rubisco. The acceptor molecule PEP is regenerated in the chloroplast by pyruvate P_i dikinase. The PEP can then move back to the cytosol to accept another CO_2.

via pyruvate P_i dikinase. A sufficient activity of this enzyme to support the photosynthetic rate has been found in *Udotea* (123). In this way, then, *Udotea* would be able to provide Rubisco with an elevated concentration of CO_2, i.e., a CO_2-concentrating mechanism, which accounts for the C_4-like photosynthetic features displayed by this alga.

LIST OF REFERENCES

1. **Ali-Ali AK, Al-Husayni H, Power DM** (1988) Purification and comparison of phosphoenolpyruvate carboxykinase from the liver and kidney of the Arabian camel (*Camelus dromedarius*). Comp Biochem Physiol **89B:** 335-338

2. **Arnelle DR, O'Leary MH** (1992) Binding of carbon dioxide to phosphoenolpyruvate carboxykinase deduced from carbon kinetic isotope effects. Biochem **31:** 4363-4368

3. **Arnon DI** (1949) Copper enzymes in isolated chloroplasts. Polyphenoloxidase in *Beta vulgaris*. Plant Physiol **24:** 1-15

4. **Ashton AR, Burnell JN, Furbank RT, Jenkins CLD, Hatch MD** (1990) Enzymes of C_4 photosynthesis. *In* PM Dey, JB Harborne, eds, Methods in Plant Biochemistry. Academic Press, New York, pp 39-72

5. **Axelsson L, Carlberg S, Ryberg H** (1989) Adaptations by macroalgae to low carbon availability. I. A buffer system in *Ascophyllum nodosum*, associated with photosynthesis. Plant Cell Environ **12:** 765-770

6. **Axelsson L, Uusitalo I** (1988) Carbon acquisition strategies for marine macroalgae. I. Utilization of proton exchanges visualized during photosynthesis in a closed system. Mar Biol **97:** 295-300

7. **Badger MR, Andrews TJ** (1982) Photosynthesis and inorganic carbon usage by the marine cyanobacterium, *Synechococcus* sp. Plant Physiol **70:** 517-523

8. **Banu MJ, Dhandayuthapani S, Nellaiappan K** (1991) Intermediary carbohydrate metabolism in the adult filiarial worm *Setaria digitata*. Int J Parasitol **21:** 795-799

9. **Beale EG, Chrapkiewicz NB, Scoble HA, Metz RJ, Quick DP, Noble RL, Donelson JE, Biemann K, Granner DK** (1985) Rat hepatic cytosolic phosphoenolpyruvate carboxykinase (GTP). Structures of the protein, messenger RNA, and gene. J Biol Chem **260:** 10748-10760

10. **Beer S, Eshel A** (1983) Photosynthesis of *Ulva* sp. II. Utilization of CO_2 and HCO_3^- when submerged. J Exp Mar Biol Ecol **70:** 99-106

11. **Beer S, Israel A** (1986) Photosynthesis of *Ulva* sp. III. O_2 effects, carboxylase activities, and the CO_2 incorporation pattern. Plant Physiol **81:** 937-938

12. **Beer S, Israel A** (1990) Photosynthesis of *Ulva fasciata*. IV. pH, carbonic anhydrase and inorganic carbon conversions in the unstirred layer. Plant Cell Environ **13:** 555-560

13. **Beer S, Israel A, Drechsler Z, Cohen Y** (1990) Photosynthesis in *Ulva fasciata*. V. Evidence for an inorganic carbon concentrating system, and ribulose-1,5-bisphosphate carboxylase/oxygenase CO_2 kinetics. Plant Physiol **94:** 1542-1546

14. **Beer S, Sand-Jensen K, Vindbaek Madsen T, Nielsen SL** (1991) The carboxylase activity of Rubisco and the photosynthetic performance in aquatic plants. Oecologia **87:** 429-434

15. **Björk M, Haglund K, Ramazanov Z, García-Reina G, Pedersén M** (1992) Inorganic-carbon assimilation in the green seaweed *Ulva rigida* C.Ag. (Chlorophyta). Planta **187:** 152-156

16. **Black CC, Jr.** (1973) Photosynthetic carbon fixation in relation to net CO_2 uptake. Annu Rev Plant Physiol **24:** 253-286

17. **Blanke MM, Hucklesby DP, Notton BA** (1988) Phosphoenolpyruvate carboxykinase in aubergine, kiwi and apple fruit. Gartenbauwissenschaft **53:** 65-70

18. **Boczoń K** (1986) The role of malic enzyme in the carbohydrate metabolism of *Trichinella spiralis spiralis* and *Trichinella spiralis pseudospiralis*. Int J Parasitol **16:** 435-440

19. **Böhm L, Fütterer D, Kaminski E** (1978) Algal calcification in some Codiaceae (Chlorophyta): ultrastructure and location of skeletal deposits. J Phycol **14:** 486-493

20. **Bold HC, Wynne MJ** (1978) Introduction to the Algae. Structure and Reproduction. Prentice-Hall, Englewood Cliffs, NJ, pp 8-14

21. **Bold HC, Wynne MJ** (1985) Introduction to the Algae, Ed 2. Prentice-Hall, Englewood Cliffs, NJ, pp 216-225

22. **Borowitzka MA** (1987) Calcification in algae: mechanisms and the role of metabolism. CRC Critical Reviews in Plant Sciences **6:** 1-45

23. **Borowitzka MA** (1984) Calcification in aquatic plants. Plant Cell Environ **7:** 457-466

24. **Borowitzka MA** (1982) Morphological and cytological aspects of algal calcification. *In* GH Bourne, JF Danielli, KW Jeon, eds, International Review of Cytology, Vol 74. Academic Press, New York, pp 127-162

25. **Bowes G** (1985) Pathways of CO_2 fixation by aquatic organisms. *In* WJ Lucas, JA Berry, eds, Inorganic Carbon Uptake by Aquatic Photosynthetic Organisms. American Society of Plant Physiologists, Rockville, MD pp 187-210

26. **Bowes G, Ogren WL** (1972) O_2 inhibition and other properties of soybean ribulose 1,5-bisphosphate carboxylase. J Biol Chem **247:** 2171-2176

27. **Bowes G, Salvucci ME** (1983) Two photosynthetic mechanisms mediating the low photorespiratory state in submersed aquatic angiosperms. Plant Physiol **73:** 488-496

28. **Bowman BJ, Slayman CW** (1979) The effects of vanadate on the plasma membrane ATPase of *Neuorspora crassa*. J Biol Chem **254:** 2928-2934

29. **Bradford MM** (1976) A rapid and sensitive method for the quantitation of microgram quantities of protein utilizing the principle of protein-dye binding. Anal Biochem **72:** 248-254

30. **Brechignac F, Andre M** (1984) Oxygen uptake and photosynthesis of the red macroalga, *Chondrus crispus*, in seawater. Effects of light and CO_2 concentration. Plant Physiol **75:** 919-923

31. **Brinkworth RI, Hanson RW, Fullin FA, Schramm VL** (1981) Mn^{2+}-sensitive and -insensitive forms of phosphoenolpyruvate carboxykinase (GTP). J Biol Chem **256:** 10795-10802

32. **Buchanan BB** (1980) Role of light in the regulation of chloroplast enzymes. Annu Rev Plant Physiol **32:** 349-383

33. **Burnell JN** (1986) Purification and properties of phosphoenolpyruvate carboxykinase from C_4 plants. Aust J Plant Physiol **13:** 577-587

34. **Burnell JN, Hatch MD** (1988) Photosynthesis in phosphoenolpyruvate carboxykinase-type C_4 plants: pathways of C_4 acid decarboxylation in bundle sheath cells of *Urochloa panicoides*. Arch Biochem Biophys **260:** 187-199

35. **Cantley LC, Jr., Josephson L, Warner R, Yanagisawa M, Lechene C, Guidotti G** (1977) Vanadate is a potent (Na,K)-ATPase inhibitor found in ATP derived from muscle. J Biol Chem **252:** 7421-7423

36. **Cardemil E, Encinas MV, Jabalquinto AM** (1990) Reactive sulfhydryl groups in *Saccharomyces cerevisiae* phospho*enol*pyruvate carboxykinase. Biochim Biophys Acta **1040:** 71-76

37. **Caspari D, Macy JM** (1983) The role of carbon dioxide in glucose metabolism of *Bacteroides fragilis*. Arch Microbiol **135:** 16-24

38. **Chau HS, Ng SK** (1986) Activation of phosphoenolpyruvate carboxykinase isolated from *Veillonella parvula*. Biochem Cell Biol **64:** 898-905

39. **Coleman JR, Berry JA, Togasaki RK, Grossman AR** (1984) Identification of extracellular carbonic anhydrase of *Chlamydomonas reinhardtii*. Plant Physiol **76:** 472-477

40. **Colman B, Cook CM** (1985) Photosynthetic characteristics of the marine macrophytic red alga *Rhodymenia palmata*: evidence for bicarbonate transport. *In* WJ Lucas, JA Berry, eds, Inorganic Carbon Uptake by Aquatic Photosynthetic Organisms. American Society of Plant Physiologists, Rockville, MD pp 97-110

41. **Colombo PM, Postai E** (1978) The process of wound repair in *Udotea petiolata* (Siphonales). Cytobios 23:7-16

42. **Cook CM, Lanaras T, Colman B** (1986) Evidence for bicarbonate transport in species of red and brown macrophytic marine algae. J Exp Bot **37:** 977-984

43. **Cook JS, Weldon SL, García-Ruíz JP, Hod Y, Hanson RW** (1986) Nucleotide sequence of the mRNA encoding the cytosolic form of phospho*enol*pyruvate carboxykinase (GTP) from the chicken. Proc Natl Acad Sci, USA **83:** 7583-7587

44. **Cooper TG, Tchen TT, Wood HG, Benedict CR** (1968) The carboxylation of phosphoenolpyruvate and pyruvate. I. The active species of "CO_2" utilized by phosphoenolpyruvate carboxykinase, carboxytransphosphorylase, and pyruvate carboxylase. J Biol Chem **243:** 3857-3863

45. **Dawes CJ** (1974) Marine Algae of the West Coast of Florida. University of Miami Press, Coral Gables, FL, pp 85-87

46. **Dixon GK, Merrett MJ** (1988) Bicarbonate utilization by the marine diatom *Phaeodactylum tricornutum* Bohlin. New Phytol **109:** 47-51

47. **Drechsler Z, Beer S** (1991) Utilization of inorganic carbon by *Ulva lactuca*. Plant Physiol **97:** 1439-1444

48. **Edwards GE, Huber SC** (1981) The C_4 pathway. *In* MD Hatch, NK Boardman, eds, The Biochemistry of Plants, Vol 8. Photosynthesis. Academic Press, New York, pp 237-281

49. **Elzenga JTM, Prins HBA** (1988) Adaptation of *Elodea* and *Potamogeton* to different inorganic carbon levels and the mechanism for photosynthetic bicarbonate utilisation. Aust J Plant Physiol **15:** 727-735

50. **Encinas MV, Quinoñes V, Cardemil E** (1990) *Saccharomyces cerevisiae* phosphoenolpyruvate carboxykinase: physicochemical characteristics of the nucleotide binding site, as deduced from fluorescent spectroscopy measurements. Biochem **29:** 4548-4553

51. **Esau K** (1977) Anatomy of Seed Plants, Ed 2. John Wiley & Sons, New York

52. **Espie GS, Kandasamy RA** (1992) Na^+-independent HCO_3^- transport and accumulation in the cyanobacterium *Synechococcus* UTEX 625. Plant Physiol **98:** 560-568

53. **Falk JJ, Chan SI** (1986) Molecular mechanisms of band 3 inhibitors. 1. Transport site inhibitors. Biochem **25:** 7888-7894

54. **Forrester ML, Krotkov G, Nelson CD** (1966) Effect of oxygen on photosynthesis, photorespiration, and respiration on detached leaves. I. Soybean. Plant Physiol **41:** 422-427

55. **Forster RM, Dring MJ** (1992) Interactions of blue light and inorganic carbon supply in the control of light-saturated photosynthesis in brown algae. Plant Cell Environ **15:** 241-247

56. **Friedmann EI, Roth WC, Turner JB, McEwer RS** (1972) Calcium oxalate crystals in the aragonite-producing green alga *Penicillus* and related genera. Science **177:** 891-893

57. **Gallagher SR, Leonard RT** (1982) Effect of vanadate, molybdate, and azide on membrane-associated ATPase and soluble phosphatase activities of corn roots. Plant Physiol **70:** 1335-1340

58. **Gallwitz WE, Jacoby GH, Ray PD, Lambeth DO** (1988) Purification and characterization of the isozymes of phospho*enol*pyruvate carboxykinase from rabbit liver. Biochem Biophys Acta **964:** 36-45

59. **Gibson AC** (1982) The anatomy of succulence. *In* IP Ting, M Gibbs, eds, Crassulacean Acid Metabolism. American Society of Plant Physiologists, Rockville, MD pp 1-17

60. **Gilmour DJ, Kaaden R, Gimmler H** (1985) Vanadate inhibition of ATPases of *Dunaliella parva in vitro* and *in vivo*. J Plant Physiol **118:** 111-126

61. **Giordano M, Maberly SC** (1989) Distribution of carbonic anhydrase in British marine macroalgae. Oecologia **81:** 534-539

62. **Goyal A, Tolbert NE** (1989) Uptake of inorganic carbon by isolated chloroplasts from air-adapted *Dunaliella*. Plant Physiol **89:** 1264-1269

63. **Haglund K, Björk M, Ramazanov Z, García-Reina G, Pedersén M** (1992) Role of carbonic anhydrase in photosynthesis and inorganic-carbon assimilation in the red alga *Gracilaria tenuistipitata*. Planta **187:** 275-281

64. **Haglund K, Ramazanov Z, Mtolera M, Pedersén M** (1992) Role of external carbonic anhydrase in light-dependent alkalization by *Fucus serratus* L. and *Laminaria saccharina* (L.) Lamour. (Phaeophyta). Planta **188:** 1-6

65. **Hall NP, Keys AJ** (1983) Temperature dependence of the enzymic carboxylation and oxygenation of ribulose 1,5-bisphosphate in relation to effects of temperature on photosynthesis. Plant Physiol **72:** 945-948

66. **Hatch MD, Agostino A, Burnell JN** (1988) Photosynthesis in phospho*enol*pyruvate carboxykinase-type C_4 plants: activity and role of mitochondria in bundle sheath cells. Arch Biochem Biophys **261:** 357-367

67. **Hatch MD, Mau S** (1977) Properties of phosphoenolpyruvate carboxykinase operative in C_4 pathway photosynthesis. Aust J Plant Physiol **4:** 207-216

68. **Hedeskov CJ, Capito K, Thams P** (1984) Phospho*enol*pyruvate carboxykinase in mouse pancreatic islets. ATP-induced changes in sensitivity to Mn^{2+} activation. Biochim Biophys Acta **791:** 37-44

69. **Hod Y, Cook JS, Weldon SL, Short JM, Wynshaw-Boris A, Hanson RW** (1982) Differential expression of the genes from the mitochondrial and cytosolic forms of phosphoenolpyruvate carboxykinase. Ann NY Acad Sci **478:** 31-44

70. **Hofslagare O, Samuelsson G, Sjöberg S, Ingri N** (1983) A precise potentiometric method for determination of algal activity in an open CO_2 system. Plant Cell Environ **6:** 195-201

71. **Holbrook GP, Beer S, Spencer WE, Reiskind JB, Davis JS, Bowes G** (1988) Photosynthesis in marine macroalgae: evidence for carbon limitation. Can J Bot **66:** 577-582

72. **Holdsworth ES, Bruck K** (1977) Enzymes concerned with β-carboxylation in marine phytoplankter. Purification and properties of phosphoenolpyruvate carboxykinase. Arch Biochem Biophys **182:** 95-106

73. **Israel A, Beer S, Bowes G** (1991) Photosynthetic carbon acquistion in the red alga *Gracilaria conferta*. I. Gas-exchange properties and the fixation pathway. Mar Biol **110:** 195-198

74. **Jenkins CLD, Burnell JN, Hatch MD** (1987) Form of inorganic carbon involved as a product and as an inhibitor of C_4 acid decarboxylases operating in C_4 photosynthesis. Plant Physiol **85:** 952-957

75. **Jensen RG, Bahr JT** (1977) Ribulose 1,5-bisphosphate carboxylase-oxygenase. Annu Rev Plant Physiol **28:** 379-400

76. **Johnson KS** (1982) Carbon dioxide hydration and dehydration kinetics in seawater. Limnol Oceanogr **27:** 849-855

77. **Johnston AM** (1991) The acquisition of inorganic carbon by marine macroalgae. Can J Bot **69:** 1123-1132

78. **Johnston AM, Raven JA** (1987) The C_4-like characteristics of the intertidal macroalga *Ascophyllum nodosum* (L.) Le Jolis (Fucales, Phaeophyta) Phycologia **26:** 159-166

79. **Johnston AM, Raven JA** (1989) Extraction, partial purification and characterization of phosphoenolpyruvate carboxykinase from *Ascophyllum nodosum* (Phaeophyceae). J Phycol **25:** 568-576

80. **Jomain-Baum M, Schramm VL, Hanson RW** (1976) Mechanism of 3-mercaptopicolinic acid inhibition of hepatic phosphoenolpyruvate carboxykinase (GTP). J Biol Chem **251:** 37-44

81. **Jordan DB, Chollet R** (1983) Inhibition of ribulose bisphosphate carboxylase by substrate ribulose 1,5-bisphosphate. J Biol Chem **258:** 13752-13758

82. **Katz A, Kabach HR, Avron M** (1986) Na^+/H^+ antiport in isolated plasma membrane vesicles from the halotolerant alga *Dunaliella salina*. FEBS Lett **202:** 141-144

83. **Keeley J** (1981) *Isoetes howellii*: a submerged aquatic CAM plant? Amer J Bot **68:** 420-424

84. **Kerby NW, Evans LV** (1983) Phosphoenolpyruvate carboxykinase activity in *Ascophyllum nodosum* (Phaeophyceae). J Phycol **19:** 1-3

85. **Kremer BP, Küppers U** (1977) Carboxylating enzymes and pathway of photosynthetic carbon assimilation in different marine algae--evidence for the C_4 pathway? Planta **133:** 191-196

86. **Ku SB, Edwards GE** (1977) Oxygen inhibition of photosynthesis. I. Temperature dependence and relation to O_2/CO_2 solubility ratio. Plant Physiol **59:** 986-990

87. **Liou B-S, Nagayama F** (1986) Properties of phosphoenolpyruvate carboxykinase from carp hepatopancreas and rainbow trout liver. Bull Jap Soc Sci Fish **52:** 2197-2202

88. **Lloyd GM** (1986) Energy metabolism and its regulation in the adult liver fluke *Fasciola hepatica*. Parasitol **93:** 217-248

89. **Lorimer GH** (1981) The carboxylation and oxygenation of ribulose 1,5-bisphosphate: the primary events in photosynthesis and photorespiration. Annu Rev Plant Physiol **32:** 349-383

90. **Lorimer GH, Andrews TJ** (1981) The C_2 chemo- and photorespiratory carbon oxidation cycle. *In* MD Hatch, NK Boardman, eds, The Biochemistry of Plants, Vol 8. Photosynthesis. Academic Press, New York, pp 330-374

91. **Lorimer GH, Badger MR, Andrews TJ** (1976) The activation of ribulose 1,5-bisphosphate carboxylase by carbon dioxide and magnesium ions. Equilibria, kinetics, a suggested mechanism, and physiological implications. Biochem **15:** 529-536

92. **Lorimer GH, Badger MR, Heldt HW** (1983) The activation of ribulose 1,5-bisphosphate carboxylase/oxygenase. *In* HW Siegelmann, G Hind, eds, Photosynthetic Carbon Assimilation. Plenum Press, New York pp 283-306

93. **Maberly SC** (1992) Carbonate ions appear to neither inhibit nor stimulate use of bicarbonate ions in photosynthesis by *Ulva lactuca*. Plant Cell Environ **15:** 255-260

94. **Maberly SC** (1990) Exogenous sources of inorganic carbon for photosynthesis by marine macroalgae. J Phycol **26:** 439-449

95. **Malebrán LP, Cardemil E** (1987) The presence of functional arginine residues in phosphoe*nol*pyruvate carboxykinase from *Saccharomyces cerevisiae*. Biochim Biophys Acta **915:** 385-392

96. **Martin DF** (1972) Salinity. *In* DF Martin, ed, Marine Chemistry, Analytical Methods, Vol 1. Mercel Dekker, Inc., New York, pp 85-91

97. **McCandless EL** (1981) Polysaccharides of the seaweeds. *In* CS Lobban, MJ Wynne, eds, Botanical Monographs, Vol 17. The Biology of Seaweeds. University of California Press, Berkeley, pp 559-588

98. **McConnaughey T** (1989) ^{13}C and ^{18}O isotopic disequilibrium in biological carbonates: II. *In vitro* simulation of kinetic isotope effects. Geochim Cosmochim Acta **53:** 163-171

99. **McConnaughey T** (1991) Calcification in *Chara corallina*: CO_2 hydroxylation generates protons for bicarbonate assimilation. Limnol Oceanogr **36:** 619-628

100. **McConnaughey T, Falk RH** (1991) Calcium-proton exchange during algal calcification. Biol Bull **180:** 185-195

101. **Meinesz A** (1969) Sur la reproduction sexuée de l'*Udotea petiolata* (Turra) Boerg. CR Acad Sci Paris **269:** 1063-1065

102. **Merrett MJ** (1991) Inorganic carbon transport in some marine microalgal species. Can J Bot **69:** 1032-1039

103. **Moroney JV, Husic DH, Tolbert NE** (1985) Effect of carbonic anhydrase inhibitors on inorganic carbon accumulation by *Chlamydomonas reinhardtii*. Plant Physiol **77:** 177-183

104. **Mortain-Bertrand A, Descolas-Gros, Jupin H** (1987) Stimulating effect of light-to-dark transitions on carbon assimilation by a marine diatom. J Exp Mar Biol Ecol **112:** 11-26

105. **Mottram JC, Coombs GH** (1985) *Leishmania mexicana*: Subcellular distribution of enzymes in amastigotes and promastigotes. Exp Parasitol **59:** 275-289

106. **Müller M, Müller H, Holzer H** (1981) Immunochemical studies on catabolite inactivation of phosphoenolpyruvate carboxykinase in *Saccharomyces cerevisiae*. J Biol Chem **256:** 723-727

107. **Ogren WL** (1984) Photorespiration: pathways, regulation, and modification. Annu Rev Plant Physiol **35:** 415-442

108. **Ohnishi J, Kanai R** (1983) Differentiation of photorespiratory activity between mesophyll and bundle sheath cells of C_4 plants. I. Glycine oxidation by mitochondria. Plant Cell Physiol **24:** 1411-1420

109. **O'Neill SD, Spanswick RM** (1984) Effects of vanadate on the plasma membrane ATPase of red beet and corn. Plant Physiol **75:** 586-591

110. **Opperdoes FR, Cottem D** (1982) Involvement of the glycosome of *Trypanosoma brucei* in carbon dioxide fixation. FEBS Lett **143:** 60-64

111. **Osmond CB** (1982) Carbon cycling and stability of the photosynthetic apparatus in CAM. *In* IP Ting, M Gibbs, eds, Crassulacean

Acid Metabolism. American Society of Plant Physiologists, Rockville, MD pp 112-127

112. **Osmond CB** (1978) Crassulacean acid metabolism: a curiosity in context. Annu Rev Plant Physiol **29:** 379-414

113. **Osmund CB, Holtum JAM** (1981) Crassulacean acid metabolism. *In* MD Hatch, NK Boardman, eds, Plant Biochemistry, Vol 8. Photosynthesis. Academic Press, New York pp 283-328

114. **Palmqvist K, Sjöberg S, Samuelsson G** (1988) Induction of inorganic carbon accumulation in the unicellular green algae *Scenedesmus obliquus* and *Chlamydomonas reinhardtii*. Plant Physiol **87:** 437-442

115. **Pearcy RW, Ehleringer J** (1984) Comparative ecophysiology of C_3 and C_4 plants. Plant Cell Environ **7:** 1-13

116. **Pietrzak Rohrer SP, Saz HJ, Nowak T** (1986) Purification and characterization of phosphoenolpyruvate carboxykinase from the parasitic helminth *Ascaris suum*. J Biol Chem **261:** 13049-13055

117. **Pönsgen-Schmidt E, Schneider T, Hammer U, Betz A** (1988) Comparison of phosphoenolpyruvate-carboxykinase from autotrophically and heterotrophically grown *Euglena* and its role during dark anaerobiosis. Plant Physiol **86:** 457-462

118. **Raven JA, Johnston AM** (1991) Photosynthetic inorganic carbon assimilation by *Prasiola stipitata* (Prasiolales, Chlorophyta) under emersed and submersed conditions: relationship to the taxonomy of *Prasiola*. Br Phycol J **26:** 247-257

119. **Raven JA, Osmond CB** (1992) Inorganic C acquisition processes and their ecological significance in inter- and sub-tidal macroalgae of North Carolina. Funct Ecol **6:** 41-47

120. **Ray TB, Black CC** (1976) Inhibition of oxalacetate decarboxylation during C_4 photosynthesis by 3-mercaptopicolinic acid. J Biol Chem **251:** 5824-5826

121. **Reiskind JB, Berg RH, Salvucci ME, Bowes G** (1989) Immunogold localization of primary carboxylases in leaves of aquatic and a C_3-C_4 intermediate species. Plant Sci **61:** 43-52

122. **Reiskind JB, Bowes G** (1991) The role of phosphoenolpyruvate carboxykinase in a marine macroalga with C_4-like photosynthetic characteristics. Proc Natl Acad Sci USA **88:** 2883-2887

123. **Reiskind JB, Seamon PT, Bowes G** (1988) Alternative methods of photosynthetic carbon assimilation in marine macroalgae. Plant Physiol **87:** 686-692

124. **Reiskind JB, Seamon PT, Bowes G** (1989) Photosynthetic responses and anatomical features of two marine macroalgae with different CO_2 compensation points. Aquat Bot **33:** 71-86

125. **Reymond P, Geourjon C, Roux B, Durand R, Fevre M** (1992) Sequence of the phosphoenolpyruvate carboxykinase-encoding cDNA from the rumen anaerobic fungus *Neocallimastix frontalis*: comparison of the amino acid sequence with animals and yeast. Gene **110:** 57-63

126. **Rotatore C, Colman B** (1991) The active uptake of carbon dioxide by the unicellular green algae *Chlorella saccharophila* and *C. ellipsoidea*. Plant Cell Environ **14:** 371-375

127. **Rotatore C, Colman B** (1991) The localization of active inorganic carbon transport at the plasma membrane in *Chlorella ellipsoidea*. Can J Bot **69:** 1025-1031

128. **Rowland-Bamford AJ, Baker JT, Allen LH, Jr., Bowes G** (1991) Acclimation of rice to changing atmospheric carbon dioxide concentration. Plant Cell Environ **14:** 577-583

129. **Salvucci ME, Portis AR, Jr., Ogren WL** (1985) A soluble chloroplast protein catalyzes activation of ribulose 1,5-bisphosphate carboxylase/oxygenase *in vivo*. Photosyn Res 7: 193-201

130. **Sato A, Suzuki T, Kochi H** (1986) Purification and characterization of cytosol-specific phosphoenolpyruvate carboxykinase from chicken liver. J Biochem **100:** 671-678

131. **Satoh Y** (1986) Effects of Mn^{2+} on the exchange reaction of phosphoenolpyruvate carboxykinase in the presence of high concentrations of Mg^{2+}. Biochim Biophys Acta **872:** 177-182

132. **Servaites JC, Ogren WL** (1978) Oxygen inhibition of photosynthesis and stimulation of photorespiration in soybean leaf cells. Plant Physiol **60:** 461-466

133. **Skirrow G** (1975) The dissolved gases--carbon dioxide. *In* JP Riley, G Skirrow, eds, Chemical Oceanography, Vol 2. Academic Press, New York pp 1-192

134. **Smith AM, HW Woolhouse** (1983) Metabolism of phosphoenolpyruvate in the C_4 (carbon pathway) cycle during photosynthesis in the phosphoenolpyruvate-carboxykinase C_4 grass *Spartina anglica* Hubb. Planta **159:** 570-578

135. **Smith RG** (1988) Inorganic carbon transport in biological systems. Comp Biochem Physiol **90B:** 639-654

136. **Smith RG, Bidwell RGS** (1987) Carbonic anhydrase-dependent inorganic carbon uptake by the red macroalga *Chondrus crispus*. Plant Physiol **83:** 735-738

137. **Smith RG, Bidwell RGS** (1989) Inorganic carbon uptake by photosynthetically active protoplasts of the red macroalga *Chondrus crispus*. Mar Biol **102:** 1-4

138. **Smith RG, Bidwell RGS** (1989) Mechanism of photosynthetic carbon dioxide uptake by the red macroalga, *Chondrus crispus*. Plant Physiol **89:** 93-99

139. **Staal M, Elzenga JTM, Prins HBA** (1989) ^{14}C fixation by leaves and leaf cell protoplasts of the submerged aquatic angiosperm *Potamogeton lucens*: carbon dioxide or bicarbonate? Plant Physiol **90:** 1035-1040

140. **Sültemeyer DF, Miller AG, Espie GS, Fock HP, Canvin DT** (1989) Active CO_2 transport by the green alga *Chlamydomonas reinhardtii*. Plant Physiol **89:** 1213-1219

141. **Surif MB, Raven JA** (1989) Exogenous inorganic carbon sources for photosynthesis in seawater by members of the Fucales and the

Laminariales (Phaeophyta): ecological and taxonomic implications. Oecol **78:** 97-105

142. **Surowy TK, Sussman MR** (1986) Immunological cross-reactivity and inhibitor sensitivities of the plasm membrane H^+-ATPase from plants and fungi. Biochim Biophys Acta **848:** 24-34

143. **Thielmann J, Tolbert NE, Boyal A, Senger H** (1990) Two systems for concentrating CO_2 and bicarbonate during photosynthesis by *Scenedesmus*. Plant Physiol **92:** 622-629

144. **Ting I** (1985) Crassulacean acid metabolism. Annu Rev Plant Physiol **36:** 595-622

145. **Tinker KA, Brosnan JT, Herzberg GR** (1983) Phosphoenolpyruvate carboxykinase is a nuclear enzyme in rats and chickens. Int J Biochem **15:** 1473-1475

146. **Tinoco I, Jr., Sauer K, Wang JC** (1985) Physical Chemistry. Principles and Application in Biological Sciences, Ed 2. Prentice-Hall, Englewood Cliffs, NJ p 135

147. **Tortora P, Hanozet GM, Guerritore A** (1985) Purification of phosphoenolpyruvate carboxykinase from *Saccharomyces cerevisiae* and its use for bicarbonate assay. Anal Biochem **144:** 179-185

148. **Turner JF, Turner DH** (1975) The regulation of carbohydrate metabolism. Annu Rev Plant Physiol **26:** 159-186

149. **Ui M, Claus TH, Exton JH, Park CR** (1973) Studies on the mechanism of action of glucagon on gluconeogenesis. J Biol Chem **248:** 5344-5349

150. **Urbina JA** (1987) The phosph*enol*pyruvate carboxykinase of *Trypanosoma (Schizotrypanum) cruzi* epimastigotes: molecular, kinetic, and regulatory properties. Arch Bioch Biophys **258:** 186-195

151. **Urbina JA, Avilan L** (1989) The kinetic mechanism of phosphoenolpyruvate carboxykinase from *Panicum maximum*. Phytochem **28:** 1349-1353

152. **Utter MF, Kolenbrander HM** (1972) Formation of oxalacetate by CO_2 fixation on phosphoenolpyruvate. *In* PD Boyer, ed, The Enzymes, Vol VI. Carboxylation and Decarboxylation (Nonoxidative). Isomerization. Academic Press, New York pp 117-168

153. **van den Hoek C** (1981) Chlorophyta: morphology and classification. *In* CS Lobban, MJ Wynne, eds, Botanical Monographs, Vol 17. The Biology of Seaweeds. University of California Press, Berkeley and Los Angeles, pp 86-132

154. **Vu CV, Allen LH, Jr., Bowes G** (1983) Effects of light and elevated atmospheric CO_2 on the ribulose bisphosphate carboxylase activity and ribulose bisphosphate level of soybean leaves. Plant Physiol **73:** 729-734

155. **Walker NA, Smith FA, Cathers IR** (1980) Bicarbonate assimilation by freshwater Charophytes and higher plants: I. Membrane transport of bicarbonate ions is not proven. J Membr Biol **57:** 51-58

156. **Watanabe M, Ohnishi J, Kanai R** (1984) Intracellular localization of phosphoenolpyruvate carboxykinase in bundle sheath cells of C_4 plants. Plant Cell Environ **25:** 69-76

157. **Watford M** (1985) Gluconeogenesis in the chicken: regulation of phosphoenolpyruvate carboxykinase gene expression. Federation Proc **44:** 2469-2474

158. **Wedding RT, Black MK, Meyer CR** (1990) Inhibition of phosphoenolpyruvate carboxylase by malate. Plant Physiol **92:** 456-461

159. **Weidner M, Küppers U** (1982) Metabolic conversion of ^{14}C-aspartate, ^{14}C-malate and ^{14}C-mannitol by tissue disks of *Laminaria hyperborea*: role of phosphoenolpyruvate carboxykinase. Z Pflanzenphysiol **108:** 353-364

160. **Wilson AJ, Bhattacharjee JK** (1986) Regulation of phosphoenolpyruvate carboxykinase and pyruvate kinase in *Saccharomyces cerevisiae* grown in the presence of glycolytic and gluconeogenic carbon sources and the role of mitochondrial function on gluconeogenesis. Can J Microbiol **32:** 969-972

161. **Yueh AY, Chung C-S, Lai Y-K** (1989) Purification and molecular properties of malate dehydrogenase from the marine diatom *Nitzschia alba*. Biochem J **258:** 221-228

162. **Zabala MT, Lorenzo P, Alvarez L, Berlanga JJ, García-Ruíz JP** (1992) Serotonin increases the cAMP concentration and the phosphoenolpyruvate carboxykinase mRNA in rat kidney, small intestine, and liver. J Cell Physiol **150:** 451-455

BIOGRAPHICAL SKETCH

Beth Ann Lilly was born in Reading, Pennsylvania, on October 1, 1963. She graduated from Governor Mifflin Senior High School in Shillington, Pennsylvania, in June 1981, matriculated at Millersville University in Millersville, Pennsylvania, as a biology major in August 1981 and graduated with a Bachelor of Science cum laude in August 1985. She then moved to Gainesville, Florida to commence graduate studies in botany under the direction of Dr. George Bowes at the University of Florida in August 1985. Beth was awarded the Master of Science degree in August 1988. She immediately began research toward the doctorate in botany, under the direction of Dr. George Bowes. In August 1992, she married Gregory Burch in Gainesville, Florida. Beth became an assistant professor of biology at Huntington College in Huntington, Indiana in September 1993 and graduated with the degree Doctor of Philosophy in December 1993.

I certify that I have read this study and that in my opinion it conforms to acceptable standards of scholarly presentation and is fully adequate, in scope and quality, as a dissertation for the degree of Doctor of Philosophy.

George Bowes

George Bowes, Chairman
Professor of Botany

I certify that I have read this study and that in my opinion it conforms to acceptable standards of scholarly presentation and is fully adequate, in scope and quality, as a dissertation for the degree of Doctor of Philosophy.

Joseph S. Davis
Professor of Botany

I certify that I have read this study and that in my opinion it conforms to acceptable standards of scholarly presentation and is fully adequate, in scope and quality, as a dissertation for the degree of Doctor of Philosophy.

Richard C. Smith
Professor of Botany

I certify that I have read this study and that in my opinion it conforms to acceptable standards of scholarly presentation and is fully adequate, in scope and quality, as a dissertation for the degree of Doctor of Philosophy.

Charles M. Allen, Jr.
Professor of Biochemistry and Molecular Biology

I certify that I have read this study and that in my opinion it conforms to acceptable standards of scholarly presentation and is fully adequate, in scope and quality, as a dissertation for the degree of Doctor of Philosophy.

Charles L. Guy
Associate Professor of Horticultural Science

This dissertation was submitted to the Graduate Faculty of the Department of Botany in the College of Liberal Arts and Sciences and to the Graduate School and was accepted as partial fulfillment of the requirements for the degree of Doctor of Philosophy.

December 1993

Dean, Graduate School